




2019

## MUTATIONS OF FUS CAUSE AGGREGATION OF RNA BINDING PROTEINS, DISRUPTIONS IN PROTEIN SYNTHESIS, AND DYSREGULATION OF NONSENSE MEDIATED DECAY

Marisa Elizabeth Kamelgarn

University of Kentucky, meka229@g.uky.edu

Author ORCID Identifier:

 <https://orcid.org/0000-0002-7433-5909>

Digital Object Identifier: <https://doi.org/10.13023/etd.2019.163>

[Right click to open a feedback form in a new tab to let us know how this document benefits you.](#)

### Recommended Citation

Kamelgarn, Marisa Elizabeth, "MUTATIONS OF FUS CAUSE AGGREGATION OF RNA BINDING PROTEINS, DISRUPTIONS IN PROTEIN SYNTHESIS, AND DYSREGULATION OF NONSENSE MEDIATED DECAY" (2019). *Theses and Dissertations--Toxicology and Cancer Biology*. 27.  
[https://uknowledge.uky.edu/toxicology\\_etds/27](https://uknowledge.uky.edu/toxicology_etds/27)

This Doctoral Dissertation is brought to you for free and open access by the Toxicology and Cancer Biology at UKnowledge. It has been accepted for inclusion in Theses and Dissertations--Toxicology and Cancer Biology by an authorized administrator of UKnowledge. For more information, please contact [UKnowledge@lsv.uky.edu](mailto:UKnowledge@lsv.uky.edu).

## **STUDENT AGREEMENT:**

I represent that my thesis or dissertation and abstract are my original work. Proper attribution has been given to all outside sources. I understand that I am solely responsible for obtaining any needed copyright permissions. I have obtained needed written permission statement(s) from the owner(s) of each third-party copyrighted matter to be included in my work, allowing electronic distribution (if such use is not permitted by the fair use doctrine) which will be submitted to UKnowledge as Additional File.

I hereby grant to The University of Kentucky and its agents the irrevocable, non-exclusive, and royalty-free license to archive and make accessible my work in whole or in part in all forms of media, now or hereafter known. I agree that the document mentioned above may be made available immediately for worldwide access unless an embargo applies.

I retain all other ownership rights to the copyright of my work. I also retain the right to use in future works (such as articles or books) all or part of my work. I understand that I am free to register the copyright to my work.

## **REVIEW, APPROVAL AND ACCEPTANCE**

The document mentioned above has been reviewed and accepted by the student's advisor, on behalf of the advisory committee, and by the Director of Graduate Studies (DGS), on behalf of the program; we verify that this is the final, approved version of the student's thesis including all changes required by the advisory committee. The undersigned agree to abide by the statements above.

Marisa Elizabeth Kamelgarn, Student

Dr. Haining Zhu, Major Professor

Dr. Isabel Mellon, Director of Graduate Studies

MUTATIONS OF FUS CAUSE AGGREGATION OF RNA BINDING PROTEINS,  
DISRUPTIONS IN PROTEIN SYNTHESIS, AND DYSREGULATION OF  
NONSENSE MEDIATED DECAY

---

DISSERTATION

---

A dissertation submitted in partial fulfillment of the  
requirements for the degree of Doctor of Philosophy in the  
College of Medicine  
at the University of Kentucky

By  
Marisa Elizabeth Kamelgarn  
Lexington, Kentucky  
Director: Dr. Haining Zhu, Professor of Molecular and Cellular Biochemistry  
Lexington, Kentucky  
2019

Copyright © Marisa Elizabeth Kamelgarn 2019  
<https://orcid.org/0000-0002-7433-5909>

## ABSTRACT OF DISSERTATION

### MUTATIONS OF FUS CAUSE AGGREGATION OF RNA BINDING PROTEINS, DISRUPTIONS IN PROTEIN SYNTHESIS, AND DYSREGULATION OF NONSENSE MEDIATED DECAY

Amyotrophic lateral sclerosis (ALS) is a fatal neurodegenerative disease characterized by motor neuron death and subsequent muscle atrophy. Approximately 15% of ALS cases are inheritable, and mutations in the Fused in Sarcoma (*FUS*) gene contribute to approximately 5% of these cases, as well as about 2% of sporadic cases. *FUS* performs a diverse set of cellular functions, including being a major regulator of RNA metabolism. *FUS* undergoes liquid-liquid phase transition *in vitro*, allowing for its participation in stress granules and RNA transport granules. Phase transition also contributes to the formation of cytoplasmic inclusions found in the cell bodies of *FUS* ALS patients motor neurons. The nature of these inclusions has remained elusive, as the proteins localized to them have not been identified. Additionally, the functional consequence of the accumulation of cytoplasmic *FUS* inclusions has not been established, nor is it understood how they contribute to selective motor neuron death.

We carried out two related, but independent studies to characterize the proteins that may be included in *FUS*-positive inclusions. In this first study, we utilized immunoprecipitation of wild-type and mutant *FUS* in the presence and absence of RNase, followed by LC MS/MS. The identified proteins represent those that directly or indirectly interact with *FUS*, with relatively high affinity that can be pulled down with immunoprecipitation. A wide variety of interacting proteins were identified and they are involved in a multitude of pathways including: chromosomal organization, transcription, RNA splicing, RNA transport, localized translation, and stress response. Their interaction with *FUS* varied greatly in their requirements for RNA. Most notably, *FUS* interacted with hnRNPA1 and Matrin-3, proteins also known to cause familial ALS. Immunofluorescent

staining of proteins interacting with mutant FUS were localized to cytoplasmic inclusions. We concluded that mis-localization of these proteins potentially lead to their dysregulation or loss of function, thus contributing to FUS pathogenesis.

In the second study, we developed a protocol to isolate dynamic FUS inclusions and employed LC MS/MS to identify all proteins associated with FUS inclusions. We identified a cohort of proteins involved in translation, splicing, and RNA export to be associated with the FUS inclusions. Further pathway and disease association analysis suggested that proteins associated with translation and RNA quality control pathways may be the most significant. Protein translation assays using both N2A and ALS patient fibroblasts demonstrated suppression of protein biosynthesis in mutant FUS expressing cells. However, translation initiation was not impaired. To understand how protein synthesis is suppressed by mutant FUS mediated defects in RNA metabolism, we examined changes in a well conserved RNA turnover pathway namely: nonsense mediated decay (NMD). We found that NMD is hyperactivated in cells expressing mutant FUS, likely due to chronic suppression of protein translation shifting the pathways autoregulatory circuit to allow for hyperactivation. We concluded that mutant FUS suppresses protein biosynthesis and disrupts NMD regulation. These defects together likely contribute to motor neuron death.

**KEYWORDS:** Fused in Sarcoma, Amyotrophic Lateral Sclerosis, RNA binding, Nonsense Mediated Decay, Protein Translation.

---

Marisa Elizabeth Kamelgarn

*(Name of Student)*

---

[03/22/2019]

Date

MUTATIONS OF FUS CAUSE AGGREGATION OF RNA BINDING PROTEINS,  
DISRUPTIONS IN PROTEIN SYNTHESIS, AND DYSREGULATION OF  
NONSENSE MEDIATED DECAY

By  
Marisa Elizabeth Kamelgarn

Dr. Haining Zhu  
\_\_\_\_\_  
Director of Dissertation

Dr. Isabel Mellon  
\_\_\_\_\_  
Director of Graduate Studies

03/22/2019  
\_\_\_\_\_  
Date

## ACKNOWLEDGMENTS

This dissertation and the research done would not have been possible without the guidance and support of Dr. Haining Zhu, the Zhu lab, and my family and friends. I would like to thank my advisor Dr. Zhu for the opportunity to work in his lab and his help developing this project. The freedom he afforded me in the lab helped develop my skills as an independent scientist, an invaluable part of my training that will be essential for my career. Not only has Dr. Zhu been an incredible mentor, helping foster creativity at the bench, but also encouraging perseverance and instilling confidence in my research. I would also like to thank my Advisory Committee: Drs. Isabel Mellon, Daret St. Clair, Edward J. Kasarskis, and Stefan Stamm for the time spent on collaborations, committee meetings, exams, and reference letters, and for the great advice and suggestions on my research projects. Lastly, I would like to give a special thanks to Dr. Steven Estus for serving as Outside Examiner of my final exam.

In nearly six years, I have made some incredible friends in the Zhu Lab. I want to give special thanks to Ms. Li Liu for taking care of basic lab needs and for helping breed mice for primary neuron culture. I also want to thank current and previous members of the Zhu Lab: Drs. Liuqing Yang, Junkai Fan, Dandan Liu, Jozsef Gal, Jing Chen, Lisha Kuang, and Sushil Dubey, as well as Alexandra Arenas and Will Na. I would like to extend a special thank you to Huan Jin, for producing data published in our PNAS paper.

I want to thank the department of Toxicology and Cancer Biology for providing both financial and educational support, as well as the department of Molecular and Cellular Biochemistry for allowing me to use their facilities. Both departments have

amazing professors, staff, postdocs, and students. I would like to give a very special thank you to Dr. Isabel Mellon for her guidance, support, and the opportunity to host the Toxicology Student Forum. Additionally, I would like to thank Ms. Madalyn Willis for helping take care of my student affairs and Dr. Carole Moncman for training me on the confocal microscope. I am forever grateful for everyone's assistance and guidance, and proud that I can take the skills you all have taught me to future research positions.

Lastly, I would like to thank my parents, Sandra and Howard Kamelgarn for their support over the past five and half years, as well as my fiancée Eugene Hinderer III for his support.

This dissertation research would not have been possible without the funding support from: the department of Toxicology and Cancer Biology's T32 training grant, the College of Medicine's Fellowship for Excellence in Graduate Research Award, the Lyman T. Johnson Fellowship, National Institute of Neurological Disorder, Stroke (NINDS) and Amyotrophic Lateral Sclerosis (ALS) Association, and the Veterans Association (VA).



## TABLE OF CONTENTS

<i>ACKNOWLEDGMENTS</i> .....	<i>iii</i>
<i>TABLE OF CONTENTS</i> .....	<i>v</i>
<i>LIST OF TABLES</i> .....	<i>viii</i>
<i>LIST OF FIGURES</i> .....	<i>ix</i>
<i>LIST OF ADDITIONAL FILES</i> .....	<i>x</i>
<i>CHAPTER 1. Introduction</i> .....	<i>1</i>
1.1    What is Amyotrophic Lateral Sclerosis?.....	1
1.2    FUS' Domain Structure and Post Translational Modifications.....	2
1.3    FUS' Nuclear Function.....	3
1.3.1    Transcription.....	4
1.3.2    Regulation of mRNA Length and Coupling Transcription to Splicing.....	6
1.3.3    Alternative Splicing.....	7
1.4    Nucleocytoplasmic Shuttling of FUS.....	10
1.5    FUS' Cytoplasmic Function.....	12
1.5.1    Protein Translation.....	12
1.5.2    RNA Triage and Stress Response.....	13
1.5.3    Regulation of RNA Stability.....	14
1.6    Study Rationale and Overview.....	16
<i>CHAPTER 2. Materials and Methods</i> .....	<i>23</i>
2.1    Cell Culture, Plasmids, and Transfection.....	23
2.2    Culture and Transfection of Primary Cortical Neurons.....	23
2.3    GST-FUS Pull-Downs.....	24
2.4    Immunoprecipitation.....	24
2.5    Proteomic identification of FUS interaction partners.....	25
2.6    Western Blot.....	26
2.7    Immunofluorescence microscopy.....	27
2.8    Patient Skin Fibroblast Culture.....	27
2.9    Membrane Filtration.....	28
2.10    Native Gel Electrophoresis.....	28
2.11    Proteomic identification of proteins captured by membrane filtration.....	29

2.12	Enrichment Analysis of roteins captured by membrane filtration .....	29
2.13	RNA FISH .....	30
2.14	RNA Immunoprecipitation followed by qPCR .....	30
2.15	Protein Translation Assays .....	31
2.16	7' Methyl-guanosine Pulldown.....	32
2.17	Bromouridine Immunoprecipitation.....	32
2.18	NMD Activity Assays .....	33
2.19	RNA Stability Assay .....	33
2.20	Statistics.....	34
<i>CHAPTER 3. Proteomic Analysis of FUS Interacting Proteins Provides Insights Into FUS Function and Its Role in ALS.....</i>		<i>38</i>
3.1	Introduction.....	38
3.2	Results .....	40
3.2.1	Identification of FUS interaction partners .....	40
3.2.2	Validation and characterization of selected FUS interactions .....	41
3.2.3	Co-localization of FUS interaction partners with cytoplasmic ALS mutant FUS inclusions.....	42
3.2.4	Significantly enriched Gene Ontology (GO) terms among the identified FUS interacting partners .....	44
3.2.5	FUS interacts with overlapping ribonucleoprotein complexes.....	45
3.3	Discussion.....	47
3.3.1	Identification and validation of FUS interaction partners .....	47
3.3.2	The RNA dependence of FUS interactions .....	48
3.3.3	The interaction of FUS with the ALS-related proteins Matrin-3 and hnRNPA1 .....	49
3.3.4	FUS interacts with regulators of protein phosphorylation.....	49
3.3.5	Loss of nuclear FUS functions due to ALS mutations.....	50
3.3.6	Mis-regulation of cytoplasmic processes by ALS mutant FUS.....	51
3.4	Conclusions.....	52
<i>CHAPTER 4. ALS Mutations of FUS Suppress Protein Translation and Disrupt the Regulation of Nonsense-Mediated Decay.....</i>		<i>66</i>
4.1	Introduction.....	66
4.2	Results .....	68
4.2.1	Proteins related to translation and mRNA surveillance are enriched in mutant FUS inclusions.....	68
4.2.2	Protein translation is impaired in the presence of mutant FUS .....	70
4.2.3	The NMD pathway is activated by mutant FUS .....	73
4.2.4	NMD factors are dysregulated in fibroblasts in FUS ALS cases.....	75

4.2.5	UPF1-mediated autoregulation of NMD is impaired in FUS ALS cases.....	76
4.2.6	Enhanced decay of NMD substrate in the presence of ALS mutant FUS.....	77
4.3	Discussion.....	79
<i>CHAPTER 5. The Role of Endogenous FUS in Nonsense Mediated Decay</i> .....		110
5.1	Introduction.....	110
5.2	Results .....	112
5.2.1	FUS Binds NMD Factor mRNA.....	112
5.2.2	FUS Binds NMD Substrate mRNA .....	113
5.2.3	FUS Knockout Downregulates Pro-NMD Factor Proteins .....	114
5.2.4	FUS KO Reduces NMD Complex Assembly.....	115
5.2.5	FUS Knockout Downregulates Pro-NMD Factor mRNA.....	115
5.2.6	Stability of NMD Factors is Unchanged when FUS is Knocked Out.....	116
5.2.7	FUS KO Reduces UPF1 Binding to NMD Factor mRNA .....	116
5.2.8	NMD Substrate mRNAs are Stabilized when FUS is Knocked Out .....	117
5.2.9	FUS KO Reduces UPF1 Binding to NMD Substrate mRNA.....	118
5.2.10	Natural NMD substrate levels are influenced by FUS KO.....	118
5.3	Conclusions and Future Directions for FUS KO/ NMD Study .....	119
<i>REFERENCES</i> .....		136
<i>Vita</i> .....		154

## LIST OF TABLES

Table 2.1 Patient Fibroblasts.....	35
Table 2.2 List of qPCR Primers .....	36
Table 3.1 Selected enriched GO Biological Processes among the identified FUS interacting partners. ....	53
Table 3.2 Selected enriched GO Molecular Functions among the identified FUS interacting partners. ....	54
Table 3.3 Selected enriched GO Cellular Components among the identified FUS interacting partners. ....	55

## LIST OF FIGURES

Figure 1.1 FUS Domain Structure.....	18
Figure 1.2 FUS Nuclear Functions.....	19
Figure 1.3 FUS' Cytoplasmic Function .....	21
Figure 3.1 .....	56
Figure 3.2 .....	57
Figure 3.3 .....	58
Figure 3.4 .....	60
Figure 3.5 .....	62
Figure 3.6 .....	64
Figure 3.7 .....	65
Figure 4.1 .....	85
Figure 4.2 .....	87
Figure 4.3 .....	88
Figure 4.4 .....	89
Figure 4.5 .....	90
Figure 4.6 .....	92
Figure 4.7 .....	93
Figure 4.8 .....	95
Figure 4.9 .....	97
Figure 4.10 .....	98
Figure 4.11 .....	99
Figure 4.12 .....	101
Figure 4.13 .....	102
Figure 4.14 .....	104
Figure 4.15 .....	106
Figure 4.16 .....	107
Figure 4.17 .....	109
Figure 5.1 Endogenous FUS binds key NMD factor mRNA .....	122
Figure 5.2 Endogenous FUS binds NMD substrate mRNA .....	123
Figure 5.3 Endogenous FUS is required for normal expression of NMD factor protein	124
Figure 5.4 Endogenous FUS is required for assembly of NMD factor complexes.....	126
Figure 5.5 Endogenous FUS is required for normal expression of NMD factor mRNA	127
Figure 5.6 NMD factor mRNA stability is unchanged when FUS is Knocked Out .....	128
Figure 5.7 FUS KO Reduces UPF1 Binding to NMD Factor mRNA.....	129
Figure 5.8 NMD substrate mRNA is stabilized when FUS is Knocked Out.....	131
Figure 5.9 UPF1 Binding to NMD Substrate mRNA is Reduced When FUS is Knocked Out .....	132
Figure 5.10 Natural NMD substrate levels are in influenced by FUS KO .....	134

## LIST OF ADDITIONAL FILES

Supplemental Table 3.1. The identified non-ribosomal FUS interacting partners.....	[PDF 176 KB]
Supplemental Table 3.2. The identified ribosomal FUS interacting partners.....	[PDF 133 KB]
Supplemental Table 4.1 FUS WT Proteomics .....	[PDF 1.2 MB]
Supplemental Table 4.2. FUS R495X Proteomics .....	[PDF 1.1 MB]
Supplemental Table 4.3 FUS P525L Proteomics .....	[PDF 1.1 MB]
Supplemental Table A. List of Primers .....	[PDF 154 KB]

## CHAPTER 1. INTRODUCTION

### 1.1 What is Amyotrophic Lateral Sclerosis?

Amyotrophic Lateral Sclerosis (ALS) is a rapidly progressing, neurodegenerative disease impacting both upper and lower motor neurons. Brought into the public eye in the 1930s by the American baseball player, Lou Gehrig, the disease is characterized by body-wide voluntary muscle weakness and paralysis, culminating in the death of the patient (1). According to the ALS Association, in the United States alone, there are approximately 20,000 individuals living with ALS and 6,000 new diagnoses each year. ALS can be classified as sporadic (sALS), where no family history of the disease is found, or familial (fALS) if a mutated allele is identified in several family members with the disease. Roughly 90% of ALS cases are considered sporadic, while the remaining 10% are from inheritable mutations. Genes most commonly mutated that result in an ALS phenotype are C9orf72, Superoxide Dismutase I (SOD1), transactive response DNA binding protein 43 kDa (TPD-43), and Fused in Sarcoma (FUS) (1).

FUS is a DNA and RNA binding protein identified in 2009 to cause approximately 5% of fALS and 2% of sALS cases when mutated (2, 3). Although FUS mutations are considered rare and only account for 5% of fALS cases, it accounts for approximately 60% of all fALS cases for patients younger than 40 years of age (4, 5). The severity of FUS related ALS varies, with specific mutations resulting in a shorter course of disease earlier in life. Severe, disease-causing mutations typically result in FUS' mis-localization from the nucleus to the cytoplasm. Presentation of FUS in the cytoplasm can vary in appearance, depending on the type of mutation an individual has (5). Mutant FUS' presentation in the

cytoplasm may range from diffuse throughout the cytoplasm to forming large inclusion bodies. These inclusions are basophilic, and ubiquitin and p62 positive (6, 7), however, the consequence of their formation in the cell body of motor neurons is unknown. Wild type FUS' cellular functions have been well characterized and include transcription, regulation of RNA length, alternative splicing, nucleocytoplasmic export, protein translation, and maintenance of RNA stability.

## 1.2 FUS' Domain Structure and Post Translational Modifications

FUS is a member of the FUS, EWSR1, TAF15 (FET) family of DNA and RNA binding proteins. These proteins are composed of a unique set of a prion-like QGYS domains, two RNA-recognition motifs (RRM), a zinc-finger (ZnF) domain, and a C-terminal nuclear localization domain (5). To better understand FUS' molecular function, several in-depth studies have been conducted to understand the importance of each domain. FUS' QGYS, or low-complexity (LC), domain has been characterized using NMR. It was determined to have a unique amino acid profile and folding dynamics compared to many other intrinsically disordered, neurodegenerative proteins (8). FUS' QGYS domain is required for formation of functional oligomeric species that can be regulated through phosphorylation of serine and threonine residues. Phosphorylation of these sites facilitates disassembly of liquid/liquid droplets formed by FUS and prevent its aggregation (8, 9). RNP granules formed through the QGYS domain are critical for regulation of mRNA stability, location, and metabolism, most notably the formation of stress granules (SGs) in times of acute cellular stress (10-12).



In addition to self-oligomerization being required for RNP granule formation and binding RNA polymerase 2 (RNAP2), RNA binding is also needed for seeding these complexes (13, 14). FUS' nucleotide (DNA and RNA) binding function is executed through its RGG, RRM and ZnF domains (15, 16). Little is understood about the mechanism through which the domains determine nucleotide binding specificity, however, this aspect of FUS' structure is central to its natural cellular function, as well as its disease phenotype. FUS' RGG and RRM domains can be methylated on arginine residues. Arginine methylation is important for regulating FUS' participation in phase separation and transportin-1 (TNPO1) binding. It has been reported that disruption of FUS' methylation profile, characteristic of FUS mutations contributes to cytoplasmic mislocalization and stabilization of oligomeric structures (17, 18). Together, FUS' amino acid sequence, domains, and types of post-translational modifications are critical for its localization and function in motor neurons (Fig. 1.1). Disturbance in one of these features due to an ALS causing mutation leads to gross changes in FUS' molecular function and contributes to a neurodegenerative phenotype.

### 1.3 FUS' Nuclear Function

FUS is largely a nuclear protein that plays critical roles in transcription, mRNA maturation, and nucleocytoplasmic export of RNA (Fig. 1.2). It is hypothesized that the first step in cellular dysfunction contributing to ALS pathogenesis is FUS' exclusion from the nucleus (19). Exclusion of FUS from the nucleus may result in defective transcription, polyadenylation, and splicing of mRNA. FUS' structure is critical to its normal function in the nucleus and is vital to maintaining the fidelity of the transcriptome.

### 1.3.1 Transcription

FUS is a potent regulator of RNA synthesis that can bind active chromatin. There are two nuclear pools of FUS: a soluble fraction and chromatin bound fraction (20). It is likely that the chromatin bound fraction contains FUS interacting with RNAP2 and directly with DNA. The soluble fraction is FUS bound to newly synthesized RNA, regulating splicing and processing mRNA for nuclear export (20). These observations are supported by FUS knockout experiments that describe lost expression of hundreds of genes (21). Additionally, formation of oligomeric species is required for WT and mutant FUS to interact with active chromatin in discrete nuclear puncta (20, 22), indicative of localization to sites of active transcription (23). Mutations that lead to exclusion of FUS from the nucleus have fewer active sites and repression of transcription (20, 22).

FUS' interaction with RNAP2 is critical for its role in the regulation of gene expression. Accumulation of FUS at transcriptional start sites (TSS) recruits RNAP2 to active chromatin (20, 22). Following recruitment, FUS binds the C-terminal domain (CTD) of RNAP2, where it regulates its phosphorylation state of specific serine residues. Classically, there are two positions within the CTD that promote or block RNAP2 translocation along DNA: serine 2 (Ser2) and serine 5 (Ser5). Upon FUS knockdown, studies demonstrated the accumulation of phosphorylation on Ser2 (13) (p-Ser2), which is illustrative of transcriptional termination (24, 25). These knockdown studies demonstrated that FUS limits p-TEFb phosphorylation of Ser2, implying that FUS functions to prevent premature termination of transcription (13). However, as RNAP2 travels down the DNA, p-Ser2 collects on the CTD, which eventually displaces FUS and terminates transcription

(26). Studies in ALS patient fibroblasts exhibited similar changes in the phosphorylation state of Ser2 as observed in FUS knockdown cells, indicating that mutations in FUS result in a nuclear loss of function (23). Mutant FUS has been observed to localize within nuclear aggregates sequestered away from TSS' and RNAP2. This sequestration away from transcriptionally active chromatin and RNAP2 likely leads to premature phosphorylation of Ser2 near the TSS and reduced mRNA levels (23).

Deeper explorations of differences between how mutant and WT FUS bind transcriptionally active chromatin demonstrate the importance of oligomerization and RNA binding. Both forms of the protein bind chromatin through their LC-domains and RNA through FUS' RGG-Zn-RGG domains (13, 27). However, compared to WT FUS, mutant FUS has reduced chromatin binding capabilities, and therefore some loss of nuclear function (20). In fact, FUS' LC-domain is required for interaction with chromatin, binding RNAP2, and effective transcription, suggesting that formation of functional oligomers is intrinsic for FUS' nuclear function (20).

Taken together, FUS is an important regulator of transcription through several different modalities. Endogenous FUS influences transcriptional activity through directly binding to chromatin and to RNAP2. These interactions are critical to signal for transcription to be initiated for a specific gene, but also to enhance complete RNA synthesis.

### 1.3.2 Regulation of mRNA Length and Coupling Transcription to Splicing

FUS plays an important role in post-transcriptionally modifying mRNA to control gene expression in tandem with transcription. Connection of transcription to mRNA splicing and polyadenylation is an important step in efficient maturation of mRNA. Without these processes, transcription would terminate prematurely, and newly synthesized mRNA would undergo premature polyadenylation (28, 29).

FUS is a potent regulator of mRNA length through selection of favorable polyadenylation sites for expression of approximately two-thirds of neuronal genes (30). FUS' binding to nascent RNA, in combination to direct interaction with RNAP2, determines transcriptional termination and polyadenylation (30). To regulate polyadenylation, FUS binds upstream (5') or downstream (3') of alternative polyadenylation (APA) sites (30). The location of FUS' binding site on RNA determines whether the short polyA or degraded isoform is favored. For short APA isoforms, FUS binds downstream (3') from the APA site, which enhances the RNA's interaction with RNAP2, allowing polyadenylation specificity factor (CPSF) complex members to bind, specifically, CPSF160. This interaction generates short polyA tails and stimulates additional proteins to bind and finish synthesizing sequence (31, 32). Conversely, if FUS binds upstream (5') of an APA site, RNAP2 stalls and terminates transcription, leading to truncated transcripts that are degraded (30).

Studies exploring the consequences of FUS' loss of function in motor neurons demonstrated dysregulation of transcription and polyadenylation (30, 33). For example, FUS knockdown caused APA sites to be differentially regulated for genes relating to

synaptic activity and motor neuron-specific activity (30). More research needs to be done looking into changes in transcription and polyadenylation that occur when FUS is mutated to gain a deeper understanding of how ALS mutations of FUS directly the transcriptome.

### 1.3.3 Alternative Splicing

FUS' interaction with RNA is complicated; several different groups have identified various sequences and secondary characteristics that FUS preferentially interacts with, however, an agreement as to FUS' specificity has not been reached in the field. Preliminary studies identified a GGUG consensus sequence that facilitated FUS binding through its RRM domain (34, 35). Advancements in technology have allowed us to identify specific secondary structures and G/C or A/U rich regions FUS also binds (21, 36, 37). Although no definitive sequence FUS binds to has been identified, the protein broadly clusters around the 5' ends of long introns (21, 30, 37, 38), as well as within introns of cassette exons (30, 39).

This consistent binding pattern of FUS to binding 5' ends of introns and within cassette exons illustrates FUS' important role as a regulator of alternative splicing. Explorations of functional defects caused by FUS knockout in neurons demonstrated changes in splicing of over 3,000 exons and expression changes in 183 genes (30). Of the 183 genes exhibiting the most significant alterations in their splicing profiles, several were involved in neuronal function and neurodegeneration. They include *Mapt*, *Camk2a*, and *Fmr1* (30). Additionally, annotation enrichment of genes regulated by FUS, demonstrated its importance in neuronal gene expression. Terms such as "neuronal impulse", "neuronal projection", and "vesicle transport" were enriched (30). Studies investigating FUS' binding

pattern within introns demonstrated enrichment within genes of RNA binding proteins in mouse and human brains, as well. The intronic sequences FUS binds are highly conserved and upon FUS knockout, are retained within the mature mRNA (35). Overall, FUS' binding of introns is required for normal expression of genes required for neuronal function and RNA metabolism. However, FUS' ability to regulate splicing is done in conjunction with other splicing factors.

FUS' role in regulation of splicing largely involves its interaction with U1snRNP and other splicing factors (40-43). Perhaps one of FUS' best-understood protein/protein relationships is between U1snRNP and Survival Motor (SMN), the protein responsible for Spinal Muscular Atrophy (SMA). U1snRNP is a core spliceosomal component responsible for recognizing the 5' splice site of an intron, the first step in the classical splicing pathway (44). During transcription, FUS recruits U1snRNP to 5' ends of introns to begin assembly of splicing complex members (45). Studies utilizing ALS FUS mutants observed reduction of U1snRNP/pre-mRNA interaction. This is likely due to defective interactions between mutant FUS and U1snRNP, U1snRNP's mis-localization to the mutant FUS inclusion, and an overall reduction of U1snRNA bioavailability due to defective SMN activity (40, 41).

SMN is considered to be the master of snRNP biogenesis (46) and mRNP assembly on pre-mRNA (47, 48), however, this is not without the help of FUS. WT and mutant FUS have been shown to directly bind to SMN and SMN complex members (42). Mutations in FUS disturb SMN's localization due to sequestration of SMN in cytoplasmic FUS inclusions, thus reducing its nuclear availability and the number of Gems (40, 42). Gems are SMN-dependent sites of snRNA biosynthesis (49). Mutations in FUS mimic the same

loss of Gems observed in FUS KO cells, resulting in the reduction in snRNA synthesis. These patterns are observed in patient fibroblasts, transfected cells, and in transgenic mouse models of FUS ALS (40, 42). This is likely due to reductions in the levels of select snRNAs. In addition to disrupting snRNP biogenesis, in a mouse motor neuron model of mutant FUS, localization of SMN to cytoplasmic inclusions leads to reduced axonal SMN, contributing to axonal defects (50).

Together, interaction between mutant FUS, U1snRNP, and SMN illustrate the detrimental effects that occur when FUS is mutated. FUS mutations lead to a complex cytoplasmic toxic gain of function/nuclear loss of function phenotype across disease models. FUS' toxic sequestration of U1snRNP and SMN in cytoplasmic inclusions contributes to splicing defects illustrative of nuclear loss of function. Overall, the splicing defects that arise for loss of snRNPs and FUS are vast, negatively impact normal neuronal function, and are likely to be a main contributor to motor neuron degeneration.

FUS' role in splicing is not limited to the classical U1 splicing pathway (5, 21, 33, 35, 37-39, 51, 52). FUS also plays a role in splicing U12-type introns of the minor splicing pathway (53). These unique introns comprise approximately 1% of the transcriptome. Of the small subset of transcripts that are included in this group, a member of the voltage-gated sodium channel required for normal muscle function is included (54, 55). In a mechanism similar to U1snRNP dependent splicing, FUS binds the 5' splice site of introns to recruit U11 (53). Moreover, mutations in FUS fail to recruit U11 and U12 to the pre-mRNA and traps them in cytoplasmic inclusions (53).

Finally, FUS also plays a role in regulation of the circular RNA (circRNA) transcriptome. circRNAs are a rare species of RNA that originate from back-splicing events in which a downstream 5' splice site covalently binds with the upstream 3' splice site (56). Their functions in the cytoplasm of cells are still elusive, however, they are thought to act as “sponges” for RBPs to regulate their activity (57). In iPSC derived motor neurons deficient for FUS, 134 different circular transcripts were discovered to be differentially regulated, with 111 being downregulated. In N2a cells expressing FUS P525L and R521C ALS mutations, the same pattern of circRNA downregulation was recapitulated, likely due to nuclear deficiencies in splicing factors. Further inquiry into FUS' role in the circularization mechanism demonstrated that FUS must bind introns flanking the circularized exons (58). This is consistent with data demonstrating that FUS is required to bind along introns for alternative splicing to occur (20, 21, 39, 51, 56).

Overall, many studies have illustrated FUS' critical importance in regulating gene expression. This regulation and control span from snRNA biogenesis through interaction with SMN, to generation of rare circRNA isoforms. FUS' function in binding the 5' end of introns to recruit splicing factors from the classical and minor splicing pathways demonstrate its broad impacts on neuronal gene expression. Changes in gene expression and splicing may provide the initial steps in a complex pathogenic mechanism culminating in motor neuron death.

#### 1.4 Nucleocytoplasmic Shuttling of FUS

A pathological hallmark of FUS-ALS is accumulation of FUS in cytoplasmic inclusion bodies in the somas of motor neurons (2, 3). A long-standing question the field



aimed to answer was how and why FUS mutants remain localized to the cytoplasm and formed potentially pathological inclusions. An interesting feature of FUS is its non-canonical nuclear localization sequence (NLS) that binds TNPO1 (59, 60) through methylation in its RGG3 domain (18, 61). TNPO1 transports FUS back into the nucleus through the nuclear pore complex upon its release from mRNA in the cytoplasm. Mutations in FUS, however, impair its TNPO1 interaction due to defective methylation (12, 18, 62, 63). FUS' regulation through methylation is a complicated set of events dictated by PRMT1 asymmetrically dimethylating FUS. Monomethylated FUS has a much higher affinity for TNPO1 and may be responsible for cytoplasmic sequestration of TNPO1 characteristic of FTLN-FUS (18, 64). In contrast, mutant FUS is hypomethylated in ALS, which results in cytoplasmic aggregation (17, 19, 62). It is speculated that neuron sub-type specific changes in methylation enzymes account for differences between FTLN and ALS (17).

Further research into the mechanism that regulates FUS' re-entry to the nucleus illustrates that binding of TNPO1 to FUS' NLS prevents phase separation required to form cytoplasmic aggregates (18). FUS mutants are prone to aggregation due to their reduced ability to interact with TNPO1 (18, 65). FUS' low complexity N-terminal domain naturally forms  $\beta$ -sheets through arginine and tyrosine residues interacting via cation- $\pi$  interactions (17). Hypomethylation of these residues promotes phase separation, as it prevents TNPO1 from acting as a molecular chaperone for FUS in the axons of motor neurons, as well as the nuclear pore (17).

## 1.5 FUS' Cytoplasmic Function

FUS' cytoplasmic role in neurons has yet to be described in detail. Recent publications have begun to describe FUS' role in regulation of stress granule dynamics, translation, and regulation of mRNA stability (Fig. 1.3).

### 1.5.1 Protein Translation

FUS' function in regulation of mRNA metabolism is ever evolving. FUS has been demonstrated to be shuttled out into the cytoplasm bound to mRNA, then chaperoned back into the nucleus. Early in FUS' characterization, it was linked to translation in adenomatous polyposis coli (APC)-RNPs. These granules included RNAs that mediate cell migration. Interestingly, both wild type and mutant FUS were localized to these translationally active granules in cell protrusions (66), however, the levels of protein biosynthesis were not measured.

More recently, FUS' cytoplasmic function has begun to be described in more detail. Transgenic mice expressing wild type or the R521 mutant were observed to have defects in axonal translation and changes in RNA expression. Specifically, it was reported that elevated levels of RNA's encoding for stress-related chaperones were observed, while genes for synaptic function like ion transporters were downregulated (67). This landmark paper provides support and a mechanism to a 2015 paper demonstrating the GluA1 subunit of the AMPA receptor is downregulated (68). Both groups described behavioral deficits in mutant animals, while only the Da Cruz lab identified motor defects. This fascinating difference in phenotype is likely due to different neuronal subtypes bearing mutations (67, 68).

### 1.5.2 RNA Triage and Stress Response

FUS involvement in stress granule (SG) formation has been described as a vital function of the protein since it was initially implicated in causing ALS. SGs are membrane-less, cytoplasmic granules that are sites of arrested translation and temporary mRNA stabilization. They function to protect mRNP complexes in times of acute cellular stress. Many proteins are recruited into SGs, including wild type and mutant FUS (12, 69). Studies that aimed to understand FUS' role in SG formation utilized FUS KO cells. Ultimately, it was found that loss of FUS does not negatively impact SG formation, indicating that FUS participates in later stages of stress response and RNA triage (69).

To investigate the mechanism by which wild type and mutant FUS localize to the cytoplasm, Pandey et.al mutated four phenylalanine residues (F305, F341, F359, and F368) to leucine in FUS' RRM (11). Mutation of these residues abolished FUS' RNA binding ability and resulted in nuclear sequestration of FUS, suggesting that RNA binding is required for FUS' nuclear export and incorporation into SGs (11). Mutant FUS follows similar rules for SG incorporation, requiring RNA binding to enter SGs, however, it is hypothesized that this initiates the formation of cytoplasmic inclusions. Additionally, FUS cannot act alone in managing SGs dynamics. Proteins like G3BP1 and TIA1 also manage the longevity, size, and mRNA stability with SGs (70, 71). Changes in the SG proteome can account for differences when comparing their formation in WT and mutant FUS cells. However, the mechanism driving the potential stabilization of SG's in cells bearing mutant FUS is unknown.

A large variety of proteins can be found localized to the SG- like mutant FUS inclusions, however, many are related to RNA binding, SG formation, protein translation, and other aspects of RNA metabolism. Early proteomic analysis of FUS' binding partners identified a number of key stress granule proteins, including Poly-A binding protein (PABP1). Additionally, FUS inclusions also colocalize with SG markers TIA1, Caprin-1, and G3BP1 (70, 72-74). P-bodies are observed adjacent to FUS inclusions, suggesting that stabilized SGs are sites of RNA decay (72). The molecular functions of these proteins in SG's remain elusive, however, they are vital to normal stress response.

One RNA binding protein that interacts with mutant FUS and whose function in the SG-like inclusions has been explored is Pur-alpha (75). Pur-alpha is a single-strand DNA binding protein found to localize to SGs when FUS is mutated (75, 76). In cells expressing mutant FUS, Pur-alpha overexpression has been demonstrated to play a protective role by preventing FUS' cytoplasmic mis-localization to SGs, thus preventing the formation of large inclusion bodies and toxicity (75).

As SG formation is thought to be a precursor event to inclusion formation, more in-depth studies must be performed. A more complete understanding of the interaction mutant FUS has with proteins and RNAs localized in SG-like inclusion bodies will illustrate the proteins whose function is most impacted by FUS mutations (11, 77).

### 1.5.3 Regulation of RNA Stability

A burgeoning avenue of research delving further into FUS' cytoplasmic function is its role in managing mRNA stability. Two different mechanisms have arisen to be controlled by

FUS to influence the stability of select RNA species: miRNA targeting and Nonsense Mediated Decay (NMD).

FUS has been established to control miRNA biogenesis for mRNAs required in neuronal development and activity through recruitment and loading of Drosha onto pri-miRNA upon transcription (78). Drosha is a critical enzyme in the miRNA biogenesis pathway required to cleave pri-miRNA to pre-miRNA (79). Upon FUS knockdown, the levels of miR-9, miR-125b, and miR-132 are all down-regulated. Loss of these miRNA species is thought to be due to defective processing of pri-mRNA due to FUS KO. These miRNA species have a key role in neuronal function, differentiation, and synaptogenesis, respectively (78). Loss of these miRNA results in toxic increases of neuronal proteins.

Mutations in FUS, specifically FUS P525L and equivalents, can result in severe disturbances in levels of the miRNA landscape due to their exclusion from the nucleus. For example, mutations result in upregulation of brain-specific miR-409-3p and miR-495-3p (80). Upregulation of these miRNAs is related to a number of neurodevelopmental disorders involved down-regulation of *Gria2*, a subunit of the AMPA receptor. Loss of this subunit results in excitotoxic events leading to defective  $Ca^{2+}$  regulation (80). miRNA species can also participate in the autoregulatory loops of many RNA binding proteins (81). In spinal motor neurons of ALS patients, miR-b2122 expression is depressed and thought to regulate TDP-43, FUS/TLS and RGNEF (81). Down-regulation of this miRNA in sporadic ALS patients may result in toxic overexpression of these proteins

In addition to regulating mRNA levels through miRNA binding and silencing, NMD has been identified to play an important role in influencing neurotoxicity in FUS

models. In early yeast studies, it was demonstrated that overexpression of UPF1 rescued mutant FUS toxicity (82). Further confirmation of NMD's importance in mediating neuronal toxicity was demonstrated in a mouse neuronal model of ALS, where overexpression of UPF1 within a particular range, was neuroprotective (83). A deeper understanding of how NMD participates in regulation of mRNA stability will be a fascinating avenue of study for the ALS field. Research of this pathway in relation to FUS ALS may provide many links to other molecular mechanisms thoroughly researched by the field, including mRNA splicing and protein translation.

## 1.6 Study Rationale and Overview

A well-defined molecular mechanism driving FUS ALS remains elusive. We aimed to demonstrate a novel mechanism that explored reported defects in RNA metabolism and to understand how they are related to the FUS inclusions. Proteins localized to the mutant inclusions had not been identified or characterized. It had been widely speculated that mutant FUS inclusions are stalled and/ or ultra-stable stress granules, however, a functional consequence of their stasis has not been ascribed to them. Additionally, early studies began to illustrate a link between FUS and protein translation. Until 2018, however, no efforts had been made in the field to further explore protein translation in ALS or its relationship with the mutant FUS inclusion. Overall, our goal was to understand the role mutant FUS inclusions play in protein translation and mRNA stability.

To address this, we designed two exploratory mass spectrometry studies to first characterize the mutant FUS inclusions: 1) to examine direct FUS interactors dependent

and independent of RNA binding and 2) proteins exclusively associated with the inclusion. These studies illustrated the link between mRNA stability, regulation of stress granule dynamics, and protein translation. From these data we proposed two hypotheses:

1. FUS mutations sequester stress granule proteins in inclusion bodies, impairing their function.
2. FUS inclusions are sites of stalled or terminated translation complexes and mRNA degradation by NMD.

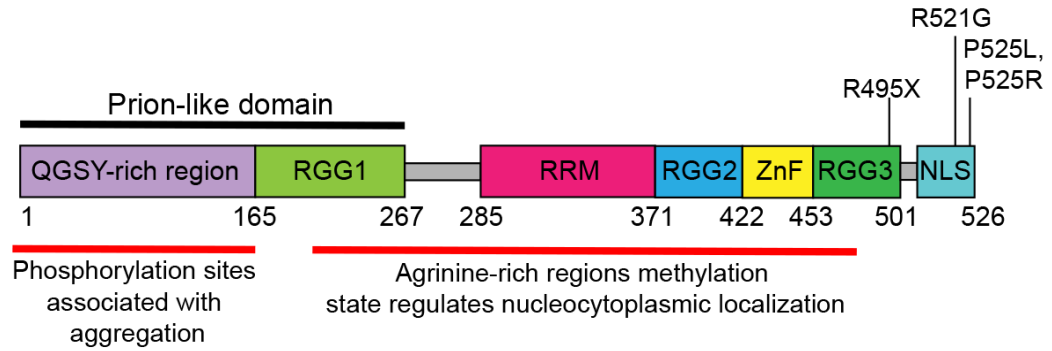


Figure 1.1 FUS Domain Structure

RGG, Arginine/glycine-rich region; RRM, RNA recognition motif; ZnF, zinc finger domain; NLS, nuclear localization sequence. R495X, R521G, P525L, and P525R are naturally occurring ALS mutations.



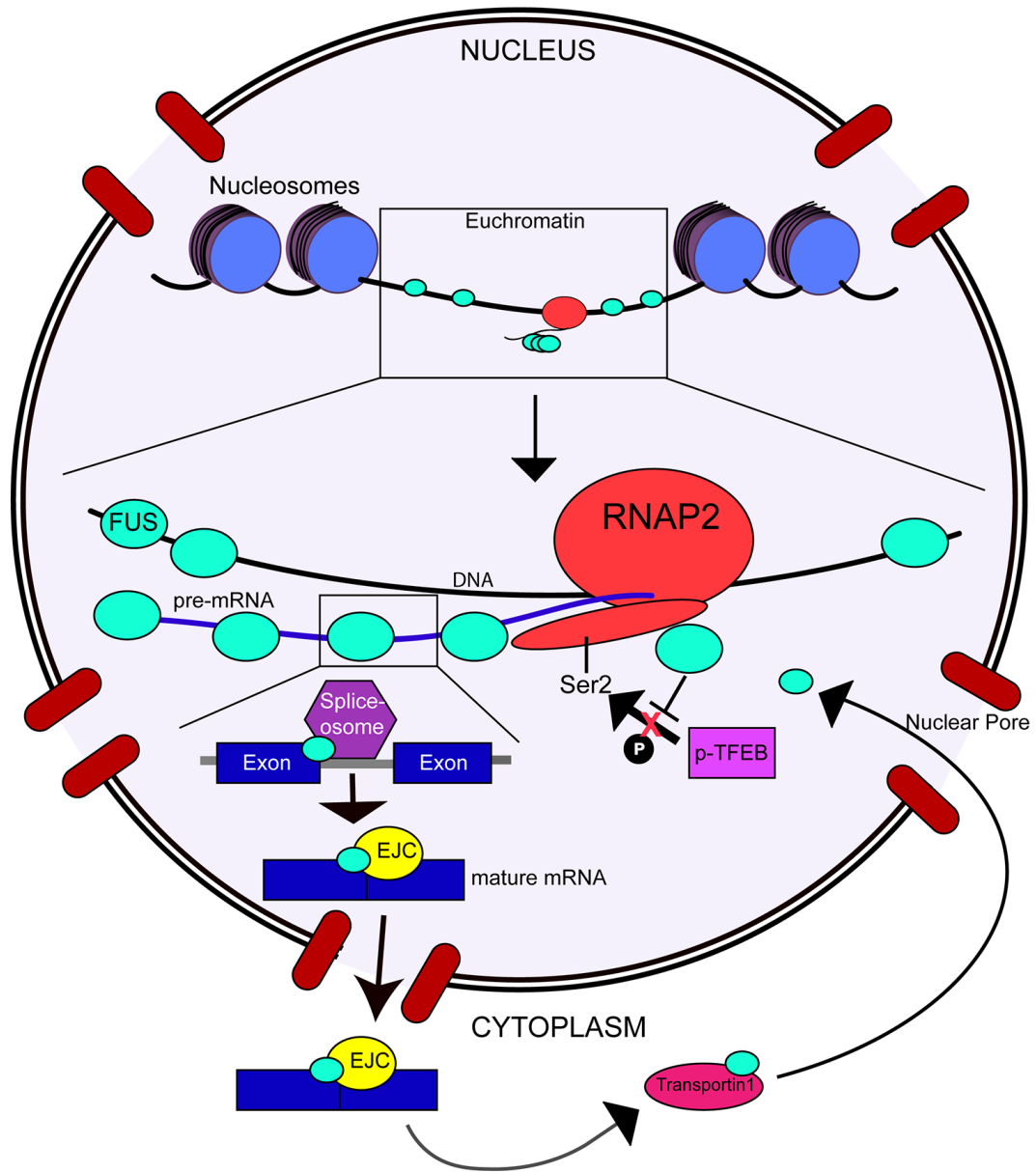


Figure 1.2 FUS Nuclear Functions

FUS binds transcriptionally active DNA directly, as well as on the C-terminal domain of RNAP2. When bound to RNAP2, FUS functions to prevent phosphorylation of Ser 2, preventing premature termination of transcription. FUS also binds pre-mRNA, facilitating formation of U1snRNP and SMN spliceosomal complexes. After splicing is complete, FUS

Figure 1.2 Continued

is exported from the nucleus on mRNA, into the cytoplasm. FUS dissociates from the mRNA, binds TNPO1, and is shuttled back into the nucleus.

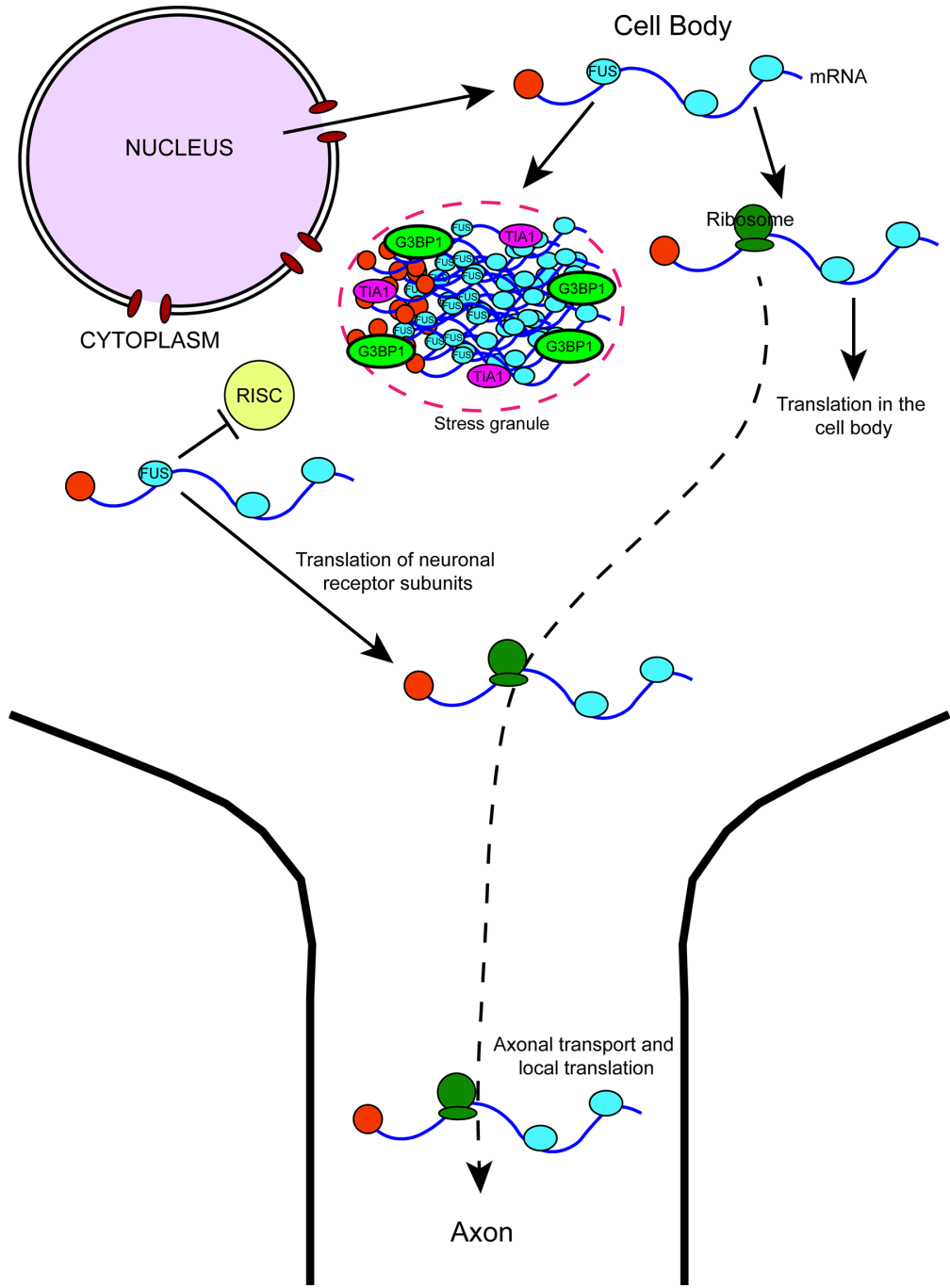


Figure 1.3 FUS' Cytoplasmic Function

FUS has several cytoplasmic functions related to maintenance and regulation of mRNA stability, and protein translation. FUS plays a role in stress granule dynamics, allowing for

### Figure 1.3 Continued

disassembly of the temporary structures once acute stress is resolved. FUS also plays an elusive role in regulation of translation and axonal protein biosynthesis. Additionally, FUS aids in preventing miRNA decay of cytosolic transcripts, facilitating expression of specific genes.

## CHAPTER 2. MATERIALS AND METHODS

### 2.1 Cell Culture, Plasmids, and Transfection

The HEK293T (293T) and N2a cells were cultured in Dulbecco's Modified Eagle's Medium (Sigma-Aldrich, D5796) with 10% fetal bovine serum and penicillin-streptomycin at 37 °C in 5% CO<sub>2</sub>/95% air. The SH-SY5Y cells were cultured in a 1:1 mixture of Dulbecco's Modified Eagle's Medium/F-12 Ham (Sigma-Aldrich, D8437) with 10% fetal bovine serum and penicillin-streptomycin at 37 °C in 5% CO<sub>2</sub>/95% air. The 293T cells were transfected with Polyethylenimine “Max” (Polysciences, Inc.). The SH-SY5Y and N2a cells were transfected with Lipofectamine 2000 (Life Technologies, 11668). The pCMV10 3X FLAG FUS and pEGFP-C3 FUS plasmids used were created for previous studies (72). The Polio IRES luciferase translation reporter construct was a generous gift from Dr. Tianyan Gao (84).  $\beta$ WT,  $\beta$ 39, GPX-1 WT, and GPX-1 PTC NMD reporters were a gift from Dr. Jens Lykke-Andersen.

### 2.2 Culture and Transfection of Primary Cortical Neurons

The mouse primary cortical neuron cultures were prepared as reported (85). Briefly, neonatal mouse pups (strain C57BL/6, Jackson Laboratory) were sacrificed via decapitation within 24 h of birth. The cells were maintained in Neurobasal Medium (Life Technologies, 21103049) with B27 supplement (Life Technologies, 17504044), l-glutamine and penicillin/streptomycin. Neurons were dissociated from glial cells using pipette lavage after incubation with trypsin. The cells were treated with 5-Fluoro-2'-deoxyuridine (Sigma-Aldrich, F0503). Fourteen days after 5-Fluoro-2'-deoxyuridine treatment, the primary neurons were transfected with EGFP-tagged WT or P525L mutant

FUS expression constructs using Lipofectamine 2000 (Life Technologies, 11668). The primary neurons were fixed 48 h post-transfection for immunofluorescence.

### 2.3 GST-FUS Pull-Downs

The GST-FUS pull-downs were performed similarly as reported before (72). Briefly, the wild type, R521G or P525L mutant human FUS coding sequences were inserted into the pEBG glutathione S-transferase (GST) fusion vector (86) using the BamHI and KpnI sites. pEBG was a gift from Dr. David Baltimore (Addgene plasmid # 22227). 293T cells were transfected with the GST-FUS constructs. Two days post-transfection, cell lysates were prepared in  $1 \times$  RIPA buffer (Millipore, 20-188) supplemented with protease inhibitor cocktail (Sigma, P-8340, 1:500) and 1 mM sodium orthovanadate with syringe homogenization. The lysates were pre-cleared with Sepharose CL-4B (Sigma, CL4B200), then subjected to overnight pull-down with Glutathione Sepharose 4B (GE Healthcare, 17-0756-01). Where indicated, a cocktail of RNase A and RNase T1 (Life Technologies, AM2286) was added to the pre-cleared lysates before the pull-down at 1:100 dilution. The bound proteins were eluted by boiling with Laemmli sample buffer (Bio-Rad, 161-0737).

### 2.4 Immunoprecipitation

Cellular extracts of SH-SY5Y or N2a cells were prepared in  $1 \times$  RIPA buffer (Millipore, 20-188) supplemented with protease inhibitor cocktail (Sigma, P-8340, 1:500) and 1 mM sodium orthovanadate with syringe homogenization. The cellular lysates were first pre-cleared with Protein G UltraLink Resin (Thermo Scientific Pierce, 53126), then

incubated with antibody against bait protein (Santa Cruz, sc-47711) and Protein G UltraLink Resin overnight. The negative control immunoprecipitation antibody was mouse anti-HA (Santa Cruz, sc-7392) or normal goat serum. The bound proteins were eluted by boiling with Laemmli sample buffer (Bio-Rad, 161-0737) or eluted using FLAG peptide.

## 2.5 Proteomic identification of FUS interaction partners

The proteins eluted from the Glutathione Sepharose 4B beads were resolved by denaturing polyacrylamide gel electrophoresis (SDS-PAGE) on 4–15% gradient gel, followed by staining with Sypro Ruby protein gel stain (Molecular Probes, S-12000). Each lane was cut into 20 slices of equal size and each slice was subjected to in-gel trypsin digestion (87). The resulting tryptic peptides were extracted and subjected to liquid chromatography-tandem mass spectrometry (LC-MS/MS) using an LTQ Orbitrap Velos mass spectrometer (Thermo Scientific). The LC-MS/MS results were processed with a local Mascot server (version 2.3, Matrix Science) for protein identification including methionine oxidation and cysteine carbamidomethylation as allowed side chain modifications. The LC-MS/MS data of the 20 slices were combined for protein identification using the MASCOT algorithm. False discovery rate of 1% was used in decoy search for the high-confidence peptides. Proteins with a score of at least 30 for single high-confidence peptides were considered positive identifications. MS/MS spectra of high-confidence peptides with scores lower than 50 were manually inspected and confirmed. UniProt protein names and identifier numbers are used throughout this work (88).

## 2.6 Western Blot

The nitrocellulose membranes were blocked, and antibodies were applied in 5% milk in TRIS-buffered saline/Tween-20 (TBST, 0.1 M TRIS-HCl, 0.9% [w/v] NaCl, 0.1% [v/v] Tween-20, pH 7.5). The antibodies used were anti-NF45/ILF2 (Bethyl, A303-147A-M), anti-DHX9 (Bethyl, A300-855A-M), anti-Matrin-3 (Bethyl, A300-591A-M), anti-hnRNPA1 (Novus, NB100-672), anti-Caprin-1 (Proteintech, 15112-1-AP), anti-GST (Santa Cruz, sc-459), anti-DDX3X (Sigma, HPA001648), anti-actin (Santa Cruz, sc-1616), anti-FLAG (Sigma, A8592.), anti-eIF4A1 (Cell Signaling, 2490), anti-eIF4G (Cell Signaling, 2469), anti-eIF4E (Cell Signaling, 9742), anti-eIF3 (Santa Cruz, sc-74507), anti-eIF4A3 (ProteinTech, 17504-1-AP), anti-RPS6 (Cell Signaling, 2217), anti-G3BP1 (ProteinTech, 13051-2-AP), anti-RPL7a (Cell Signaling, 2415), anti-K48 TUBE (Tandem Ubiquitin Binding Entity, LifeSensors, UM305), anti-K63 TUBE (LifeSensors, UM304), anti-pan ubiquitin (Santa Cruz, sc8017), anti-HA (Santa Cruz, sc-805), anti-UPF1 (Bethyl, A300-038A), anti-phospho Ser/Thr 4 ATM/ AMR substrate (i.e. p-S/T, Cell Signaling, 2851), anti-phospho UPF1 S1089 (Millipore 07-1015), anti-PABP1 (Santa Cruz, sc-32318), anti-eRF3b (Santa Cruz, 515615), anti-BrdU (Abcam, ab6326), anti-p62 (ProteinTech, 18420-1-AP) anti-Actin (Santa Cruz, sc-81178), antiGAPDH (Santa Cruz, sc-32233), anti-puromycin (Millipore, MABE343), anti-UPF3a (Proteintech, 17114-1-AP), anti-XRN1 (Bethyl, A300-443A-M), Anti-UPF3b (Invitrogen, PA5- 51652), anti-SMG6 (Abcam, ab87539), anti-SMG1 (Abcam, ab30916), anti-SMG5 (ThermoFisher, PA5-44295), anti-SMG7 (ThermoFisher, PA5-38140), anti-RNPS1 (PA5- 35967), and anti-FUS (Santa Cruz, sc-47711). The immunoblotting images were acquired with the



Chemidoc MP Imaging System (Bio-Rad) and quantified with the Image Lab software (Bio-Rad).

## 2.7 Immunofluorescence microscopy

SH-SY5Y or N2a cells were seeded on gelatin-treated glass coverslips and transfected with EGFP-tagged FUS constructs (72). After 48 hours, the cells were fixed in 4% (w/v) paraformaldehyde in  $1 \times$  PBS, permeabilized with 0.25% (v/v) Triton X-100 in  $1 \times$  PBS and blocked with 10% (w/v) bovine serum albumin (BSA) in  $1 \times$  PBS. The slides were incubated with primary antibodies diluted in 3% (w/v) BSA/ $1 \times$  PBS. The primary antibodies were the same as those used for immunoblotting. The secondary antibodies were Alexa Fluor 568 Donkey Anti-Rabbit IgG or Alexa Fluor 568 Donkey Anti-Mouse IgG (Life Technologies, A10042 and A10037, respectively). The nuclei were visualized with 4',6-diamidino-2-phenylindole (DAPI). The coverslips were mounted on glass slides with Vectashield Mounting Medium (Vector Laboratories, H-1000-10). Confocal microscopic images were acquired using a Nikon A1 confocal microscope with a  $60 \times$  objective.

## 2.8 Patient Skin Fibroblast Culture

Human skin fibroblasts were prepared and maintained as previously described (89). Briefly, a skin punch was obtained from consenting patients with symptomatic ALS and family members free of disease. Brief information on the subjects is shown below. The biopsies were washed in phosphate-buffered saline (PBS), minced, and incubated in fibroblast growth media (MEM [Sigma-Aldrich, M5650]) supplemented with 20% FBS, 2 mM L-glutamine, 100 unit/mL penicillin, and 100  $\mu$ g/mL streptomycin at 37°C under 5%

3 CO<sub>2</sub>/95% air. Informed consent was obtained from all participants who donated a skin biopsy. Information on the 11 subjects (five patients with familial ALS with the R521G mutation, one patient with the P525R mutation, and five healthy controls with WT FUS) is shown in Table 2.1. The study was approved by the Institutional Review Board of the University of Kentucky.

## 2.9 Membrane Filtration

N2a cells were transfected with 3X FLAG FUS construct. After 48 hours, the cells were lysed in either RIPA buffer (Millipore, 20-188) or a hypotonic lysis buffer (20 mM HEPES (pH 7.4), 2 mM EGTA, 2 mM MgCl<sub>2</sub>: Cold Spring Harbor Laboratory). The lysates were centrifuged at 20,000xg and the supernatant removed. The protein concentrations were measured. Hydrophilic PVDF membranes (ThermoFisher, 88518) were applied to the BioRad Dot Blot Filtration Manifold (1706545) and the wells were rinsed with ACN. 100ug of protein lysate was applied to each well and vacuum pressure was applied. The wells were washed with lysis buffer three times and the membrane removed for either western blotting using anti-FLAG antibody (Sigma-Aldrich, A8592) or mass spectrometric analysis.

## 2.10 Native Gel Electrophoresis

Cells were harvested with RPIA or hypotonic low detergent lysis buffer and homogenized by either passing through a 23-gauge needle. Cell lysates were centrifuged at 20,000 × g at 4 °C for 10 min. The supernatant (50 μL) was taken out and mixed with 10 μL 6× loading buffer (350 mM Tris·Cl, pH 6.8, 30% (vol/vol) glycerol, 0.24% SDS,

0.02% bromophenol blue). Samples were loaded on a 6% (wt/vol) polyacrylamide gel soaked in detergent-free running buffer (25 mM Tris, 192 mM glycine). A total of 75 V was applied for stacking and 120 V was applied for separating. Subsequently, the gel was incubated with transfer buffer (25 mM Tris, 192 mM glycine, 10% (vol/vol) methanol) supplemented with 0.25% SDS at 70 °C for 10 min. After the denaturation step, the gel was ready for transferring and Western blotting following the same procedure as described earlier.

#### 2.11 Proteomic identification of proteins captured by membrane filtration

The membrane dots were subjected to trypsin digestion and the resulting tryptic peptides were subjected to liquid chromatography-tandem mass spectrometry (LC-MS/MS) as previously described in (2.V). False discovery rate of 1% was used in decoy search for the high-confidence peptides. Proteins were considered significant identifications if they met the following criteria: 1) the proteins had at least one unique peptide; 2) the identified protein had a score above 36; 3) they were unique in any of the samples.

#### 2.12 Enrichment Analysis of proteins captured by membrane filtration

Proteins identified in FUS inclusions were subjected to functional enrichment analysis using an integrative online enrichment analysis tool Enrichr (90, 91) that allows the examination of protein lists using a variety of libraries. Using the mouse exome as the universe for the enrichment, proteins were analyzed based on their function using the GO:

Molecular Function database (92, 93) and their disease relevance using the DISEASES database (94).

### 2.13 RNA FISH

N2a cells or primary neurons were transfected with EGFP-C3 FUS constructs and fixed with 4% w/v paraformaldehyde (Pierce, 28908) 48 hours post transfection. Cells were then permeabilized with 0.25% (v/v) Triton X-100 in 2x saline-sodium citrate (SSC) buffer (Invitrogen, AM9763) and blocked in Salmon sperm DNA in 2X SSC for one hour. Slides were incubated with 1ug/uL stock diluted 1:1000 oligo d(T)21 or anti-FUS (exon 4) probe for one hour at 37°C and then washed three times with 4x SSC and 3x with 2x SSC. The anti-FUS probe was generated by amplifying FUS exon 4 mRNA and was inserted into a pCRII-TOPO vector (ThermoFisher, 452640) for in vitro transcription. The anti-FUS probe was made using ThermoFisher FISH Tag RNA Multicolor Kit nuclei (ThermoFisher, F32956). Nuclei were visualized using DAPI. Coverslips were mounted on glass slides using Vectashied Mounting Media (Vector Laboratories, H-1000-10) and confocal images were acquired using a Nikon A1 confocal microscope.

### 2.14 RNA Immunoprecipitation followed by qPCR

To measure mRNA bound with protein of interest, immunoprecipitation was performed as described above. One difference is that SUPERaseIn (ThermoScientific; AM2696) was included in the RIPA buffer along with protease inhibitors. After immunoprecipitation, the bead slurry was split into two aliquots. One was for protein elution and immunoblotting as described above. The other was transferred to a new tube

for RNA isolation using Trizol reagent per manufacturer instructions. Equal amounts of isolated RNA were used for cDNA synthesis using the SuperScript III First Strand Synthesis System (ThermoScientific; 18080051). qPCR was performed using SYBR Green (ThermoScientific; 4309155) and quantitative results were obtained using the  $\Delta\Delta CT$  method. Primers used in this study are listed in Table 2.2.

### 2.15 Protein Translation Assays

For the Cap-dependent translation reporter assay: Protein translation efficiency was measured using a cap-dependent translation reporter assay as previously described (84). Briefly, N2a cells were transfected with the reporter plasmid along with empty vector, WT or mutant FUS. After 48 hours, cells were harvested and lysed followed with luminescence measurement using the Promega luciferase assay kit (Promega, E2940). The cap-dependent Renilla luciferase activity was compared to that with empty vector. The Firefly luciferase activity was used as a transfection control.

For the 35S-Met incorporation assay: N2a cells were transfected with 3X FLAG FUS and after 48 hours incubated with 1 $\mu$ M puromycin (P8833, Sigma) for thirty minutes. Cells were washed with PBS to remove residual puromycin. Cells were lysed using 1x RIPA buffer and centrifuged at 1,000xg. Lysates were then run on an SDS-PAGE gel and transferred to a nitrocellulose membrane for western blotting with anti-puromycin antibody (Millipore, MABE343). Puromycin staining in lanes was measured using Bio-Rad imaging software and normalized to actin.

For the SUnSET Assay: N2a cells were transfected with 3X FLAG FUS and after 48 hours and lysed in water. Lysates were syringe homogenized and centrifuged at 1,000xg to remove cellular debris. Lysate was then incubated with rabbit reticulocyte lysate, ATP, and <sup>35</sup>S-Methionine. The mixture was incubated at 37°C for one hour. We then precipitated the protein to remove excess <sup>35</sup>S-Methionine and took the beta particle count on the scintillation counter.

#### 2.16 7' Methyl-guanosine Pulldown

N2a cells were transfected with 3X FLAG FUS and after 48 hours, lysed using 1x RIPA buffer. The lysate was spun at 1,000xg and precleared using Sepharose beads (Sigma-Aldrich, CL4B200). After preclearing, the lysates were incubated with 7' Methyl-guanosine residues conjugated to agarose beads and incubated at 4°C overnight (JenaBiosciences, AC-155S). Beads were washed three times and the bound proteins were eluted by boiling with Laemmli sample buffer (Bio-Rad, 161-0737). Eluates were run on SDS-PAGE gels.

#### 2.17 Bromouridine Immunoprecipitation

N2a cells were transfected with 3X FLAG FUS and after 24 hours incubated with 1µM bromouridine (BrU) (Sigma Aldrich, 850187) for 24 hours. Cells were washed with PBS to remove residual BrU. Protein and RNA were crosslinked using a StrataLink Crosslinker (254nm, 1200kJ). Cells were lysed using 1x RIPA buffer and centrifuged at 1,000xg. Crosslinked lysate was incubated with anti-bromodeoxyuridine to immunoprecipitate RNA and Protein G UltraLink Resin (Thermo Scientific Pierce, 53126)

overnight at 4°C. Beads were washed three times and the bound proteins were eluted by boiling with Laemmli sample buffer (Bio-Rad, 161-0737). Eluates were run on SDS-PAGE gels followed by immunoblotting.

### 2.18 NMD Activity Assays

For the NMD Reporter Assay: N2a cells are co-transfected with 3X FLAG FUS and pcDNA NMD reporter ( $\beta$ -globin WT,  $\beta$ -globin PTC39, GPX-1 WT, GPX-1 PTC) that were previously reported (10). Cells were harvested 48 hours after transfection and RNA was extracted using Trizol, purified of plasmid using RQ1 RNase free DNase (Promega, M6101), purified again using a phenol/chlorophorm method, and subjected to qPCR.

For the Endogenous NMD substrate qPCR: Trizol reagent was used to isolate RNA from N2a cells or fibroblasts per manufacturer instructions. Equal amounts of isolated RNA were used for cDNA synthesis using the SuperScript III First Strand Synthesis System (ThermoScientific; 18080051). qPCR was performed using SYBR Green (ThermoScientific; 4309155) and quantitative results were obtained using the  $\Delta\Delta CT$  method.

### 2.19 RNA Stability Assay

N2a cells were transfected with 3x FLAG FUS constructs. After 48 hours, cells were treated with 1  $\mu$ M ActinomycinD (Sigma-Aldrich; A1410) for two or four hours, or DMSO for four hours for experiments examining UPF1, UPF3b, and UPF3a stability. The same concentration of ActinomycinD was used for examining the stability of ATF3, ATF4,

TBL2, and CyclophilinD, but a time course of one, two, or three hours, or three hours with DMSO was used. RNA was isolated using Trizol as described above and subject to qPCR.

## 2.20 Statistics

Western blot band and lane quantification was done using BioRad Imaging Software. In assays using patient fibroblasts, mutant band intensity ratios were pooled into one group. ANOVA with post hoc Tukey HSD (honest significant difference) test was used to determine p values for multiple pair-wise comparisons. Student's t test (two-tailed distribution, two-sample unequal variance) was used to determine p values for simple pair-wise comparison. Authors were not blinded to control or experimental groups. All experiments, except immunofluorescent assay, were done in triplicate.



Table 2.1 Patient Fibroblasts

ID Group	ID Group	FUS Genotype	Gender	Age at Biopsy
017	Control	WT	F	43
010	Control	WT	F	36
012	Control	WT	F	63
008	Control	WT	F	24
089	Control	WT	M	20
091	ALS	R521G	F	31
001	ALS	R521G	M	56
014	ALS	R521G	M	42
007	ALS	R521G	M	58
018	ALS	R521G	F	40
090	ALS	P525R	F	26

Table 2.2 List of qPCR Primers

GENE	FORWARD	REVERSE
MOUSE UPF1	AGAGCAGCCTGAAGGACATC	TCCAGCTTGTTGATCTGCTG
MOUSE UPF3B	GAGTGACCCTGTTTACGCC	TCAAAGTGGGAGGTAATCTTCG
MOUSE UPF3A	ATGCGCTCGGAAGAGG	CTACTGGGCCTTGTGTCC
MOUSE FUS (EXON 4)	CCAGGGATATGGTTCCACTG	CTGCTAGGAGCTGGCTGTTG
MOUSE ATF3	ATAAACACCTCTGCCATCGG	GCCTCCTTTTCCTCTCATCTTC
MOUSE ATF4	GGTTCTCCAGCGACAAGG	GCATCGAAGTCAAACCTTTTCAG
MOUSE TBL2	TCCACGATCAACACTAACCAG	CGAAACAGACCTCCCAGAC
MOUSE CYCLOPHIIN D	CCCTCCAACCTCCAAGAACC	TTCTCCTGTACACAACGCAC
MOUSE RPL13A	CTGTGAAGGCATCAACATTTCTG	GACCACCATCCGCTTTTCTT

HUMAN UPF1	AGAGCAGCCTCAAGGACATC	TCCAGCTTGTTGATCTGCTG
HUMAN UPF3B	GTTTCATATCCCGTTCCTCTC	TGCCCAAGCGTTCTGATAG
HUMAN UPF3A	TCCAGCTTGTTGATCTGCTG	GGCAATCTTCTGGAATGGAG
HUMAN ATF3	GTTTGCCATCCAGAACAAGC	GTCGCCTCTTTTTCCTTTCATC
HUMAN ATF4	CCAAGCACTTCAAACCTCATG	ATCCATTTTCTCCAACATCCAATC
HUMAN TBL2	AATATCAGCGGATTCGGAAGG	ACAGGTAGCCAGGTATTTGC
HUMAN B- ACTIN	AGAGCTACGAGCTGCCTGAC	GGATGTCCACGTCACACTTC
NMD REPORTER:  HUMAN B- GLOBIN	AGGAGAAGTCTGCCGTTACT	GAGCCAGGCCATCACTAAAG
NMD REPORTER:  RAT GPX-1	GGGACTACACCGAAATGAATGA	GGACAGCAGGGCTTCTATATC

## CHAPTER 3. PROTEOMIC ANALYSIS OF FUS INTERACTING PROTEINS PROVIDES INSIGHTS INTO FUS FUNCTION AND ITS ROLE IN ALS

*Modified from the manuscript “Proteomic analysis of FUS interacting proteins provides insights into FUS function and its role in ALS”, published in the Biochimica et biophysica acta. 2016;1862(10):2004-14. Epub 2016/07/28. doi: 10.1016/j.bbadis.2016.07.015. PubMed PMID: 27460707; PMCID: PMC5055831. The introduction was simplified for fluidity and experiments not performed by M.K were excluded.*

### 3.1 Introduction

Amyotrophic lateral sclerosis (ALS), also known as Lou Gehrig's disease, is a progressive and ultimately fatal neurodegenerative disease of the upper and lower motor neurons of the brain and spinal cord. At any given time, approximately 30,000 people in the United States are living with the disease (95). There is currently no cure available for those afflicted (96). General symptoms of ALS are muscle weakness and wasting triggered by the degeneration of motor neurons. In order to develop effective preventive measures or cures, we have to gain a better understanding of the molecular etiology of the disease.

Approximately 10% of the ALS cases are familial (fALS) and caused by heritable mutations in a number of different genes. A subset of fALS cases is caused by autosomal dominant mutations in the gene encoding Fused in Sarcoma/Translocated in Liposarcoma (FUS/TLS) (2, 3). FUS mutations were also identified in a subset of the sporadic ALS (sALS) cases (97-99). In most tissues, FUS is predominantly localized to the nucleus with a notable cytoplasmic presence in neurons (100). FUS has several known functions in

multiple cellular pathways. FUS binds RNA and shuttles between the nucleus and the cytoplasm, participating in nucleo-cytoplasmic RNA shuttling (101). FUS also plays roles in DNA repair (102-104), transcription (13, 20, 33, 61, 105-111), RNA splicing (20, 112, 113), dendritic RNA transport (114-116), and miRNA biogenesis and function (78, 117). However, the physiological functions of FUS are still not fully understood. The ALS-related FUS mutations cause varied degrees of cytoplasmic mis-localization of FUS and the formation of stress granule-like structures (12, 62, 63, 72). In a subset of frontotemporal dementia cases, pathological cytoplasmic mis-localization of FUS was found without FUS mutations (118, 119). The depletion of FUS in the nucleus likely results in partial loss of its nuclear function(s). In addition, its cytoplasmic accumulation and the formation of stress granule-like structures and other ribonucleoprotein complexes might lead to a gained toxicity phenotype. These loss-of-function and gain-of-function/gain-of-toxicity mechanisms are both plausible and are not mutually exclusive (40, 120).

To gain insight into the normal functions of FUS and the pathogenesis caused by its mutations, we performed GST-FUS pull-downs from human cells expressing wild-type and R521G mutant FUS, followed by proteomic identification of the FUS interacting partners. In addition to previously reported interacting proteins, many novel interacting partners were identified in this study, including members of the spliceosome, IMP1-dependent ribonucleoprotein particles, transport RNA granules and stress granules. Many of the identified interacting partners are shared between two or more of these ribonucleoprotein particles. We selected a set of the identified FUS interacting partners that participate in a wide range of functions for further analysis. We validated the interaction of FUS with the selected partners and determined the RNA dependence of those

interactions. We found that the interactions of FUS with some partners were enhanced, whereas with others were partly or completely abrogated by RNase digestion. Importantly, we found that FUS interacted with hnRNPA1 and Matrin-3, proteins whose mutations were also identified to cause familial ALS (121, 122). We found that ALS mutants of FUS co-localized with Caprin-1, DDX3X, and DHX9 in cytoplasmic inclusions that could lead to the mis-regulation of their respective pathways, providing further clues to the mechanism of ALS pathogenesis.

## 3.2 Results

### 3.2.1 Identification of FUS interaction partners

We generated GST-FUS expression constructs using the pEBG vector that expresses the glutathione *S*-transferase (GST) gene of *Schistosoma japonicum* under control of the human EF-1 $\alpha$  promoter (86). We performed GST pull-downs from human HEK293T (293T) cells transfected with wild-type (WT) or R521G mutant GST-FUS or the GST vector. The GST-FUS pull-downs were performed both in the presence and absence of added RNase in the cellular lysates. SDS-PAGE revealed major banding pattern differences between the GST vector control and the GST-FUS lanes (Fig. 3.1). Proteins that were identified in the vector lane (several human glutathione *S*-transferases and other proteins) and common contaminants such as keratin, heat shock proteins and abundant cytoskeletal components were excluded from the analysis of the GST-FUS lanes. It is noted that no endogenous FUS was identified in the GST vector control lane, suggesting that the endogenous FUS did not bind non-specifically to the Glutathione Sepharose 4B beads.

We identified the FUS interacting proteins using the Mascot software (Matrix Science). Mascot uses probability-based scoring to judge whether identifications are significant. The peptide score shows the probability of whether the observed match is a random event. Scores are reported as  $-10 \times \log_{10}(P)$ , where P is the probability. For example, a Mascot score of 30 means that the probability of a peptide identification being a random event is 0.001. The protein score is calculated from the scores of the individual peptides. A total of 112 proteins were identified as FUS-interacting partners in this study. Among them, 70 were non-ribosomal proteins (Supplemental Table 3.1) and 42 were ribosomal proteins (Supplemental Table 3.2). The count of the peptides identified at high confidence level (false discovery rate < 1% in decoy search) is shown in the tables, and only proteins identified with a compounded score of 30 or higher are listed. The MS/MS spectra of high-confidence peptides with scores lower than 50 were manually inspected and confirmed. Proteins identified with these parameters are considered highly confident identifications.

### 3.2.2 Validation and characterization of selected FUS interactions

We demonstrated the co-precipitation of endogenous DHX9, Matrin-3, ILF2 and hnRNPA1 with endogenous FUS immunoprecipitated from SH-SY5Y cells (Fig. 3.2). We also validated the interaction of FUS with endogenous DHX9, Matrin-3, DDX3X, Caprin-1, ILF2 and hnRNPA1 in 293T cells using GST-FUS pull-down followed by immunoblot with specific antibodies (Fig. 3.3A–B, lanes 1 and 3). We determined whether the interactions of FUS with the above proteins depended on RNA. Cells were transfected with GST vector or GST-tagged WT, R521G or P525L FUS expression constructs and the cell

lysates were subjected to GST pull-down either with or without the addition of RNase (Fig 3.3A). The precipitation of the baits was verified with anti-GST immunoblot (Fig. 3.3B). The immunoblots of the co-precipitating proteins were quantified from three independent experiments (Fig. 3.3C). The binding of FUS to its interaction partners was differentially affected by RNase treatment (Fig. 3.3A and C). The amounts of the co-precipitated Matrin-3 and that of the RNA helicases DHX9 and DDX3X were significantly enhanced by RNase treatment. The interactions of FUS with Caprin-1 and ILF2 were weakened, but not fully abrogated, by the RNase treatment. The interaction of FUS with hnRNPA1 was entirely dependent on RNA, as the RNase treatment completely abolished its interaction with FUS. Thus, the interactions of FUS with DHX9, Matrin-3 and DDX3X are likely protein-protein interactions that do not require RNA, whereas the interactions with Caprin-1, ILF2, and hnRNPA1 are partly or fully RNA-dependent.

### 3.2.3 Co-localization of FUS interaction partners with cytoplasmic ALS mutant FUS inclusions

We tested whether the selected interaction partners co-localized with cytoplasmic inclusions of mutant FUS in the SH-SY5Y human neuroblastoma cell line transfected with EGFP-tagged WT, R521G or P525L FUS. We found that EGFP-tagged WT FUS localized to the nuclei of SH-SY5Y cells. The localization of R521G mutant FUS ranged widely from mostly nuclear to mostly cytoplasmic. The localization of P525L FUS was even further shifted towards the cytoplasm. Both the R521G and the P525L FUS mutants formed cytoplasmic inclusions (Fig. 3.4). The DHX9 protein was primarily localized to the nuclei of SH-SY5Y cells sharing a similar distribution pattern with that of nuclear FUS (Fig.



3.4A). The expression of both R521G and P525L FUS resulted in the accumulation of small amounts of DHX9 in cytoplasmic mutant FUS inclusions (Fig. 3.4A). The DDX3X protein was mostly localized to the cytoplasm (Fig. 3.4B). DDX3X was efficiently sequestered by the cytoplasmic inclusions of both R521G and P525L mutant FUS (Fig. 3.4B). We had similar observations with the mostly cytoplasmic CAPR1/Caprin-1. The expression of R521G and P525L FUS induced the formation of cytoplasmic Caprin-1-positive inclusions, most of which co-localized with the mutant FUS inclusions (Fig. 3.4C). We also demonstrated the co-localization of DHX9, DDX3X and Caprin-1 with cytoplasmic EGFP-P525L mutant FUS inclusions in primary cortical neurons (Fig. 3.5)

The co-localization of DHX9, DDX3X and Caprin-1 with mutant FUS inclusions was quantified in SH-SY5Y cells transfected with EGFP-tagged P525L mutant FUS in four independent experiments, each representing over 400 transfected cells. On average, 24.5% of the transfected cells contained cytoplasmic P525L mutant FUS inclusions. DHX9 co-localized with 89.7%, DDX3X with 97.9%, and Caprin-1 with 88.7% of the cytoplasmic P525L mutant FUS inclusions, respectively.

The FUS interaction partners Matrin-3 and hnRNPA1 were localized to the nuclei of SH-SY5Y cells and were not detected in cytoplasmic mutant FUS inclusions (Fig 3.6A–B). The ILF2 protein was primarily in the nuclei and was not detected in cytoplasmic mutant FUS inclusions, either (Fig. 3.6C). These results suggest that the detected complexes of FUS with Matrin-3, hnRNPA1, and ILF2 were likely nuclear that will be explored in future studies.

### 3.2.4 Significantly enriched Gene Ontology (GO) terms among the identified FUS interacting partners

We searched for significantly enriched GO terms for the identified FUS interacting partners using the STRING server (<http://www.string-db.org/>, (123)). The enriched GO Biological Processes, Molecular Functions and Cellular Components of FUS interacting partners are summarized in (Tables 3.3- 3.5), respectively. The p-values shown in the tables are Benjamini-Hochberg corrected p-values for enrichment of the terms in question, representing the estimated false discovery rate (124).

Based on the GO Biological Processes, the majority of significantly enriched terms were related to various aspects of gene expression and RNA metabolism, such as chromosomal organization, transcription, RNA splicing, RNA processing, RNA transport, translation and RNA stability (Table 3.1). Based on the GO Molecular Functions, the majority of the identified FUS interaction partners are RNA and/or DNA binding proteins with a considerable enrichment for RNA helicases (Table 3.2). The FUS interacting partners CN166, CTR9 and ZN326 represent three of the 21 UniProt entries annotated with the significantly enriched GO Molecular Function “RNA polymerase II core binding” (Table 3.2). Among the significantly enriched GO Cellular Components were various ribonucleoprotein complexes including ribosomes, splicing complexes, the SMN-Sm protein complex and cytoplasmic stress granules (SGs). Also enriched were chromosomal proteins and components of extracellular exosomes (Table 3.3).

### 3.2.5 FUS interacts with overlapping ribonucleoprotein complexes

Our analysis showed that the majority of the identified non-ribosomal FUS interaction partners (Supplemental Table 3.1) are known members of at least one of four types of ribonucleoprotein complexes: spliceosomes, IMP1-dependent ribonucleoprotein (RNP) granules, transport granules or stress granules (Fig. 3.7). In Fig. 3.7, only the FUS-interacting ribosomal proteins that were specifically identified as part of the above complexes are shown.

This study identified the following FUS-interacting proteins that were previously identified as spliceosomal components: ROA1/hnRNPA1, ROA2/hnRNPA2B1, ROA3/hnRNPA3, HNRPC/hnRNPC, RBMX/hnRNPG, HNRH1/hnRNPH, HNRPK/hnRNPK, HNRPM/hnRNPM, HNRPR/hnRNPR, HNRPU/hnRNPU, PABP1, RSMB/SNRPB, SMD1, SMD3, RUXE/SNRPE, SF3B1, SF3B3, U520/SNRNP200, SK2L2, DDX5 and ZCHC8 (125), and SR140 and SRSF7 (126, 127). In addition, FUS-interacting proteins are involved in a tRNA splicing ligase complex that is not part of the spliceosome: RTCB/HSPC117, CN166/CGI-99 and DDX1 (128).

Another group of FUS interacting proteins identified in this study belong to the IMP1-dependent mRNP granules. They include: DHX9, HNRPU/hnRNPU, NUCL/Nucleolin, PABP1, ILF2, ILF3, HNRPR/hnRNPR, PABP4, ROA1/hnRNPA1, ROA2/hnRNPA2B1, RLA0, RS3, RS3a, RS4X, RS6, RS8 (129), as well as HNRPK/hnRNPK, ROA3/hnRNPA3, and ELAV1/HuR (130).

The third group of our identified FUS-interacting proteins contains components of RNA transporting granules. DDX1, DDX3X, DDX5, RTCB/HSPC117, CN166/CGI-99, FMR1, FXR1, RL3, ROA1/hnRNPA1, HNRPU/hnRNPU, and NUCL are components of a FUS-positive kinesin-mediated RNA transporting dendritic granule complex (131). Moreover, the DHX9, FMR1, HNRPU/hnRNPU, ILF3, NUCL, PABP1, RLA0, RL6, RL7A, RL10, RL14, RS2, RS3A, RS6, and RS8 proteins identified in this study were reported as components of Staufen-containing transport ribonucleoprotein complexes (132, 133). In addition, ROA2/hnRNPA2 (134) and CAPR1/Caprin-1 (74) were also identified in RNA transport granules.

The fourth group among our identified FUS-interacting proteins belongs to stress granules. They include ATX2L, CAPR1/Caprin-1, DDX1, DDX3X, DDX6, DHX36/RHAU, ELAV1/HuR, FMR1, FXR1, G3BP2, ROA1/hnRNPA1, ROA2/hnRNPA2, HNRPK/hnRNPK, ILF3, PABP1, RS3, RS6, RS18, RBP56/TAF15 and PABP4 (73, 135). Moreover, the two FUS-interacting proteins DDX6/RCK and MOV10 are components of processing bodies (P-bodies) (136-138) that functionally interact with stress granules (139). NPM, PARP1 and NUCL were identified as part of the SWAP complex, a B-cell-specific DNA recombination complex (140).

NPM, PARP1 and NUCL were identified as part of the SWAP complex, a B-cell-specific DNA recombination complex (140).

### 3.3 Discussion

#### 3.3.1 Identification and validation of FUS interaction partners

We identified 70 non-ribosomal and 42 ribosomal proteins as FUS interaction partners in this study (Fig. 3.1 and Fig. 3.6). No endogenous FUS was identified in the GST vector control pull-down. Proteins identified in the GST vector control experiment were excluded from the analysis of the GST-FUS pull-downs. Most FUS interaction partners we identified are known RNA and DNA binding proteins (Table 3.1) involved in pathways regulating various aspects of gene expression and RNA metabolism including transcription, splicing, RNA processing, RNA stability, RNA transport and translation (Table 3.1). Selected interactions were validated by immunoprecipitation and GST pull-down followed by immunoblotting (Fig. 3.2, Fig. 3.3). Immunostaining followed by confocal microscopy showed that the FUS interaction partners DHX9, DDX3X and Caprin-1 localized to cytoplasmic FUS inclusions (Fig. 3.4, Fig. 3.5).

Our method to generate cellular lysates efficiently extracted not only cytosolic proteins but also predominantly nuclear proteins such as WT FUS, DHX9, Matrin-3 and hnRNPA1 (Fig. 3.2, Fig. 3.3, Fig. 3.4, Fig. 3.5, and Fig 3.6). In the pull-down studies, we detected interactions between proteins mostly residing in different cellular compartments such as the interactions between the predominantly nuclear WT FUS and the almost exclusively cytoplasmic DDX3X or Caprin-1 (Fig. 3.3, Fig. 3.4, Fig. 3.5). This observation demonstrates the significance of examining interacting proteins with imaging techniques in cells to determine whether the proteins interact with each other in live cells under physiological conditions.

Many FUS interacting partners participate in two or more of the ribonucleoprotein complexes shown in Fig. 3.7. Ribonucleoprotein complexes are highly dynamic structures that can exchange components and transition from one kind of complex to another. It is conceivable that FUS cycles between different molecular complexes and ribonucleoprotein granules depending on a number of cellular influences including subcellular localization and stress conditions.

### 3.3.2 The RNA dependence of FUS interactions

The identified interactions were differentially impacted by the introduction of RNase into the pull-down mixtures. Whereas the interactions of FUS with DHX9, Matrin-3 and DDX3X are likely protein-protein interactions that were enhanced by RNase digestion, the interactions of FUS with CAPR1, ILF2, and hnRNPA1 were partly or fully RNA-dependent (Fig. 3.3). It is likely that FUS molecules cycle between RNA-bound and RNA-unbound states as they interact with successive target RNA molecules. Our results showed that FUS displayed differential affinities to its protein interacting partners in the RNA bound and RNA-unbound states, suggesting that the protein interacting partners of FUS likely also change during the RNA binding cycles. RNase treatment can free up molecular surfaces for protein-protein interactions otherwise occupied by RNA. Alternatively, the RNA-bound and unbound states of FUS might assume different conformations, regulating the preference of FUS to varied interaction partners.

### 3.3.3 The interaction of FUS with the ALS-related proteins Matrin-3 and hnRNPA1

We discovered that FUS interacted with MATR3/Matrin-3 and ROA1/hnRNPA1 (Figs. 3.2, 3.3 and Supplemental Table 3.1), proteins whose mutations were also identified to cause familial ALS (121, 122). This suggests that FUS might be involved in common pathogenic pathways with Matrin-3 and hnRNPA1. There are intriguing differences between these complexes, though. The interaction between FUS and Matrin-3 was enhanced by RNase treatment, whereas the FUS-hnRNPA1 interaction was entirely dependent on RNA (Fig. 3.3). It is relevant that hnRNPA1 was reported to localize to stress granules (121, 141) similarly to FUS (10, 12, 62, 63, 72, 100, 142). The analysis of the role of the FUS-Matrin-3 and FUS-hnRNPA1 complexes in ALS pathogenesis is underway.

### 3.3.4 FUS interacts with regulators of protein phosphorylation

We identified the FUS interaction partners KHDR1, ILF2, ILF3 and RBMX/hnRNPG that were previously reported to be in a complex with the serine/threonine-protein phosphatase PP1- $\alpha$  catalytic subunit PP1A (Fig. 3.7) (143). The ILF2 and ILF3 proteins were also reported to interact with and regulate the DNA-dependent protein kinase (DNA-PK) (144). The phosphorylation of FUS by DNA-PK was recently reported (145). Our results suggest that the KHDR1/ILF2/ ILF3/RBMX complex might regulate FUS phosphorylation. FUS also interacted with CSK21, the catalytic alpha subunit of casein kinase II and the serine/threonine-protein kinase Nek10. The casein kinase II-mediated

FUS phosphorylation and its functional relevance are currently being investigated in our laboratory.

### 3.3.5 Loss of nuclear FUS functions due to ALS mutations

We found that FUS interacted with numerous proteins that regulate nuclear processes. Twenty-six of the FUS interacting partners we isolated were annotated as regulators of DNA-templated transcription (Table 3.1). Twenty-three of the FUS interaction partners we identified are known spliceosomal components (Table 3.1, Fig 3.7). The splicing-related “Survival motor neuron” (SMN)-Sm protein complex was also among the significantly enriched GO Cellular Components (Table 3.3). Additionally, the FUS interacting partners RTCB, CN166 and DDX1 are components of a tRNA splicing ligase complex that is not part of the spliceosome (Fig 3.8) (128). Although we did not identify FA98B/FAM98B, a fourth component of the tRNA splicing ligase complex as a FUS interacting partner, we did identify its closest human homolog, FA98A/FAM98A (Supplemental Table 3.1). The FUS-interacting RTCB/CN166/DDX1 complex was also reported to play a role in nucleo-cytoplasmic RNA shuttling (146), a function shared by FUS (101), suggesting potential functional co-operation. The familial ALS-related FUS mutations cause cytoplasmic mis-localization of FUS (2, 3, 12, 62, 63, 72). It is conceivable that the resulting lower nuclear FUS level leads to depletion of its nuclear complexes and loss of its nuclear functions.



### 3.3.6 Mis-regulation of cytoplasmic processes by ALS mutant FUS

We identified 34 FUS interacting partners that are known components of either IMP1-dependent RNP granules, RNA transport granules, or both (Fig 3.8). IMP1, also called insulin-like growth factor 2 mRNA-binding protein 1 is an RNA binding protein that recruits target mRNAs to cytoplasmic protein-RNA complexes. IMP1 stabilizes the recruited mRNAs allowing their storage and transport and modulates the location at which the target mRNAs are translated (130, 147-149). IMP1 plays a direct role in the transport and translation of transcripts required for axonal regeneration (150). The IMP1-dependent RNP granules are distinct from RNA transport granules and stress granules (129), although they share components (Fig 3.7). The ALS-related FUS mutations cause the formation of FUS-positive cytoplasmic inclusions (12, 62, 63, 72) that sequestered the IMP1-dependent RNP granule and/or transport granule components DHX9, DDX3X, and CAPR1 (Fig. 3.4, Fig. 3.5, Fig 3.7). The sequestration of these FUS interacting partners could lead to loss of their function in RNA transport and localized translation. Because of the extreme proportions of motor neurons, they rely on mRNA transport and localized translation more than other cell types. Accordingly, motor neurons could be especially sensitive to the sequestration of mRNA transport granule components.

We identified 21 reported stress granule (SG) components as FUS interacting partners (Fig. 3.7). We found that the cytoplasmic ALS mutant FUS inclusions were immunopositive for the SG components DDX3X and CAPR1 (Fig. 3.4, Fig. 3.5, Fig. 3.7). We previously reported that the mutant FUS inclusions were also immunopositive for another SG component, PABP1 (72). Stress granules are stress-induced ribonucleoprotein

complexes in eukaryotic cells that contain translationally silent pre-initiation complexes and a host of RNA-binding proteins (73, 151). Two of the FUS interacting proteins we identified were processing body or P-body components (Fig. 3.7). P-bodies are discrete cytoplasmic foci where mRNA degradation takes place (152). P-bodies functionally interact with stress granules (139). Among normal conditions, stress granules exist for up to a few hours. The normal dynamics of stress granules is critical for the survival of stressed neurons (73). The perturbation of stress granule dynamics might be a pathological process of central importance in ALS (138, 153, 154). Accordingly, triggering the formation of unusually stable stress granule-like structures by mutant FUS and the resulting perturbation of stress granule dynamics might cause a gained toxicity phenotype.

During the revision of this manuscript, a comparative interactomics study of varied ALS-associated proteins was published that identified a partially overlapping set of FUS interacting partners (155).

### 3.4 Conclusions

In summary, our results demonstrate that the FUS interacting partners participate in multiple pathways, providing insights into the physiological functions of FUS as well as the potential mis-regulation of these pathways by ALS mutant FUS. Among the pathways, mRNA transport and stress granule dynamics are particularly important for the health of motor neurons. Mis-regulation of the dendritic and/or axonal mRNA transport and the generation of abnormally stable ectopic stress granule-like structures by ALS mutant FUS are likely contributors to ALS pathogenesis.

Table 3.1 Selected enriched GO Biological Processes among the identified FUS interacting partners.

The corresponding p-values and the numbers of FUS interaction partners are shown without/with the inclusion of ribosomal FUS interaction partners in the search.

<b>Term</b>	<b>p-Value</b>	<b>Number of FUS interaction partners</b>
<b>RNA processing</b>	1.659e <sup>-32</sup> /3.050e <sup>-36</sup>	37/46
<b>RNA splicing</b>	4.750e <sup>-27</sup> /2.960e <sup>-22</sup>	27/27
<b>mRNA processing</b>	9.890e <sup>-27</sup> /1.499e <sup>-21</sup>	28/28
<b>mRNA metabolic process</b>	1.149e <sup>-25</sup> /6.829e <sup>-73</sup>	30/67
<b>mRNA splicing, via spliceosome</b>	1.149e <sup>-25</sup> /1.760e <sup>-21</sup>	23/23
<b>Gene expression</b>	1.220e <sup>-18</sup> /3.089e <sup>-33</sup>	49/80
<b>Posttranscriptional regulation of gene expression</b>	6.050e <sup>-13</sup> /1.650e <sup>-13</sup>	17/20
<b>mRNA stabilization</b>	2.940e <sup>-7</sup> /1.150e <sup>-6</sup>	6/6
<b>Regulation of translation</b>	8.299e <sup>-7</sup> /3.019e <sup>-8</sup>	11/14
<b>RNA localization</b>	1.980e <sup>-5</sup> /2.180e <sup>-4</sup>	8/8
<b>Transcription, DNA-templated</b>	6.779e <sup>-5</sup> /4.710e <sup>-2</sup>	25/26
<b>mRNA 3'-end processing</b>	3.570e <sup>-4</sup> /1.649e <sup>-3</sup>	5/5
<b>tRNA splicing, via endonucleolytic cleavage and ligation</b>	8.429e <sup>-4</sup> /1.699e <sup>-3</sup>	3/3
<b>ncRNA metabolic process</b>	1.000e <sup>-3</sup> /3.459e <sup>-10</sup>	9/18
<b>Termination of RNA polymerase II transcription</b>	2.360e <sup>-3</sup> /8.259e <sup>-3</sup>	4/4
<b>Transcription from RNA polymerase II promoter</b>	5.130e <sup>-3</sup> /1.499e <sup>-1</sup>	11/11
<b>Chromosome organization</b>	1.149e <sup>-2</sup> /2.939e <sup>-1</sup>	11/11

Table 3.2 Selected enriched GO Molecular Functions among the identified FUS interacting partners.

The corresponding p-values and the numbers of FUS interaction partners are shown without/with the inclusion of ribosomal FUS interaction partners in the search.

<b>Term</b>	<b>p-Value</b>	<b>Number of FUS interaction partners</b>
<b>RNA binding</b>	5.000e <sup>-43</sup> /6.379e <sup>-74</sup>	53/87
<b>Single-stranded RNA binding</b>	2.070e <sup>-10</sup> /9.300e <sup>-9</sup>	9/9
<b>ATP-dependent RNA helicase activity</b>	2.220e <sup>-10</sup> /1.099e <sup>-8</sup>	9/9
<b>Double-stranded RNA binding</b>	8.889e <sup>-6</sup> /1.289e <sup>-4</sup>	6/6
<b>mRNA 3'-UTR binding</b>	4.350e <sup>-5</sup> /4.180e <sup>-4</sup>	5/5
<b>DNA binding</b>	3.330e <sup>-4</sup> /2.750e <sup>-2</sup>	22/25
<b>RNA polymerase II core binding</b>	1.690e <sup>-3</sup> /7.629e <sup>-3</sup>	3/3
<b>mRNA 5'-UTR binding</b>	1.359e <sup>-2</sup> /5.000e <sup>-4</sup>	2/3

Table 3.3 Selected enriched GO Cellular Components among the identified FUS interacting partners.

<b>Term</b>	<b>p-Value</b>	<b>Number of FUS interaction partners</b>
<b>Ribonucleoprotein complex</b>	2.369e <sup>-68</sup>	66
<b>Ribosome</b>	1.769e <sup>-46</sup>	38
<b>Spliceosomal complex</b>	1.080e <sup>-20</sup>	20
<b>Ribonucleoprotein granule</b>	3.200e <sup>-16</sup>	16
<b>Cytoplasmic stress granule</b>	3.430e <sup>-10</sup>	8
<b>Extracellular exosome</b>	1.430e <sup>-9</sup>	42
<b>tRNA-splicing ligase complex</b>	1.919e <sup>-6</sup>	4
<b>SMN-Sm protein complex</b>	5.140e <sup>-5</sup>	4
<b>Chromosome</b>	2.449e <sup>-3</sup>	13

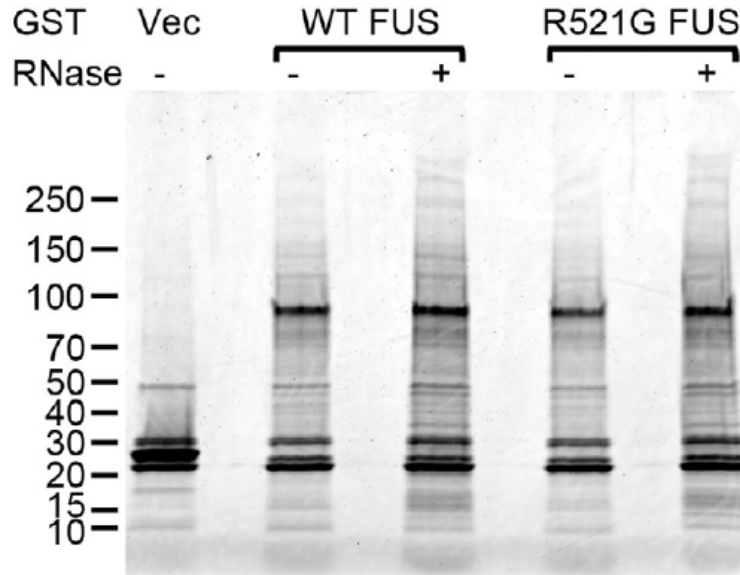


Figure 3.1

The identification of FUS interaction partners. GST pull-downs were performed from cellular extracts of 293T cells transfected with the indicated GST expression constructs. RNase was included in the cellular lysates as indicated. The pull-down mixtures were subjected to SDS-PAGE on 4–15% gradient gel, followed by Sypro Ruby staining. Vec, vector. The molecular weights of marker bands are shown on the left (kDa).

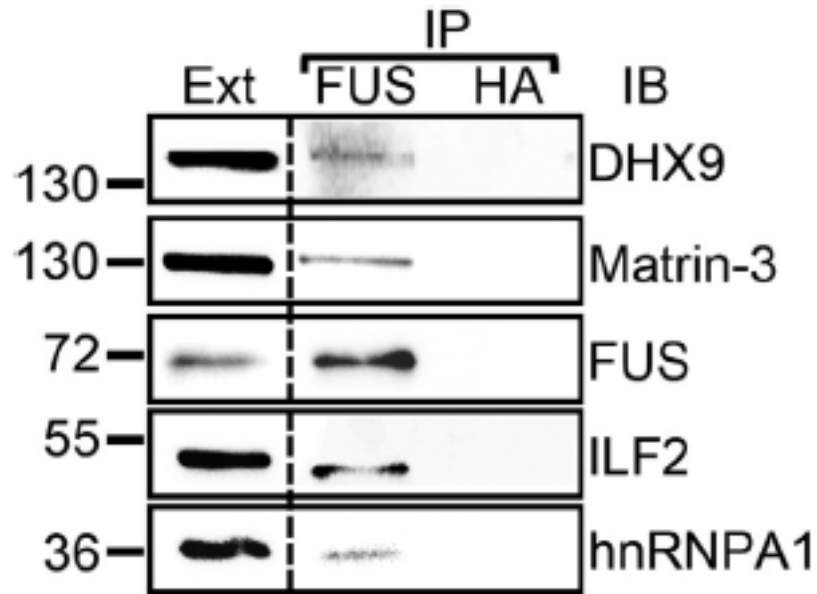


Figure 3.2

Verification of selected FUS interacting partners with endogenous FUS immunoprecipitation. Immunoprecipitations were performed from cellular extracts of SH-SY5Y cells with a FUS-specific and a control (HA) antibody. The immunoprecipitates were subjected to SDS-PAGE followed by immunoblot with the indicated antibodies. IP, immunoprecipitation; Ext, extract; IB, immunoblot. The molecular weights of nearby marker bands are shown on the left (kDa).

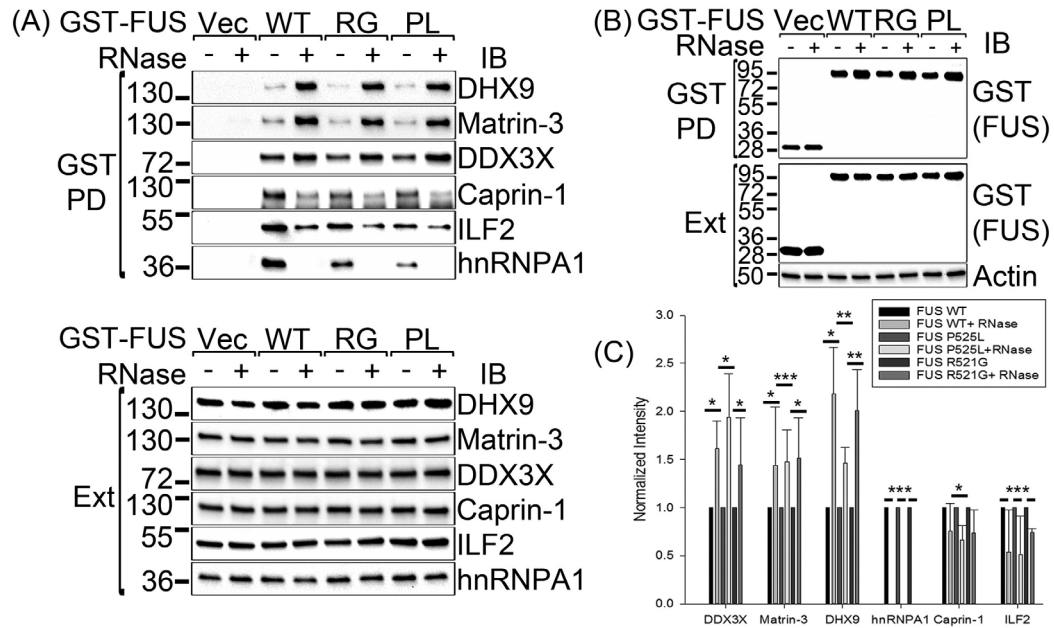
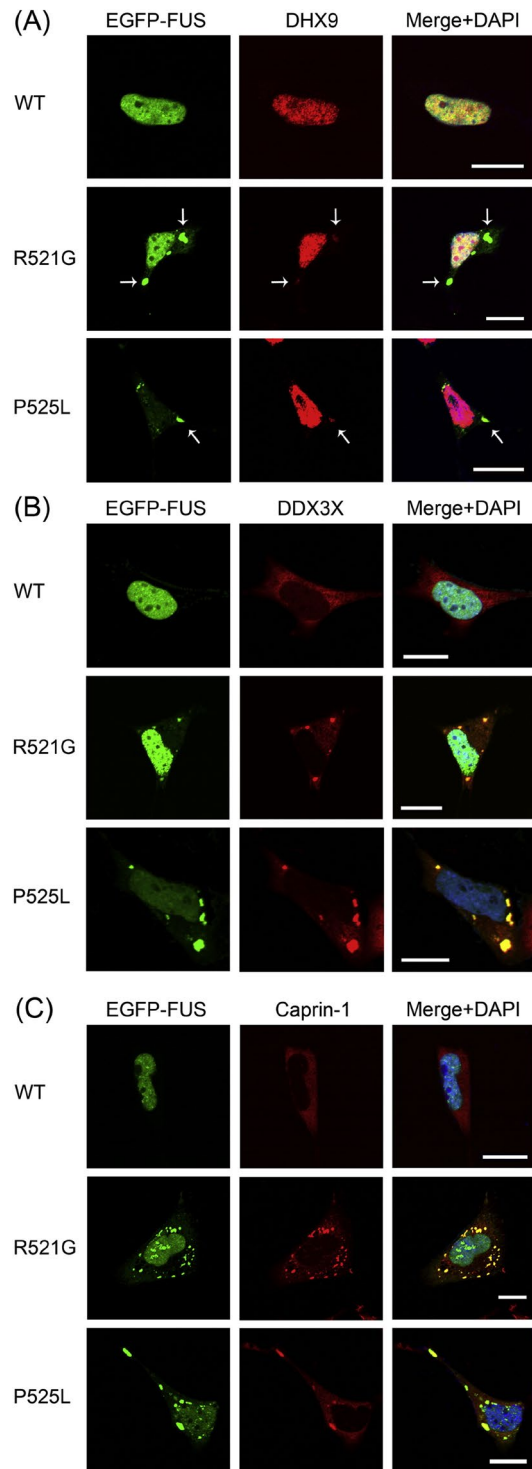


Figure 3.3

Verification of selected FUS interacting partners with GST-FUS pulldown. (A–B) GST pull-downs were performed from cellular extracts of 293T cells transfected with the indicated GST expression constructs. RNase was included in the cellular lysates as indicated. The pull-down mixtures were subjected to SDS-PAGE followed by immunoblot with the indicated antibodies. PD, pull-down; Ext, extract; Vec, vector; RG, R521G; PL, P525L; IB, immunoblot. The molecular weights of nearby marker bands are shown on the left (kDa). (C) Quantification of the RNA dependence of the FUS interactions shown in panel A. The band intensities from three independent experiments were quantified and normalized to the respective band with no RNase added. The error bars stand for standard deviation. Statistical significance was determined with Student's *t*-test. \*: 0.01 < *p* < 0.05; \*\*: 0.001 < *p* < 0.01; \*\*\*: *p* < 0.001.





### Figure 3.4

The co-localization of DHX9, DDX3X and Caprin-1 with ALS mutant FUS inclusions in SH-SY5Y cells. Confocal microscopic images of EGFP-tagged FUS (WT, R521G or P525L) fluorescence and DHX9 (A), DDX3X (B) and Caprin-1 (C) immunofluorescence in SH-SY5Y cells. The co-localization of mutant FUS and DHX9 in cytoplasmic inclusions is shown by arrows in (A). Scale bars, 10  $\mu\text{m}$ .

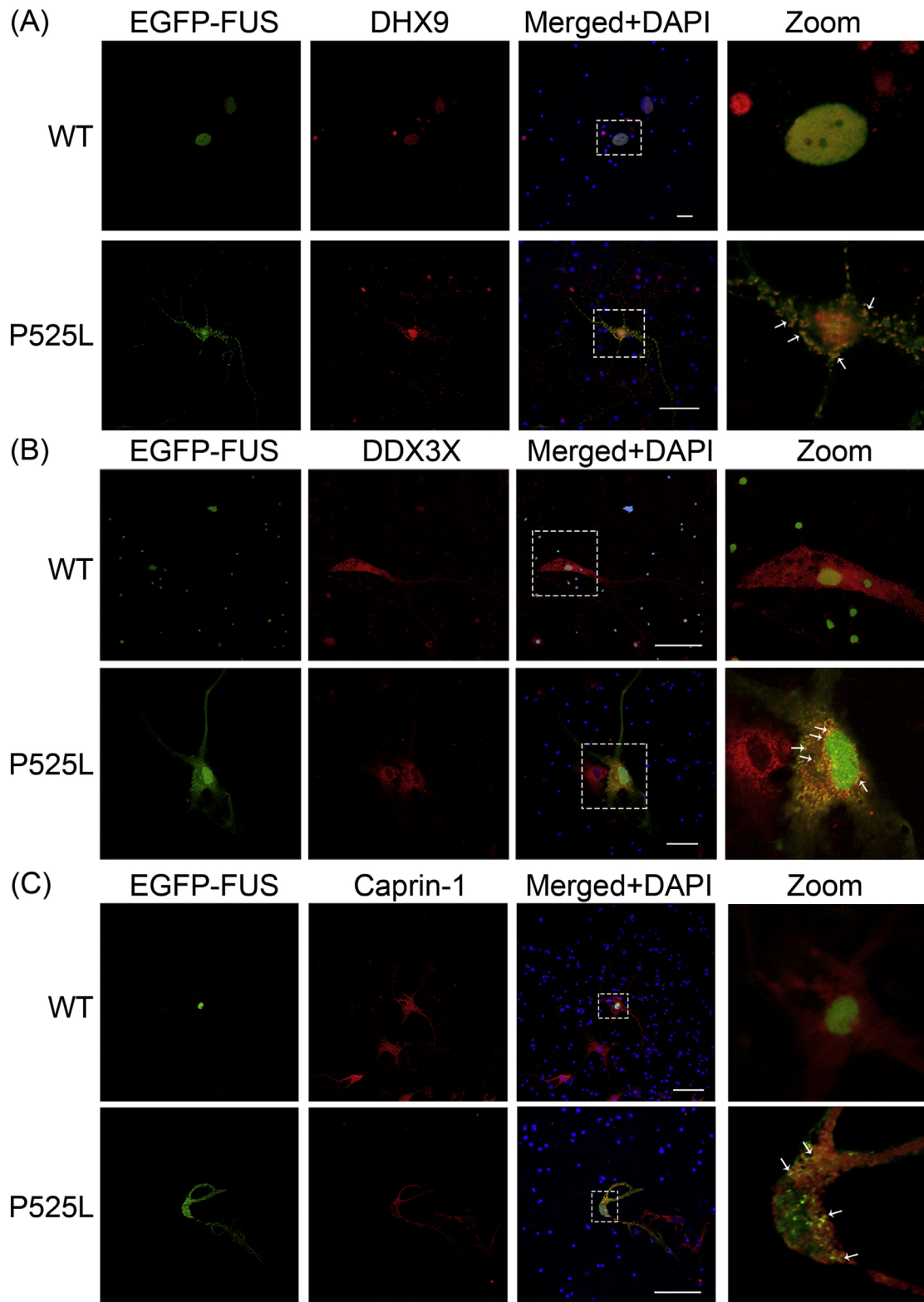


### Figure 3.5

The co-localization of DHX9, DDX3X and Caprin-1 with ALS mutant FUS inclusions in primary cortical neurons. Confocal microscopic images of EGFP-tagged WT and P525L mutant FUS fluorescence and DHX9 (A), DDX3X (B) and Caprin-1 (C) immunofluorescence in cultured mouse primary cortical neurons. The boxed areas are magnified in the respective panels on the right. The co-localization of mutant FUS with the respective interaction partners in cytoplasmic inclusions is shown by arrows. Scale bars, 50  $\mu\text{m}$ .

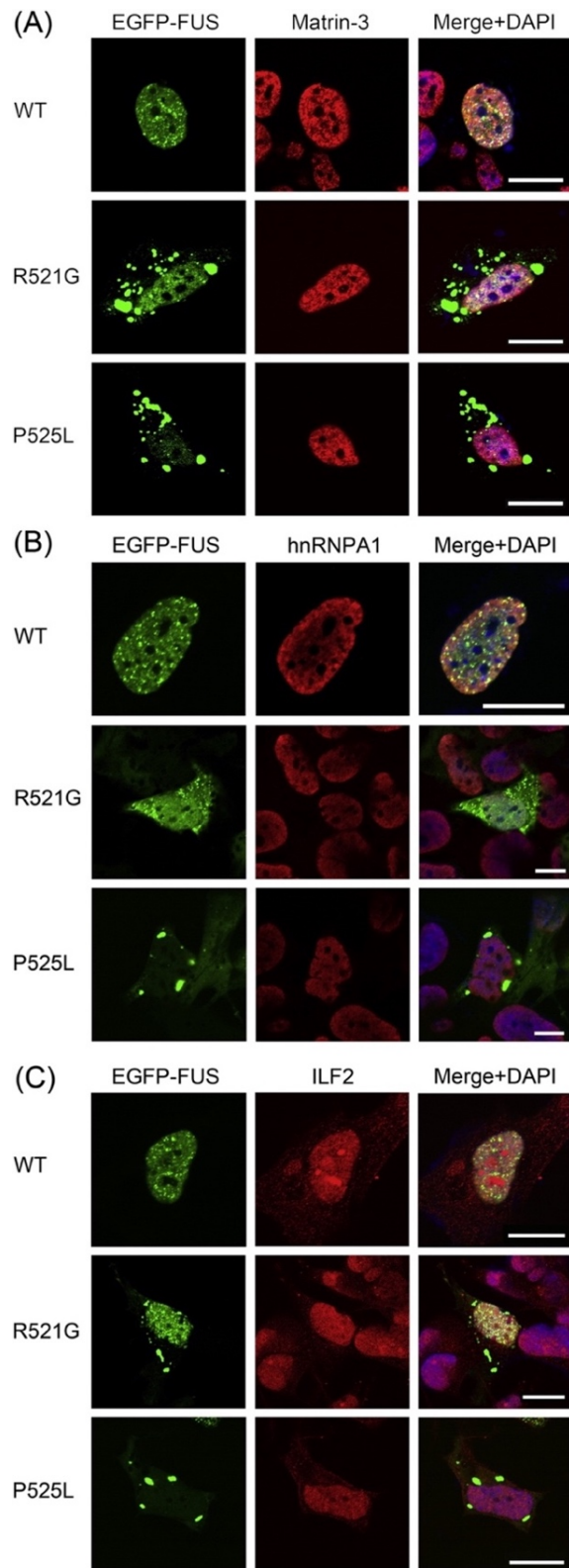


Figure 3.6

The Matrin-3, hnRNPA1 and ILF2 proteins do not localize to ALS mutant FUS inclusions in SH-SY5Y cells. Confocal microscopic images of EGFP-tagged FUS (WT, R521G or P525L) fluorescence and Matrin-3 (A), hnRNPA1 (B) and ILF2 (C) immunofluorescence in SH-SY5Y cells. Scale bars, 10  $\mu$ m.

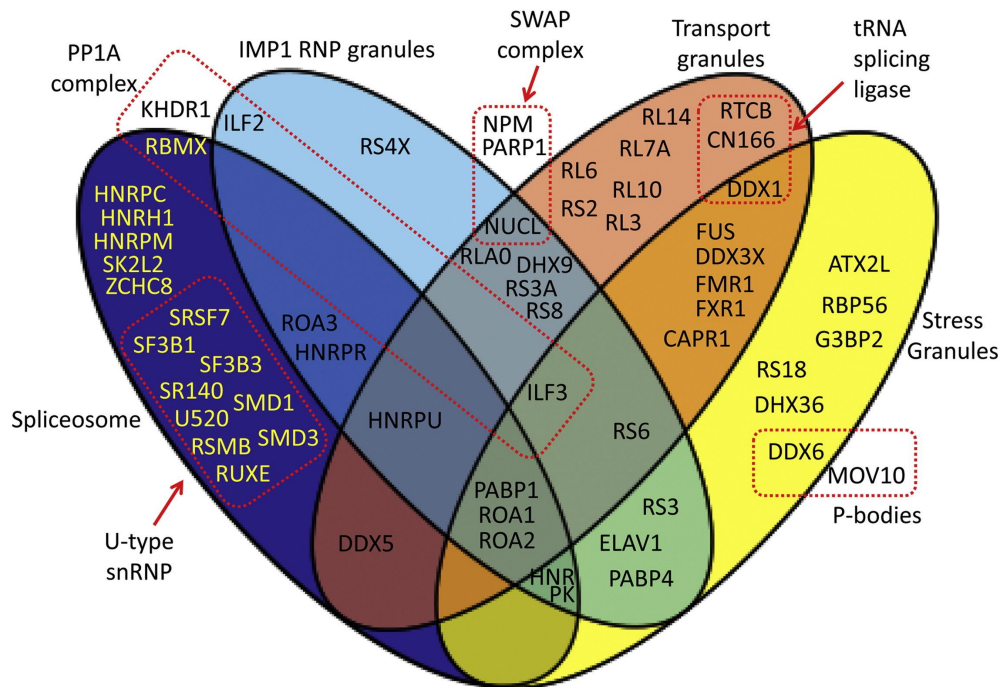


Figure 3.7

FUS interacts with overlapping ribonucleoprotein complexes. Venn diagram of a subset of the identified FUS interacting partners. Venn diagram of a subset of the identified FUS interacting partners. The background diagram was obtained from Wikimedia Commons, [https://commons.wikimedia.org/wiki/File:4-way-venn\\_vector.svg](https://commons.wikimedia.org/wiki/File:4-way-venn_vector.svg)

## CHAPTER 4. ALS MUTATIONS OF FUS SUPPRESS PROTEIN TRANSLATION AND DISRUPT THE REGULATION OF NONSENSE-MEDIATED DECAY

*Modified from the manuscript “ALS mutations of FUS suppress protein translation and disrupt the regulation of nonsense-mediated decay”, published in PNAS. 2018. Epub 2018/11/21. doi: 10.1073/pnas.1810413115. PubMed PMID: 30455313. The introduction was simplified for fluidity.*

### 4.1 Introduction

FUS is a DNA- and RNA-binding protein that is primarily localized to the nucleus, where it forms dynamic ribonucleoprotein granules. In contrast, ALS-related mutant FUS accumulates in the cytoplasm and forms stable ribonucleoprotein granules, which can lead to inclusion bodies and potentially contribute to neurotoxicity (2, 3, 156). FUS mutations have also been shown to impact many RNA metabolic processes, including transcription (9, 13, 20, 22), splicing (37-39), mRNA transport (131), and stabilization (68), ultimately contributing to neuronal dysfunction. Recent studies demonstrated that mutations in FUS cause the liquid–liquid phase separation (LLPS) of FUS protein and the formation of self-assembled hydrogels or liquid droplets in vitro (8, 157). It is noted that LLPS has also been reported for other RNA metabolic proteins involved in ALS, including TDP-43 (158), C9ORF72 dipeptide repeat (159), hnRNPA1 (158), and TIA1 (70). Thus, other cellular proteins are likely to be included in granules during LLPS in living cells, but the identities of such proteins remain to be determined.

This study started with testing the hypothesis that the identification of proteins associated with mutant FUS-dependent cytoplasmic granules is likely to provide critical



insights into the toxic mechanism of mutant FUS. We developed a protocol to capture the dynamic mutant FUS-positive granules (22, 156) by membrane filtration and identified protein components by proteomic approaches. The bioinformatics analysis of proteins identified in wild-type (WT) and mutant FUS granules revealed multiple RNA metabolism pathways, among which protein translation and mRNA surveillance appeared to be novel.

We thus hypothesize that mutant FUS plays a role in protein translation. Two previous studies reported that ALS-linked FUS mutations were recruited to ribonucleoprotein granules; thus, FUS was speculated to be involved in protein translation (66, 156). However, protein translation was not measured in either study. Using three independent assays, we found that mutant FUS indeed impaired protein translation and that the cytoplasmic inclusions of mutant FUS were positive for stalled ribosomal complexes.

Mutations in FUS have been demonstrated to cause aberrant splicing (160); however, the molecular mechanism by which cells handle defective mRNA has not been explored in ALS. Nonsense-mediated decay (NMD) is a major mRNA surveillance system that is known to degrade defective mRNA and ~3–20% of all mRNAs (161). NMD and protein translation are interrelated, as NMD utilizes the translocating ribosome as a proofreading mechanism for sensing defective mRNAs (162-164). We demonstrate that the phosphorylation level of a critical NMD regulator UPF1 (163), the NMD complex assembly, and the UPF1-mRNA binding all increased in the presence of mutant FUS, supporting that NMD is activated by mutant FUS. Additionally, two potent NMD-activating regulators UPF1 and UPF3b (163, 165, 166) were up-regulated, while the negative NMD regulator UPF3a (167) was down-regulated in skin fibroblast cells derived

from a cohort of patients with ALS with FUS mutations compared with cells from control subjects, indicating disruption of the autoregulation of NMD. The hyperactivation of NMD was demonstrated using an NMD reporter assay in N2a cells and measuring endogenous mRNAs in the fibroblast cells of FUS ALS cases. Overall, the findings from this study thus provide an in-depth understanding of how RNA metabolism and protein translation are impacted by mutations in FUS and produce insights into the disease-causing mechanism of the mutant FUS subtype of ALS.

## 4.2 Results

### 4.2.1 Proteins related to translation and mRNA surveillance are enriched in mutant FUS inclusions.

A more complete understanding of the protein composition that makes up the inclusions characteristic of mutant FUS-dependent ALS would provide a better understanding of the mechanism(s) driving the disease. To achieve this, we adapted a membrane filtration assay that was originally developed for detecting differentially soluble protein complexes (168). Utilizing previously described conditions in which radioimmunoprecipitation assay (RIPA) buffer was used to lyse cells (169), none of the WT, R495X, P525L, or R521G mutant FUS proteins were detected on the PVDF membrane (Fig. 4.1A). As a positive control and negative control, respectively, A4V mutant SOD1 was detected on the PVDF membrane filter, while WT SOD1 was not. The results suggest that, unlike A4V mutant SOD1-dependent cytoplasmic aggregates, mutant

FUS cytoplasmic inclusions are dynamic and disassembled under the experimental conditions.

A protocol using a hypotonic lysis buffer with a low detergent concentration was developed (Fig. 4.2A). Using these conditions, P525L and R495X mutant FUS was detected on the membrane filter along with A4V mutant SOD1, whereas less WT FUS was detected and no WT SOD1 was detected (Fig. 4.1B). Native gel electrophoresis (20) also confirmed that FUS protein remained as an oligomeric species under these conditions, whereas FUS protein prepared in the RIPA buffer migrated faster (Fig. 4.2B). We subjected the membrane “dots” to trypsin digestion followed by liquid chromatography-tandem mass spectrometry (LC-MS/MS) using a published protocol (169). A total of 291, 268, and 278 proteins in FUS WT (Supplemental Table 4.1), R495X (Supplemental Table 4.2), and P525L (Supplemental Table 4.3), respectively, met the protein identification criteria described in SI Appendix and were considered significant identifications

Proteins identified in the granules were subjected to functional enrichment analysis using the integrative tool, Enrichr (90, 91). The Gene Ontology (GO): Molecular Function database (93) and the DISEASES database (94) were utilized for analyzing protein functions and disease relevance, respectively. The top 20 most significant molecular function annotations aggregated from the GO: Molecular Function database by Enrichr revealed a variety of RNA-binding functions associated with WT (Fig. 4.1C) and mutant FUS (Fig. 4.1D). It is noted that several properties, including translation factor activity, tRNA binding, and RNA cap binding, are related to protein translation and mRNA surveillance mechanisms. The top 10 most significant results from the disease-gene

association analysis for WT and mutant FUS (Fig. 4.3A) show a number of neurodegenerative diseases, including lateral sclerosis and Charcot–Marie–Tooth disease. Interestingly, the disease identified with a high significance was Diamond–Blackfan anemia, a severe ribosomopathy that results in defective protein synthesis (Fig. 4.3B) (170). This association suggests that proteins identified in FUS granules are likely to be involved in protein translation. We therefore focused on testing the function of FUS in protein synthesis and related mRNA surveillance pathways.

We next examined the subcellular localization of critical proteins involved in protein translation (eIF3, eIF4A1, eIF4G, and rpS6) and mRNA surveillance (eIF4A3) that were identified in the MS results. In primary cortical neurons transfected with EGFP-tagged FUS, eIF4A3 (Fig. 4.1E), eIF3 (Fig. 4.1F), eIF4A1, eIF4G, and rpS6 (Fig. 4.4 A–C, respectively) were all colocalized with cytoplasmic inclusions of mutant FUS. As a positive control, mutant FUS inclusions in primary neurons were positive for the stress granule marker G3BP1 (Fig. 4.4D) as previously reported (22). The immunoprecipitation (IP) results also demonstrated that eIF3, eIF4G, and eIF4A3 interacted more with the mutant than WT FUS (Fig. 4.1G), validating the proteomic and colocalization results.

#### 4.2.2 Protein translation is impaired in the presence of mutant FUS

Based on the above proteomic identifications, GO enrichment analysis, and colocalization of translation machinery to the mutant FUS inclusions, we set out to test whether protein translation is impaired by ALS mutants of FUS using three independent assays. Utilizing a translation reporter assay (84), we examined how mutant FUS changed cap-dependent protein translation. Co-transfection of R495X or P525L mutant FUS with the reporter

construct resulted in 50% and 70% reductions in the translation of the Renilla reporter gene, respectively (Fig. 2A). No detectable change was observed in cells transfected with empty vector (EV) or WT FUS. The control internal ribosomal entry site (IRES)-dependent translation of the luciferase gene was not changed (Fig. 4.5A). The second assay using an in vitro 35S-methionine (35S-Met) incorporation assay to measure translation of native mRNA showed that 35S-Met incorporation decreased by 25% and 35%, respectively, in the presence of mutant FUS compared with WT FUS or the EV control (Fig. 2B). Third, to examine endogenous protein translation, we used the surface sensing of translation (SUnSET) assay in which puromycin was used as a structural analog of aminoacyl tRNAs to prevent elongation after being incorporated into the nascent polypeptide chain (171). N2a cells were transfected with either EV, WT, or mutant FUS and treated with puromycin. Western blot analysis using an anti-puromycin antibody showed reduced translation in cells expressing mutant FUS (Fig. 4.5C and D). Finally, we carried out the SUnSET assay to examine protein translation in the skin fibroblast cells derived from patients with familial ALS who were carrying R521G or P525R (89) FUS mutations and from healthy controls with WT FUS (Fig. 4.5E and F). Protein translation decreased by ~30% in fibroblast cells from FUS ALS cases. The above results consistently support that mutant FUS represses protein translation.

We next examined whether FUS inclusions contained puromycinlated proteins. Immunofluorescence using the same anti-puromycin antibody showed that puromycinlated proteins were colocalized with mutant FUS inclusions (Fig. 2G), suggesting that translation complexes are localized in mutant FUS inclusions. Moreover, to test whether mRNA was also localized to the inclusion, we performed RNA fluorescence in situ hybridization

(FISH) with two different RNA probes in N2a cells expressing WT or P525L mutant FUS. A generic Cy3 oligo d(T)<sub>21</sub> probe was used to test mature polyadenylated mRNAs (Fig. 4.5H). Mature mRNA was distributed throughout the cytoplasm in cells with EV or WT FUS. However, a significant accumulation of mRNA in the mutant FUS inclusions was observed, which is consistent with previous observations (172). FUS has been reported to regulate the splicing of its own transcript (39); thus, we tested a probe specific to FUS transcript (exon 4) and found that FUS mRNA was also localized to the mutant FUS inclusions (Fig. 4.4E). The results support that mutant FUS inclusions were colocalized with translation machinery and mature mRNAs.

We next examined whether translation initiation is impaired by mutant FUS. Binding of the initiation factor eIF4E to the 5' cap of mRNA is the rate-limiting step in translation initiation where regulation often occurs (173). We performed a 7'-methylguanosine (7'MG) pulldown as an *in vitro* cap-binding assay (174) in the presence of WT or mutant FUS. After 7'MG pulldown, key members of the preinitiation complex were observed (Fig. 4.5I). Similar levels of eIF4G, eIF4E, and eIF4A1 were pulled down regardless of the presence of WT or mutant FUS. Neither WT nor mutant FUS bound to the 5' cap. As a negative control, eIF4A3 also did not bind to the 5' cap. The results suggest that mutant FUS does not interfere with the binding of the initiation complex to the 5' cap structure in the translation initiation stage. Thus, it is likely that translation is disrupted by mutant FUS after the initiation step, resulting in premature termination.

We hypothesized that prematurely terminated polypeptides resulting from defective translation in the presence of mutant FUS will be polyubiquitinated and targeted for

degradation. Therefore, we examined the level of K48-linked polyubiquitination in cells expressing WT or mutant FUS, since it is the major signal for targeting substrates for proteasomal degradation. Using an antiK48 polyubiquitination tandem ubiquitin-binding entity (175), we found that the K48 polyubiquitination level increased ~1.5- to 1.8- fold in cells expressing mutant FUS compared with WT FUS and the EV control (Fig. 4.5J and K). In contrast, the level of K63-linked polyubiquitination, which is involved with other non-proteasomal processes, did not change with either WT or mutant FUS (Fig. 4.6). These results collectively support that ALS mutations in FUS cause defects in protein translation.

#### 4.2.3 The NMD pathway is activated by mutant FUS

Protein translation and mRNA surveillance pathways are interrelated(162, 164). It has been reported that the inhibition of protein translation elongation by cycloheximide (176) can up-regulate NMD factors and activate NMD (177). Thus, we set to examine whether mutations in FUS can impact the mRNA degradative pathway NMD. UPF1 (163, 166) and UPF3b (167) are two critical positive regulators of NMD, and UPF1 phosphorylation (p-UPF1) is a critical step in NMD activation (163, 178). We evaluated the levels of UPF1, p-UPF1, and UPF3b in the skin fibroblast cells derived from six FUS ALS cases and five healthy controls (Fig. 4.7A). The antibody used for pUPF1 was an anti-phospho-Ser/Thr ATM/AMR substrate (p-S/T) previously reported (179). Quantitative results show that the protein level of UPF1 (Fig. 4.7B), p-UPF1 (Fig. 4.7C), and UPF3b (Fig. 4.7D) increased in patients with ALS compared with healthy controls by 25%, 70%, and 35%, respectively. Similarly, N2a cells expressing P525L or R495X mutant FUS had increased levels of UPF1 and UPF3b (Fig. 4.8) and p-UPF1 (Fig. 4.9A). The results provide initial evidence that

NMD activation is elevated in the presence of mutant FUS in the cells of patients with ALS with mutations in FUS.

We next examined the subcellular localization of endogenous NMD factors in primary cortical neurons transfected with WT or mutant FUS. The colocalization of mutant FUS with UPF1 and pUPF1 was demonstrated using two different p-UPF1 antibodies: the p-S/T antibody used in the Western blot analysis (Fig. 4.7E) and a different antibody against phosphor-S1089 of UPF1 (180) (Fig. 4.7F). Two additional NMD factors, UPF3b (Fig. 4.7G) and XRN1 (Fig. 4.10A), were also localized in cytoplasmic inclusions of mutant FUS in primary neurons. SMG6 was not localized in mutant FUS inclusions serving as a control (Fig. 4.10B). Similar results were obtained from N2a cells expressing WT or mutant FUS. Cytoplasmic inclusions of FUS were positive for UPF1 and p-UPF1, UPF3b, and XRN1 (Fig. 4.9A– C). SMG6 and eRF3b showed little localization to mutant FUS inclusions in N2a cells (Fig. 4.9D and E). The colocalization of NMD factors in mutant FUS inclusions further suggests that mutant FUS may impact the NMD pathway.

Since the assembly of key NMD factors with UPF1 is a critical aspect of pathway activation (181, 182), we next examined the assembly of NMD factors in the presence of WT or mutant FUS. Endogenous UPF1 IP followed by Western blots for various NMD factors is shown in Fig. 4.11A. Quantitative analysis showed that the UPF1 interaction with p-UPF1, UPF3b, the endonuclease SMG6, and FUS increased ~1.5- to 2.0-fold, with statistical significance in the presence of mutant FUS (Fig. 4.11B). In addition, the translation termination factor eRF3b increased in the presence of mutant FUS (Fig. 4.11B).



Enhanced assembly of NMD factors is additional evidence that NMD was activated by mutant FUS.

We also tested the interaction of core NMD factors with mRNAs. We treated cells with bromouridine to label mRNAs, immunoprecipitated the labeled RNA with anti-BrdU antibody (183), and assessed NMD proteins by Western blot (Fig. 4.11C). Quantitative analysis showed that higher levels of NMD components responsible for triggering NMD (eIF4A3 and UPF1) and mRNA degradation (SMG6 and XRN1) were bound to RNAs in the presence of mutant FUS (Fig. 4.11D). An RNA-binding protein, PABP1, was used as a loading control and showed similar loading in all samples. The above results consistently support that the NMD pathway was activated by mutant FUS.

#### 4.2.4 NMD factors are dysregulated in fibroblasts in FUS ALS cases

We demonstrated earlier that two positive regulators of NMD (UPF1 and UPF3b) and UPF1 phosphorylation increased in the skin fibroblast cells derived from six FUS ALS cases compared with five healthy controls (Fig. 4.7A–D). The NMD pathway is tightly regulated by multiple mechanisms, including the molecular brake UPF3a (167). UPF3a competitively blocks the interaction of UPF3b with UPF2, thus delaying the activation of NMD. We examined protein levels of UPF3a in six FUS ALS cases (Fig. 4.12A) and found ~30% lower levels of UPF3a protein in the fibroblast cells from these patients (Fig. 4.12B). Similarly, UPF3a protein levels decreased in N2a cells overexpressing the R495X and P525L mutants (SI Fig. 4.13A and B).

We further examined how the mRNA levels of UPF1, UPF3b, and UPF3a changed in the FUS ALS cases. The qPCR results show elevated levels of UPF1 (Fig. 4.12C) and UPF3b (Fig. 4.12D) and decreased levels of UPF3a (Fig. 5E) in the fibroblast cells of FUS ALS cases. Similar results were obtained for mRNA levels of these factors in N2a cells expressing WT or mutant FUS (Figs. 4.8C and D and Fig 4.13C). Consistent changes in both mRNA and protein levels of the pro-NMD factors (UPF1 and UPF3b) and the negative regulator (UPF3a) illustrate a pattern of NMD dysregulation in the mutant FUS-linked familial patients with ALS, which will contribute to NMD hyperactivation.

#### 4.2.5 UPF1-mediated autoregulation of NMD is impaired in FUS ALS cases

Core NMD factors, including UPF1 and UPF3b, are regulated through an intricate autoregulatory mechanism, by which their own mRNAs are targeted for NMD (177, 184). Given the dysregulation of NMD factors as shown above, we hypothesized that the ALS mutations in FUS disrupt the autoregulatory mechanism of NMD. To test this hypothesis, we first performed endogenous UPF1 IP followed by qPCR to examine whether the UPF1 protein binds its own mRNA and UPF3b mRNA. Using normal goat serum as a control, UPF1 protein was specifically pulled down by a UPF1 antibody (Fig. 4.14A). Along with the UPF1 protein, UPF1 mRNA (Fig. 4.14B) and UPF3b mRNA (Fig. 4.14C) were also pulled down. We then overexpressed WT, P525L, or R495X mutant FUS in N2a cells and performed a similar RNA IP experiment (Fig. 4.14D–F). Quantitative analysis showed that, consistent with earlier results (Fig. 4.7A), higher levels of mutant FUS were pulled down with the UPF1 protein (Fig. 4.14D). More importantly, lower levels of UPF1 mRNA (Fig. 4.14E) and UPF3b mRNA (Fig. 4.14F) were pulled down along with the UPF1 protein in

the presence of mutant FUS, suggesting that mutant FUS led to a lower turnover of UPF1 and UPF3b mRNA by NMD. The dampened autoregulatory mechanism through UPF1 binding supports the observation of increases in the mRNA and protein levels of UPF1 and UPF3b.

To further examine how decay is influenced by FUS mutations, we measured the UPF1, UPF3b, and UPF3a mRNA levels by qPCR after treating N2a cells expressing WT, P525L, or R495X mutant FUS with the transcriptional inhibitor actinomycin D. In cells expressing mutant FUS, the decay of UPF1 (Fig. 4.14G) and UPF3b (Fig. 4.14H) mRNA was significantly slower than in controls. In contrast, the mRNA decay of the NMD negative regulator UPF3a was significantly faster in cells expressing mutant FUS (Fig. 4.14I). The results collectively support that the stability of NMD factor mRNA was dysregulated by mutant FUS in a UPF1-dependent manner (i.e., the NMD autoregulatory circuit is impaired).

#### 4.2.6 Enhanced decay of NMD substrate in the presence of ALS mutant FUS

Based on the above findings on the dysregulation of NMD factors, we next tested whether the NMD activity is hyperactivated using four well-characterized NMD reporters [ $\beta$ -globin and GPX-1 with and without a premature stop codon (PTC)] (185), as well as a cohort of documented endogenous NMD substrates(186, 187). The levels of all four reporter transcripts (WT  $\beta$ -globin, WT GPX-1, PTC  $\beta$ -globin, and PTC GPX-1) were consistently lower in N2a cells expressing mutant FUS than in cells expressing WT FUS (Fig. 4.15). It is noted that the transcript levels in WT FUS-expressing cells were unchanged compared with the EV control, with the exception of PTC GPX1 (Fig. 4.15D).

The NMD reporter assays support higher NMD turnover of normal and PTC-containing mRNAs in the presence of mutant FUS.

To better characterize NMD activity, we measured the mRNA levels of three NMD substrates: ATF3, ATF4, and TBL2 (186, 187). Total mRNA levels of ATF3, ATF4, and TBL2 (Fig. 4.16A–C) decreased in N2a cells expressing R495X or P525L mutant FUS compared with cells expressing EV and WT FUS. As a control, mRNA levels of cyclophilin D did not change (Fig. 4.16D). We next measured the time course of mRNA levels after transcription inhibition by actinomycin D. The mRNA decay of ATF3, ATF4, and TBL2 (Fig. 4.16E–G) was significantly faster in cells expressing R495X or P525L mutant FUS compared with cells expressing WT FUS. As a control, the decay of cyclophilin D did not differ between cells expressing mutant and WT FUS (Fig. 4.16H). Furthermore, we examined whether higher levels of these mRNAs were associated with UPF1. UPF1 protein IP was performed followed by qPCR to measure the amount of UPF1-bound mRNAs. While similar levels of UPF1 protein were immunoprecipitated (Fig. 4.16I), higher levels of ATF3, ATF4, and TBL2 mRNAs were bound to UPF1 in the presence of mutant FUS (Fig. 4.16J–L). All three lines of evidence support the enhanced NMD decay of these endogenous substrates in cells expressing mutant FUS.

We next examined the mRNA levels of ATF3, ATF4, and TBL2 in fibroblast cells derived from patients with familial ALS. Indeed, the levels of all three mRNAs were lower in cells of patients with ALS than in healthy controls with WT FUS (Fig. 4.16M–O). The results suggest that the NMD activity is induced in clinically relevant samples.

### 4.3 Discussion

FUS (8, 157) and other proteins implicated in ALS (70, 158, 159, 188) have been reported to undergo LLPS and form liquid droplets, which facilitates the formation of membrane-less RNA-protein granules and inclusions (9, 22, 156). This study started with developing a method to isolate dynamic FUS-containing granules and identifying their protein compositions. Enrichment analysis of identified proteins implied that both WT and mutant FUS are involved in protein translation and mRNA surveillance (Fig. 4.1C and D and Fig. 4.3). Tight spatiotemporal regulation of protein synthesis in a motor neuron is critical for its function and survival (189), and reduced protein synthesis can be detrimental to normal neuronal function (190, 191). Moreover, mRNA surveillance is intimately integrated into protein translation (162). For instance, eIF4A3 is a core exon junction complex member that aids in initiating NMD (182). eIF3 is classically known as a critical initiation factor; however, it is also required for efficient translation termination in the event of NMD and promotes ribosomal recycling (192, 193). However, it is unknown how defects in mRNA surveillance are linked to suppression of protein synthesis by ALS mutation in FUS. The colocalization of eIF4A3 and eIF3 in mutant FUS inclusions (Fig. 4.1E and F) led us to probe how protein translation and NMD are altered by mutant FUS and to discover the underlying mechanisms.

We used three independent assays to provide direct evidence that mutant FUS negatively impacted global protein production (Fig. 4.5A–D). Furthermore, the SUnSET assay also detected significant reduction of protein translation in fibroblast cells derived from patients with familial ALS with two different FUS mutations (Fig. 4.5E and F). In addition, mutant FUS inclusions were colocalized with mRNAs (Fig. 4.5H) and

puromycinylated peptides (Fig. 4.5G), suggesting that such inclusions are sites of defective protein synthesis with stalled translation complexes. Mutant FUS inclusions have been reported as stress granule-like with stress granule markers such as G3BP1 and TIA1, but they display altered dynamics compared with healthy cells with endogenous WT FUS (10, 72, 194, 195). We suggest that the impairment of protein translation as shown in this study is a functional consequence of the sequestration of the translation machinery in mutant FUS inclusions.

The above results raised the question how mRNAs resulting from impaired translation would be handled. It was reported that suppression of translation using cycloheximide up-regulated proteins involved in the NMD pathway, particularly UPF1 and UPF3b (177). Our proteomic analysis also suggested that proteins involved in the mRNA surveillance pathway were enriched in mutant FUS inclusions. We observed increased pro-NMD proteins UPF1 and UPF3b in fibroblast cells derived from a cohort of patients with familial ALS bearing two different FUS mutations, R521G and P525R (Fig. 4.7A–D), as well as in N2a cells expressing mutant FUS (Fig. 4.8). In addition, UPF1 phosphorylation (Fig. 4.7E and F), NMD complex assembly (Fig. 4.7A and B), and UPF1- mRNA binding (Fig. 4.7C and D) all increased in the presence of mutant FUS, suggesting an elevated level of NMD activity as we demonstrated with an NMD reporter assay (Fig. 4.15), in three endogenous NMD substrates in N2a cells expressing mutant FUS (Fig. 4.16A–H), and in fibroblast cells from patients with FUS ALS (Fig. 4.16M–O). We rationalized that higher levels of core NMD factors in mutant FUS inclusions would aid in the degradation of RNAs associated with prematurely terminated translation complexes, thus playing a protective role in FUS ALS. A yeast genetic screen identified that UPF1 rescued mutant FUS toxicity

in *Saccharomyces cerevisiae* (82), and follow-up studies showed a similar protective effect of UPF1 overexpression in primary neurons (83) and TDP-43 rat models (196).

Different from UPF1 and UPF3b, UPF3a functions as a molecular brake by competing with UPF3b for interaction with UPF2 and delaying activation of the pathway (167). To our surprise, we found that both protein and mRNA levels of UPF3a decreased in the same cells of patients with familial ALS with mutations in FUS (Fig. 4.12). Loss of the down-regulatory mechanism could result in aberrant activation of NMD. Moreover, NMD is regulated by an intricate autoregulatory circuit to prevent overt activation of NMD. Specifically, the mRNA levels of NMD factors UPF1 and UPF3b are degraded through the NMD pathway itself(177, 184). Our results from mRNA decay experiments demonstrate the stabilization of the pro-NMD factors UPF1 and UPF3b and an increased degradation of the negative regulator UPF3a (Fig. 4.15G–I), suggesting a disruption in the autoregulatory circuit. These results consistently support a model (Fig. 8) in which the NMD pathway is dysregulated and hyperactivated in the presence of mutant FUS. It was reported that UPF1 overexpression could increase the available pool of UPF1 to reactivate the autoregulatory feedback (184), thus enabling the degradation of UPF1 and UPF3b mRNAs and dampening the hyperactivation of NMD. This mechanism can provide an explanation of the reported protective effect of UPF1 overexpression in TDP-43 and FUS ALS models (82, 83, 196).

Dysregulation of NMD factors can, in turn, contribute to suppressing protein translation. For instance, besides its function of promoting NMD, UPF3b was reported to recruit termination factor eRFs to stalled ribosomes and to terminate protein translation

(197). Interestingly, mutations in UPF3b can result in intellectual disabilities, autism spectrum disorder, and schizophrenia. These disorders are likely the consequence of defective NMD in dendrites and neurons, which results in deficient neuronal maturation and dendritic branching (198, 199).

In mutant FUS ALS, translation suppression and subsequent NMD activation appear to constitute a vicious cycle, as illustrated in Fig. 8. Increased translation termination events, potentially due to increased binding of mutant FUS to mRNAs, activate NMD at higher levels. Furthermore, the autoregulation of NMD is disrupted as the pro-NMD factors UPF1 and UPF3b increase and the molecular brake UPF3a decreases, contributing to the hyperactivation of NMD and increased degradation of natural NMD targets, such as ATF3, ATF4, and TBL2. This hyperactivity resulting from defects in translation termination may contribute to toxicity in motor neurons (Fig. 4.17). It is noted that critical steps in this model, including suppressed protein translation (Fig. 4.5E and F); increased levels of UPF1, p-UPF1, and UPF3b protein (Fig. 4.7A–D) and mRNA (Fig. 4.12C and D); decreased levels of UPF3a protein (Fig. 4.12A and B) and mRNA (Fig. 4.12E); and increased NMD degradation of ATF3, ATF4, and TBL2 mRNAs (Fig. 4.16 M–O), were consistently supported by results from fibroblast cells derived from patients with familial ALS carrying two different FUS mutations.

Although this study only demonstrated that mutant FUS suppressed global protein translation, it is conceivable that local translation in dendrites and axon terminals may also be impaired by mutant FUS. FUS has been demonstrated to be part of RNA transport granules and to be recruited to activated synapses (33, 66, 200). In cells bearing FUS



mutations, however, there are defects in synaptic morphology and function (33, 191, 200-202). Decreases in proteins required for synaptic maintenance and function may contribute to an ALS phenotype. Additionally, overactivation of NMD may produce deleterious effects in stress response pathways, including how cells respond to misfolded proteins, hypoxia, and DNA damage (161, 177). NMD also functions in fine-tuning the immune response by degrading mRNAs of proinflammatory factors (203). As neuroinflammation plays a role in ALS in a non-cell autonomous fashion (204, 205), it is conceivable that dysregulation of NMD in astrocytes and microglia may also impact the immune response and contribute to the ALS phenotypes.

In summary, the mechanistic insights gained from this study begin to describe the role of FUS in protein translation and a critical mRNA quality control pathway, both of which are required for neuronal maintenance and function. Sequestration of UPF1 in mutant FUS inclusions, decrease in protein synthesis, NMD hyperactivation, or a combination of these events likely plays a role in neurodegeneration in ALS. It is noted that suppressed protein translation (Fig. 4.5E and F), NMD activation (Fig. 4.7A–D), disrupted NMD autoregulation (Fig. 4.12), and hyperactivity of NMD (Fig. 4.16M– O) were consistently demonstrated in the fibroblast cells of patients with ALS with mutations in FUS.

These mechanistic understandings support the notion that regulation of NMD and protein translation can serve as potential therapeutic targets for future development of new ALS treatment. The results also have a broader impact, since other RNA-binding proteins all undergo LLPS and form cytoplasmic granules, including TDP-43, C9ORF72 dipeptide

repeat, hnRNPA1, and TIA1 (70, 158, 159, 188). Future studies will investigate whether these proteins, which are implicated in ALS, frontotemporal dementia, and related disorders, also influence the mRNA quality control pathway and impair protein translation.

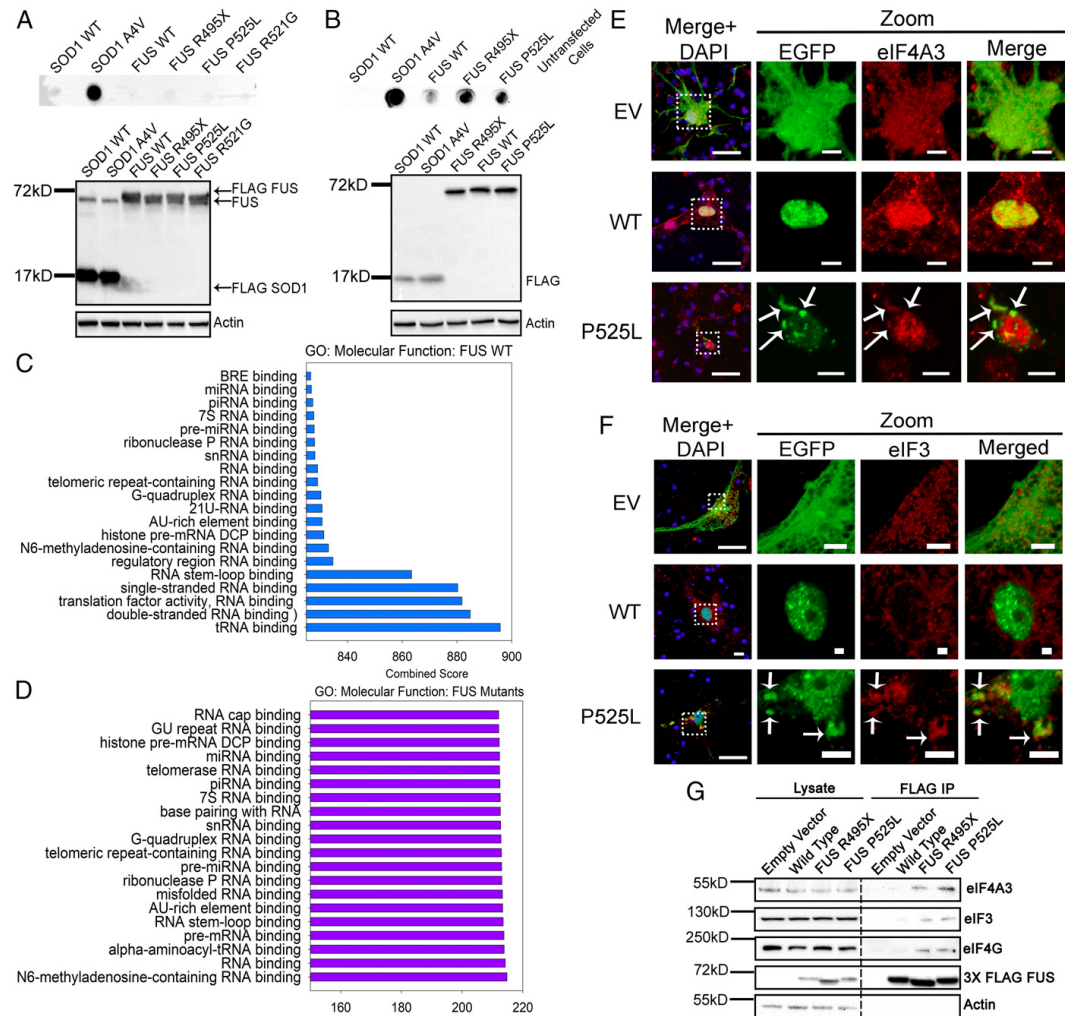


Figure 4.1

Proteomic identification, enrichment analysis, and validation of proteins in WT or mutant FUS inclusions isolated by membrane filtration. Membrane filtration, followed by dot blotting of granules isolated using the RIPA buffer (A) or the low-detergent hypotonic lysis buffer (B), was performed. The molecular function of proteins identified in WT (C) or mutant (D) FUS inclusions was analyzed using Enrichr software with the GO: Molecular Functions database. The top 20 most significant ( $P < 0.05$ ) molecular functions are represented. Immunofluorescent staining of eIF4A3 (E) and eIF3 (F) in mouse primary

Figure 4.1 Continued

cortical neurons was performed. Arrows indicate inclusions where proteins of interest are colocalized. (Scale bars: regular view, 20  $\mu\text{m}$ ; zoomed-in views, 5  $\mu\text{m}$ .) (G) FUS IP, followed by Western blot for translation initiation factors (eIF4AIII, eIF3, and eIF4G) that were uniquely identified in mutant FUS inclusions.

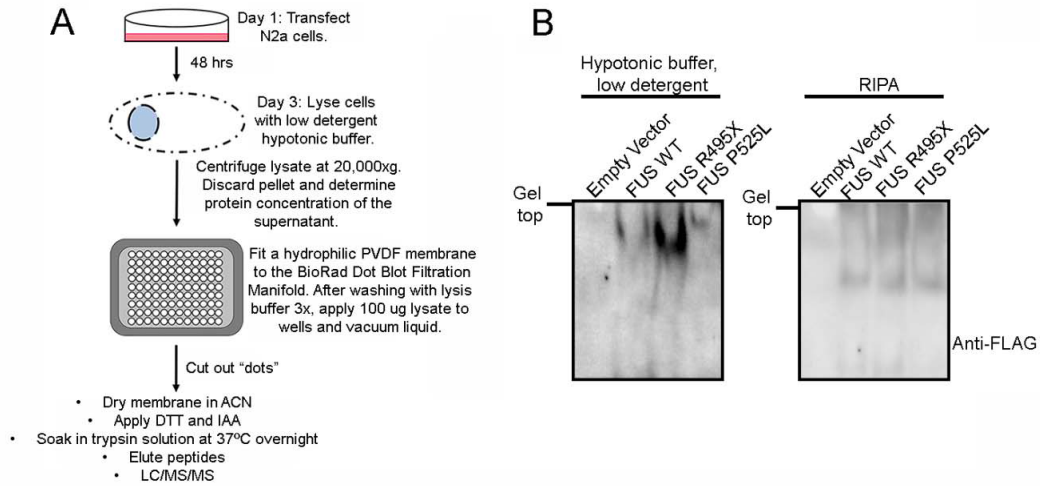


Figure 4.2

Native gel electrophoresis of FUS protein in a low detergent hypotonic lysis buffer. Workflow of the membrane filtration protocol to isolate FUS inclusions using a low detergent hypotonic lysis buffer. (B). Native gel electrophoresis to assess the migration of WT FUS and mutant (R495X and P525L) FUS in the low detergent hypotonic lysis buffer. WT and A4V mutant SOD1 were included as controls.

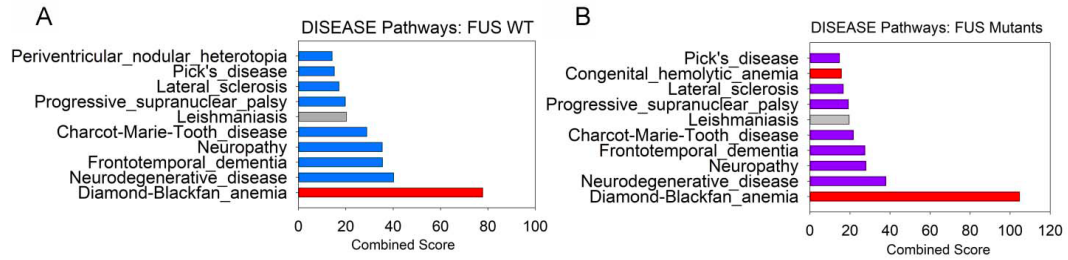


Figure 4.3

Diseases associated with proteins identified in WT (A) or mutant (B) FUS inclusions as analyzed using Enrichr software. The top 10 most significant ( $p < 0.05$ ) diseases are presented. Blue bars represent neurological or neurodegenerative diseases, while the red bar represent a ribosomopathy

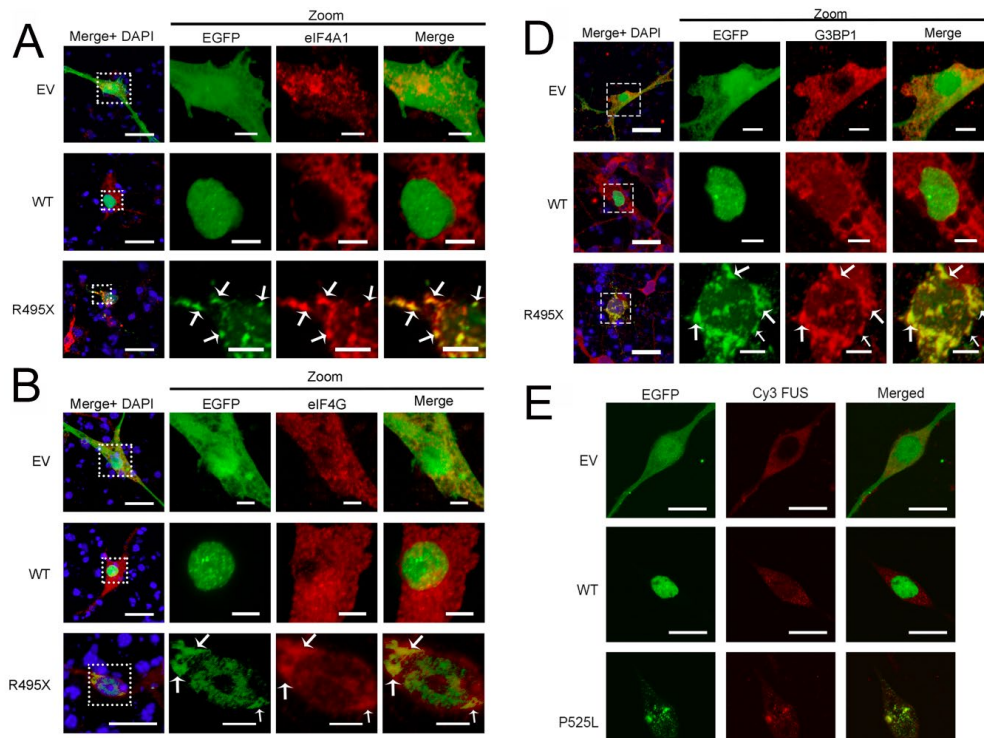


Figure 4.4

Colocalization of mutant FUS with selected proteins in mouse primary neurons (A-D) and RNA (E) in N2a cells. Immunofluorescent staining of eIF4A1 (a), eIF4G (b), RPS6 (c), and G3BP1 (d) in primary neurons transfected with EGFP-tagged WT or mutant FUS. (e). RNA FISH using an anti-FUS exon 4 RNA probe. Arrows indicate inclusions where proteins of interest are colocalized. Scale bars equal to 20  $\mu\text{m}$  in regular views and 5  $\mu\text{m}$  in zoomed views.

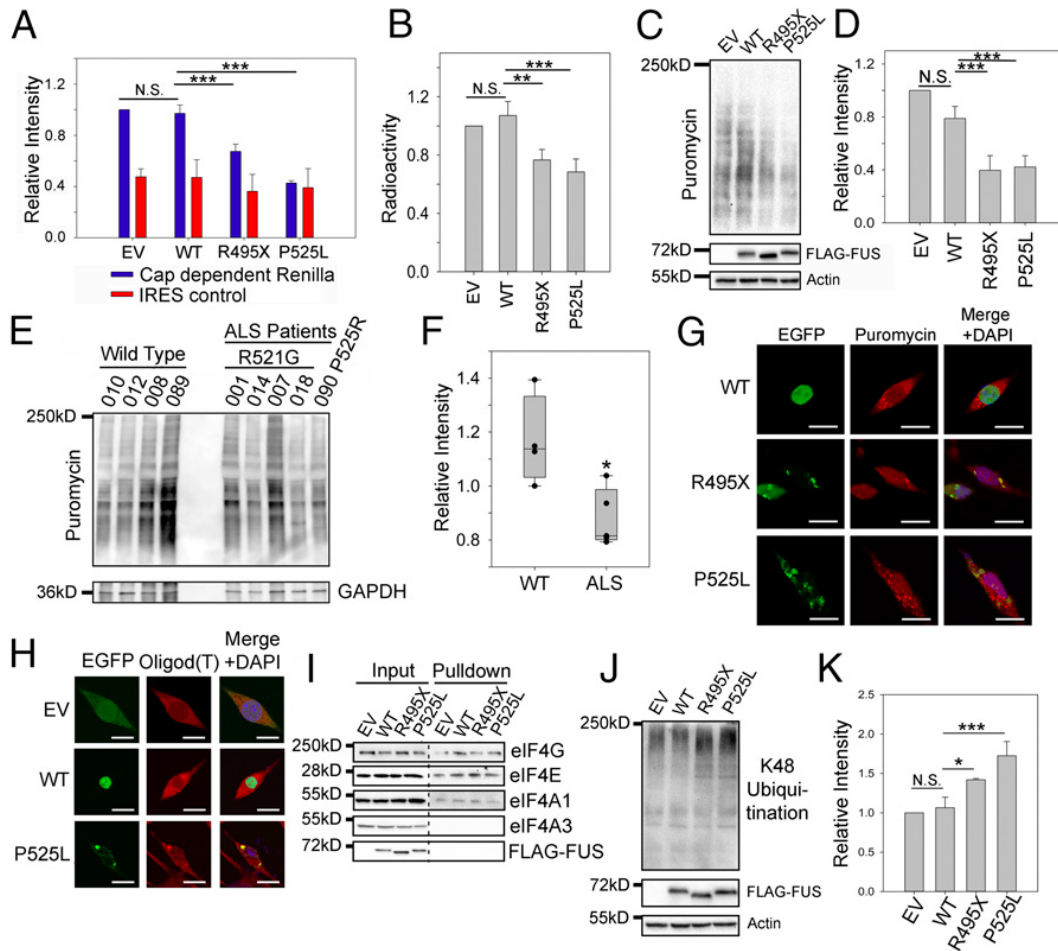


Figure 4.5

Protein translation is impaired in the presence of mutant FUS. (A) Cap-dependent translation assay using the luciferase reporter in N2a cells expressing EV, WT, or mutant FUS. Blue and red bars represent the luminescence of the Renilla cap dependent reporter and the Firefly luciferase transfection control, respectively. (B) In vitro 35S-Met incorporation assay using rabbit reticulocyte lysate mixed with N2a cell lysate containing EV, WT, or mutant FUS. After 1 h of incubation, proteins were precipitated, and radioactivity was measured using a scintillation counter. Counts were normalized to the



## Figure 4.5 Continued

EV. (C and D) SUnSET assay measuring puromycin incorporated into proteins during translation in N2a cells expressing EV, WT, or mutant FUS. Western blots of puromycinylated proteins, FUS, and actin loading control are shown in C. Quantification in D was performed using the intensity of puromycinylated proteins in each lane to normalize against Actin and EV. (E and F) SUnSET assay measuring puromycin incorporated into proteins during translation in fibroblast cells of patients with FUS ALS. Western blots of puromycinylated proteins and a GAPDH loading control are shown in E, and quantification results are shown in F. (G) Immunofluorescent staining of puromycinylated proteins in N2a cells expressing EV or EGFP-tagged WT or mutant FUS. Cells were incubated with puromycin for 30 min, fixed using paraformaldehyde (PFA), and stained with the antipuromycin antibody. (Scale bars: 20  $\mu\text{m}$ .) (H) RNA FISH using a Cy3-tagged 21-mer oligo d(T) probe in N2a cells expressing WT or mutant FUS. (Scale bars: 20  $\mu\text{m}$ .) (I) 7'MG pulldown to assess the cap binding and protein translation initiation in N2a cell lysate containing WT or mutant FUS. Various initiation complex members (eIF4E, eIF4G, and eIF4AI), FUS, and a negative control (eIF4AIII) were blotted. (J) K48 polyubiquitination in N2a cells expressing EV, WT, or mutant FUS with FUS expression and actin loading control. (K) Quantification of J using the K48 polyubiquitination intensity in each lane to normalize against actin and EV. Error bars in the figure represent SDs for three biological replicates. \* $P \leq 0.05$ ; \*\* $P \leq 0.005$ ; \*\*\* $P \leq 0.001$ . N.S., not significant. ANOVA with a post hoc Tukey honest significant difference test was used to determine P values for multiple pairwise comparisons in A, B, D, and K. A Student's t test was used to determine P values for simple pairwise comparison in F.

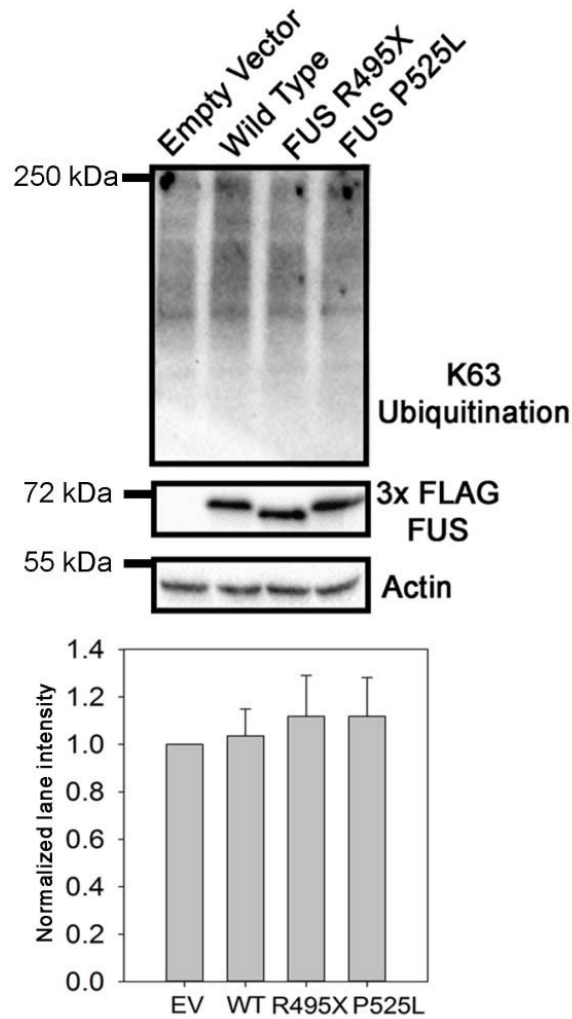


Figure 4.6

K63-linked polyubiquitination did not change in the presence of mutant FUS. (A). Western blot for K63 polyubiquitinated proteins in N2a cells transfected with WT or mutant FUS. (B). Quantification of (a) using intensities in each lane normalized against Actin and compared to EV. Error bars represent the standard deviation for three biological replicates. No statistical significance was found among samples using a Students T-test.

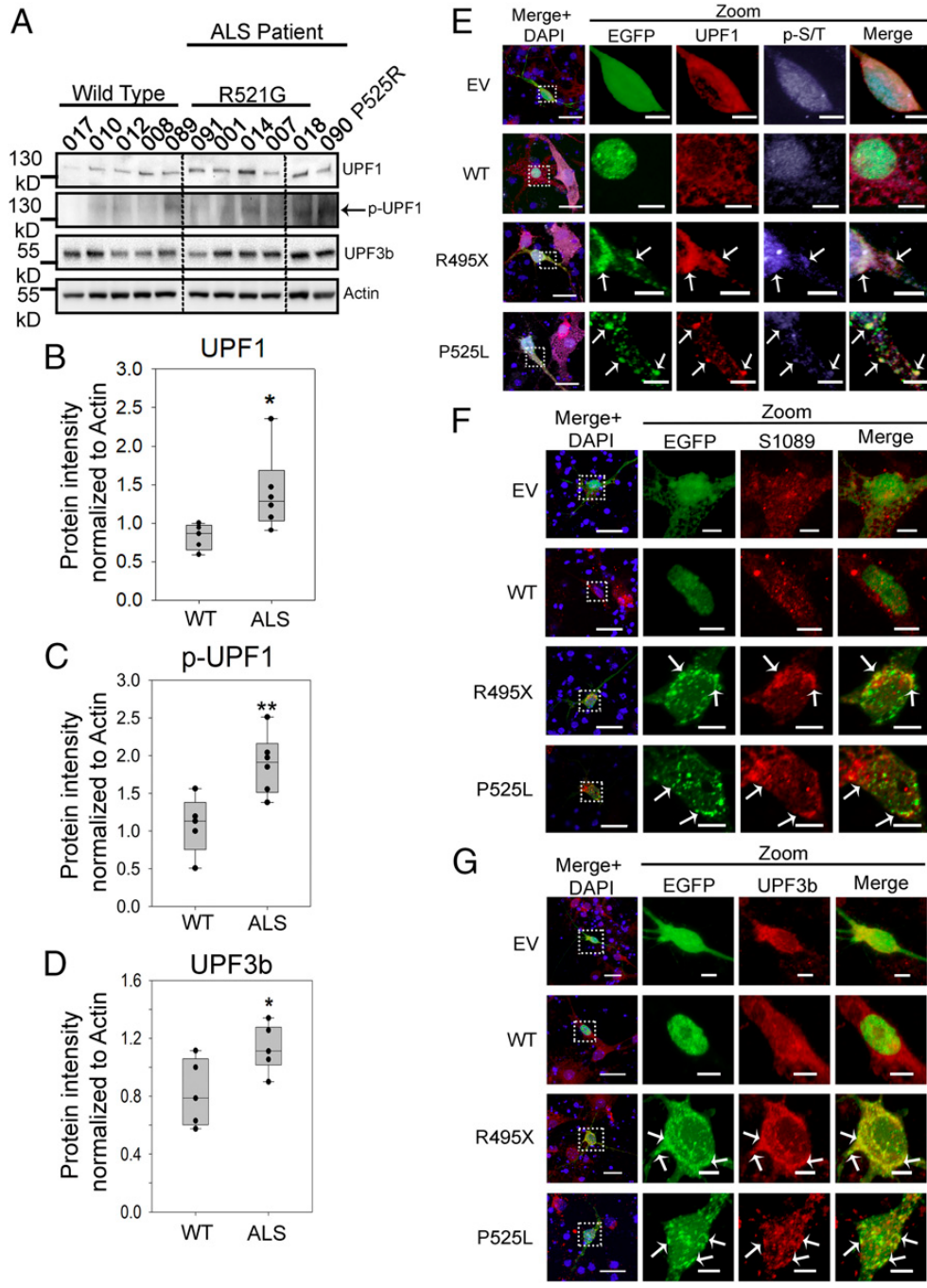


Figure 4.7

Up-regulation of pro-NMD factors in cells of patients with familial ALS and in primary neurons expressing mutant FUS. (A–D) Levels of pro-NMD factors in patients with ALS

Figure 4.7 Continued

Fig. 4.17 Continued carrying the R521G or P525R mutation and in control subjects with WT FUS. Western blots of UPF1, p-UPF1, UPF3b, and actin control were performed (A), and quantification of UPF1 (B), p-UPF1 (C), and UPF3b (D) was normalized against actin and obtained from three replicates. Error bars represent the SD between individuals. Quantifications were compared with healthy controls using a Student's t test. \* $P \leq 0.05$ ; \*\* $P \leq 0.005$ . (E–G) Immunofluorescent staining of UPF1, p-UPF1, and UPF3b in mouse primary neurons transfected with EV, EGFP-tagged WT, or mutant FUS at day 4 of in vitro culture. (E) Immunofluorescent staining of UPF1 and p-UPF1 using an anti-p-S/T ATM/AMR substrate antibody. (F) Immunofluorescent staining of p-UPF1 using an antibody against phosphor-S1089 in UPF1. (G) Immunofluorescent staining of UPF3b. Arrows indicate inclusions where proteins of interest are colocalized. (Scale bars: regular views, 20  $\mu\text{m}$ ; zoomed-in views, 5  $\mu\text{m}$ .)

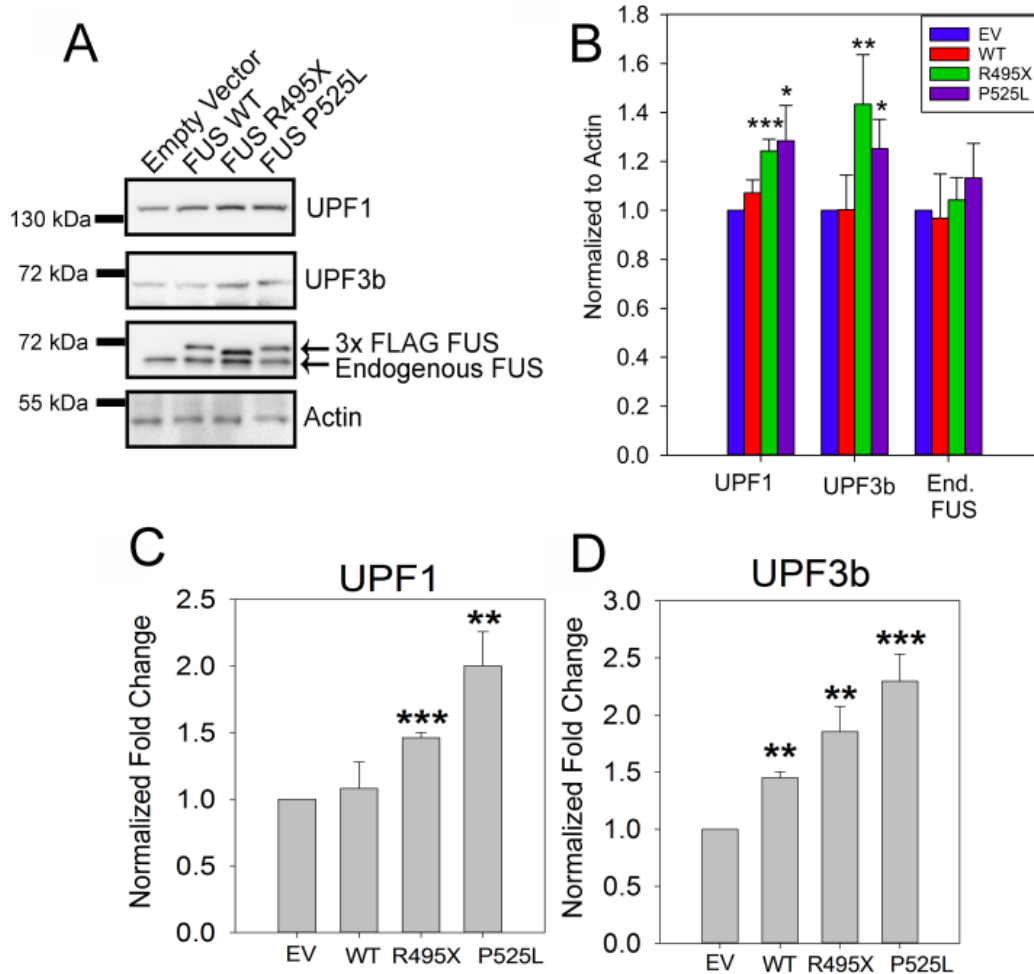


Figure 4.8

Increased protein (A-B) and mRNA (C-D) levels of UPF1 and UPF3b in N2a cells expressing mutant FUS. (A). N2a cells were transfected with WT or mutant FUS and the protein levels of UPF1 and UPF3b were assessed by SDS-PAGE followed by Western blot. (B). Quantification of UPF1 and UPF3b Western blot as normalized to Actin and compared to the EV. (C-D) qPCR quantification of the mRNA levels of UPF1 (c) and UPF3b (d) in

Figure 4.8 continued

N2a cells transfected with WT or mutant FUS. Quantification was performed using the  $\Delta\Delta C_T$  method and presented as fold changes as compared to EV. Error bars represent standard deviations for three biological replicates. P values are determined using a Students T-test. \*  $p \leq 0.05$ , \*\*  $p \leq 0.005$ , and \*\*\*  $p \leq 0.001$ .

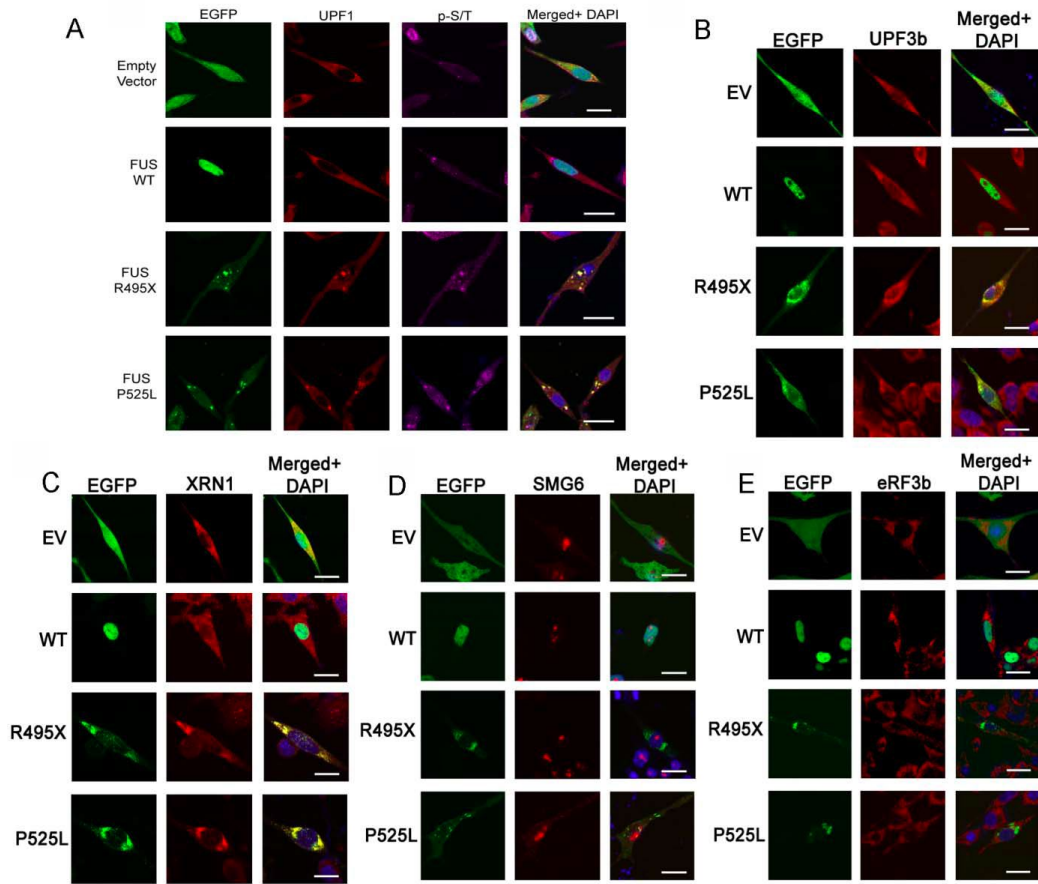


Figure 4.9

Immunostaining of NMD factors and FUS in N2a cells. N2a cells were transfected with empty vector (EV), or EGFP-tagged WT or mutant FUS, and stained for endogenous UPF1 (A), phospho-UPF1 (A), UPF3b (B), XRN1 (C), SMG6 (D), and eRF3b (E), respectively.

All scale bars equal to 20  $\mu\text{m}$ .

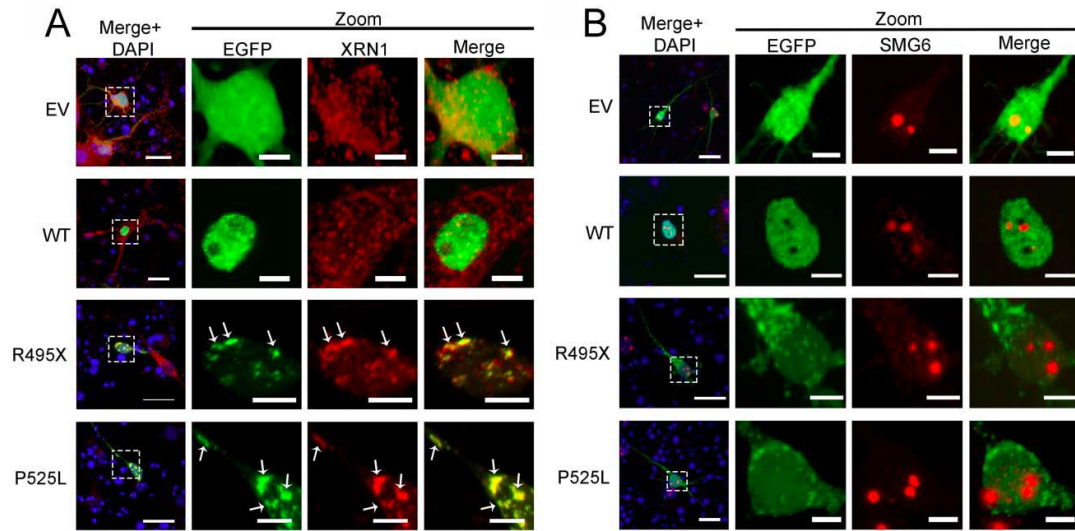


Figure 4.10

Immunostaining of XRN1 (A), SMG1 (B) and SMG6 (C) in mouse primary neurons. Mouse primary cortical neurons were transfected with empty vector (EV), or EGFP-tagged WT or mutant FUS and stained for the indicated proteins. Arrows indicate inclusions where proteins of interest are colocalized. Scale bars equal to 20  $\mu\text{m}$  in regular views and 5  $\mu\text{m}$  in zoomed views.



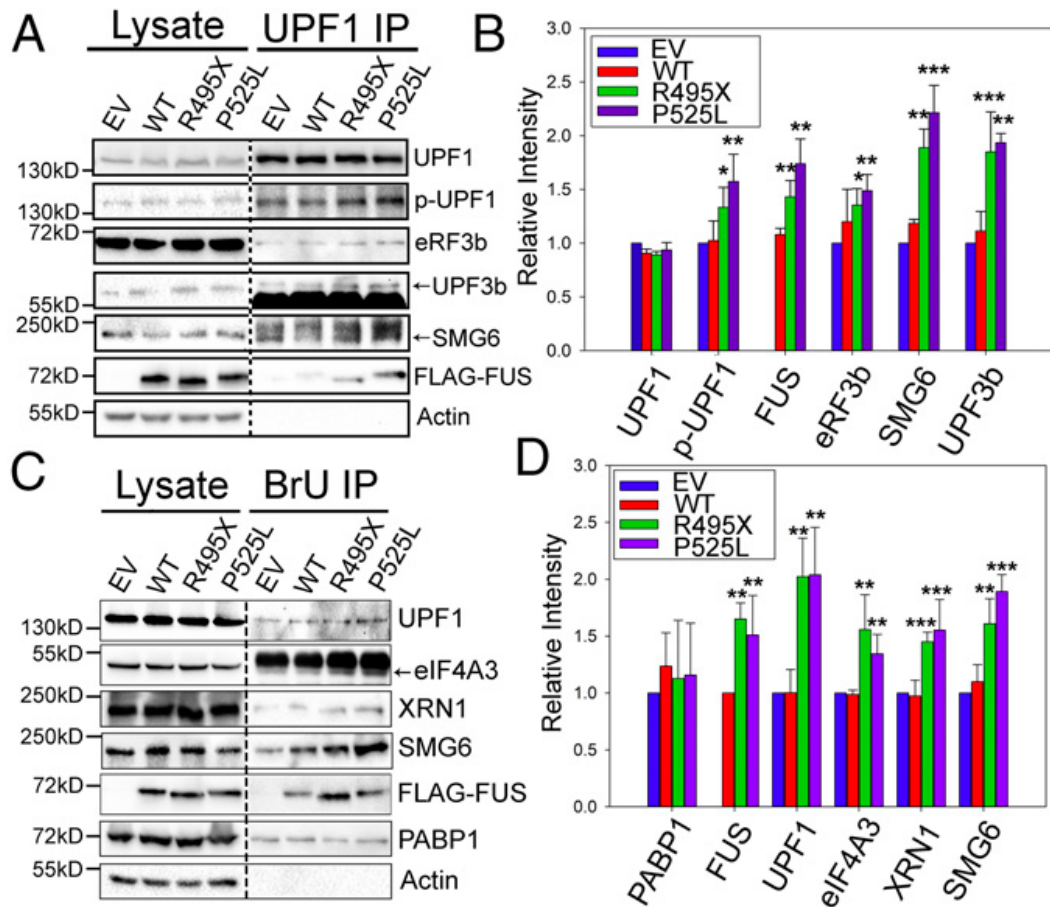


Figure 4.11

Interaction of NMD factors with UPF1 and RNAs increased in the presence of mutant FUS. (A and B) NMD factors coprecipitated with endogenous UPF1 from N2a cells expressing EV, WT, or mutant FUS. Immunoblots of UPF1, p-UPF1, eRF3b, UPF3b, SMG6, and 3 $\beta$ -FLAG-FUS are shown in A, and quantitative results are shown in B. Protein intensities were normalized to corresponding UPF1 bands and compared with EV. (C and D) NMD factors coprecipitated with BrdU-containing RNAs. N2a cells expressing

Figure 4.11 Continued

EV, WT, or mutant FUS were incubated with 1  $\mu$ M BrdU, and RNAs were UV cross-linked to proteins. BrdU IP was performed using an anti-BrdU antibody, followed by Western blots for UPF1, eIF4A3, XRN1, SMG6, FUS, PABP1, and actin. BrU, bromouridine. Quantification of proteins in C is shown in D. Proteins were normalized to the loading control, PABP1, and compared with EV. The purple, green, blue, and red bars represent EV, WT FUS, R495X FUS, and P525L FUS, respectively. Error bars represent SDs for three biological replicates. \* $P \leq 0.05$ ; \*\* $P \leq 0.005$ ; \*\*\* $P \leq 0.001$ . Quantifications were compared with EV using a Student's t test.

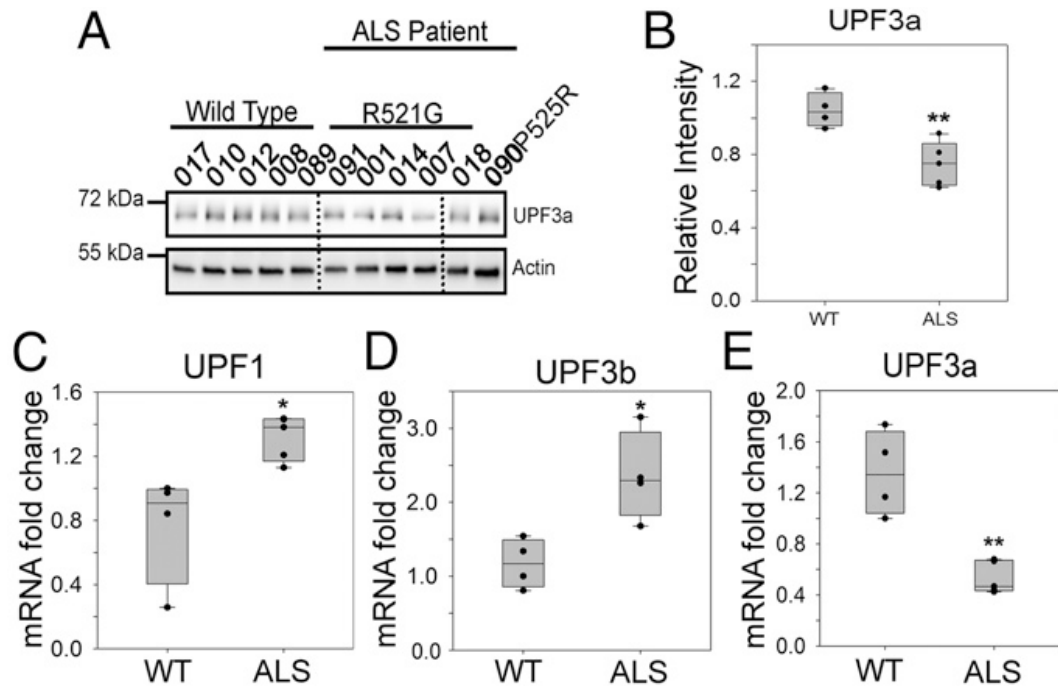


Figure 4.12

Down-regulation of the NMD negative regulator UPF3a in cells of patients with familial ALS. (A and B) Protein levels of the NMD negative regulator UPF3a in six patients with ALS and five control subjects, as shown in Fig. 3 A and B. Western blots of UPF3a and an actin control (A) and quantification of UPF3a normalized against actin (B) are shown. (C–E) Quantification of mRNA levels of dysregulated NMD factors. qPCR of UPF1 (C), UPF3b (D), and UPF3a (E) was performed using the cycle threshold method and is presented as the fold change in patients with ALS versus controls. Actin was used to normalize cycle threshold values. Error bars represent the SD between individuals. \* $P \leq 0.05$ ; \*\* $P \leq 0.005$ . Quantifications were compared with healthy controls using a Student's t test.

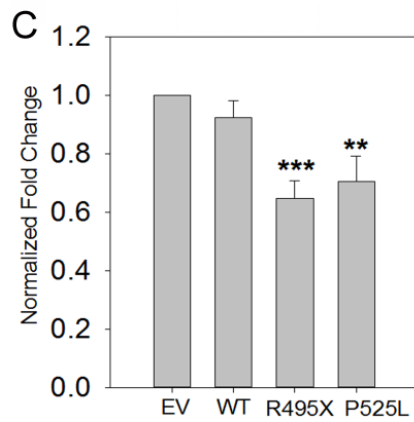
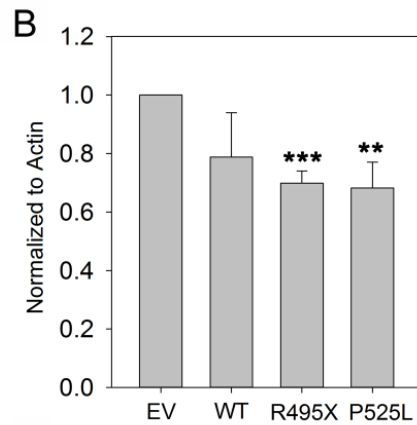
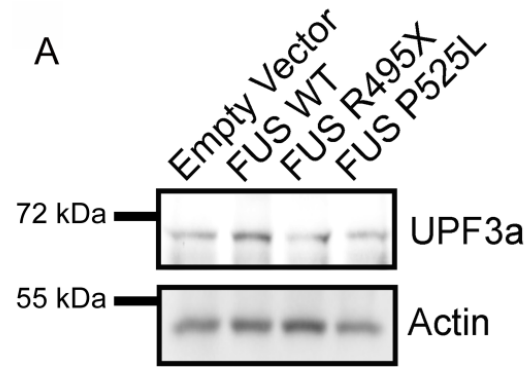
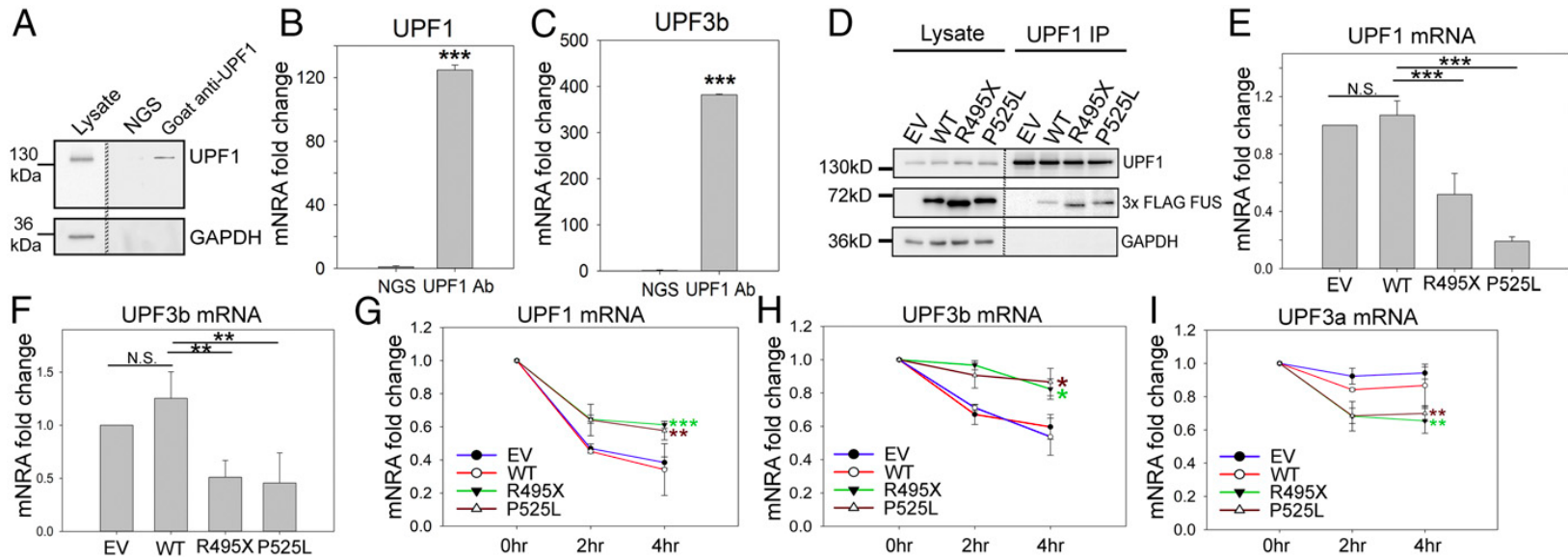


Figure 4.13

Decreased protein (A-B) and mRNA (C) levels of UPF3a in N2a cells expressing mutant FUS. N2a cells were transfected with empty vector (EV), or WT or mutant FUS and the protein levels of UPF3a were assessed by SDS-PAGE followed by Western blot. (B).

Fig. 4.13 Continued

Quantification of UPF3a Western blot as normalized to Actin and compared to the EV.  
(C). qPCR quantification of the mRNA levels of UPF3a in N2a cells transfected with WT or mutant FUS. Quantification was performed using the  $\Delta\Delta\text{Ct}$  method and presented as fold changes as compared to EV. Error bars represent standard deviations for three biological replicates. \*\*  $p \leq 0.005$ , and \*\*\*  $p \leq 0.001$ . Students T-test was used to determine p values.



104

Figure 4.14

Disruption in the NMD autoregulation loop. Endogenous UPF1 IP from N2a cells was performed, followed by Western blot (A) and qPCR measurement of UPF1 (B) and UPF3b (C) mRNAs. N2a cell lysate was subjected to IP using normal goat serum (NGS) or goat anti-UPF1 antibody. The IP samples were aliquoted for Western blot (A) and qPCR quantification (B and C) comparing RNA coprecipitated with UPF1 protein versus NGS control. UPF1 IP from N2a cells expressing EV, WT, or mutant FUS was performed, followed by Western blot (D) and qPCR measurement of UPF1 (E) and UPF3b (F) mRNAs. UPF1, FUS, and GAPDH were assessed by Western blot, as shown in D. qPCR quantification was normalized to UPF1 protein precipitate

Figure 4.14 Continued

and presented as fold change compared with EV. Turnover rates of UPF1 (G), UPF3b (H), and UPF3a (I) mRNAs in N2a cells expressing EV, WT, or mutant FUS are shown. Actinomycin D or DMSO control was added 2 or 4 h before harvesting for RNA isolation. Individual mRNAs of interest were quantified by qPCR, normalized against RPL13a, and presented as fold change versus DMSO treatment over time. Error bars represent the SD from three replicates. \* $P \leq 0.05$ ; \*\* $P \leq 0.005$ ; \*\*\* $P \leq 0.001$ . N.S., not significant. ANOVA with a post hoc Tukey honest significant difference test was used in E–I, and a Student's t test was used in B and C.

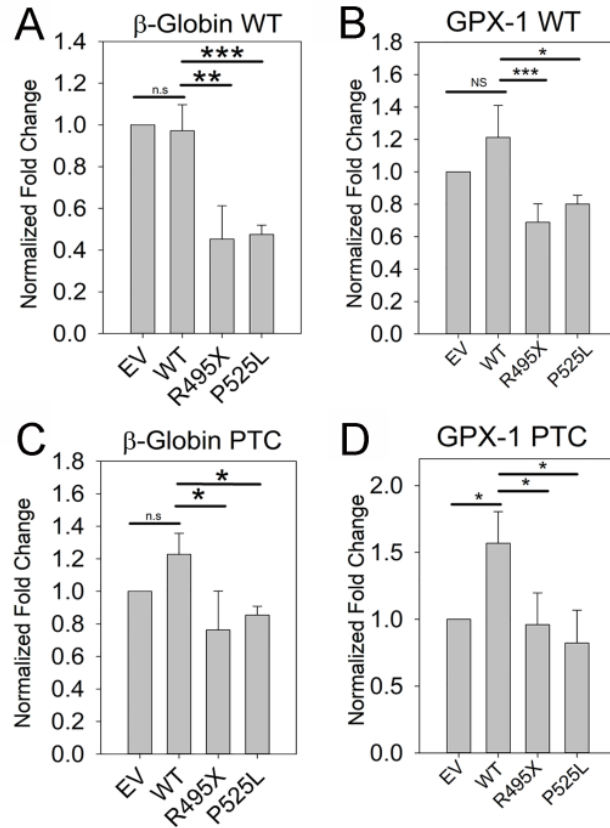


Figure 4.15

The NMD activity in the presence of WT or mutant FUS using an NMD reporter assay.

NMD activity assay was carried out using the WT  $\beta$ -globin (A), WT GPX-1 (B),  $\beta$ -globin PTC (C), or GPX-1 PTC (D) reporter. N2a cells were cotransfected with empty vector (EV), or WT or mutant FUS and an NMD reporter as indicated. The levels of the indicated reporter transcript were quantified by qPCR using the  $\Delta\Delta\text{Ct}$  method. The fold changes as compared to EV are presented. ANOVA with post hoc Tukey HSD test was used to determine p-values for multiple pair-wise comparisons.



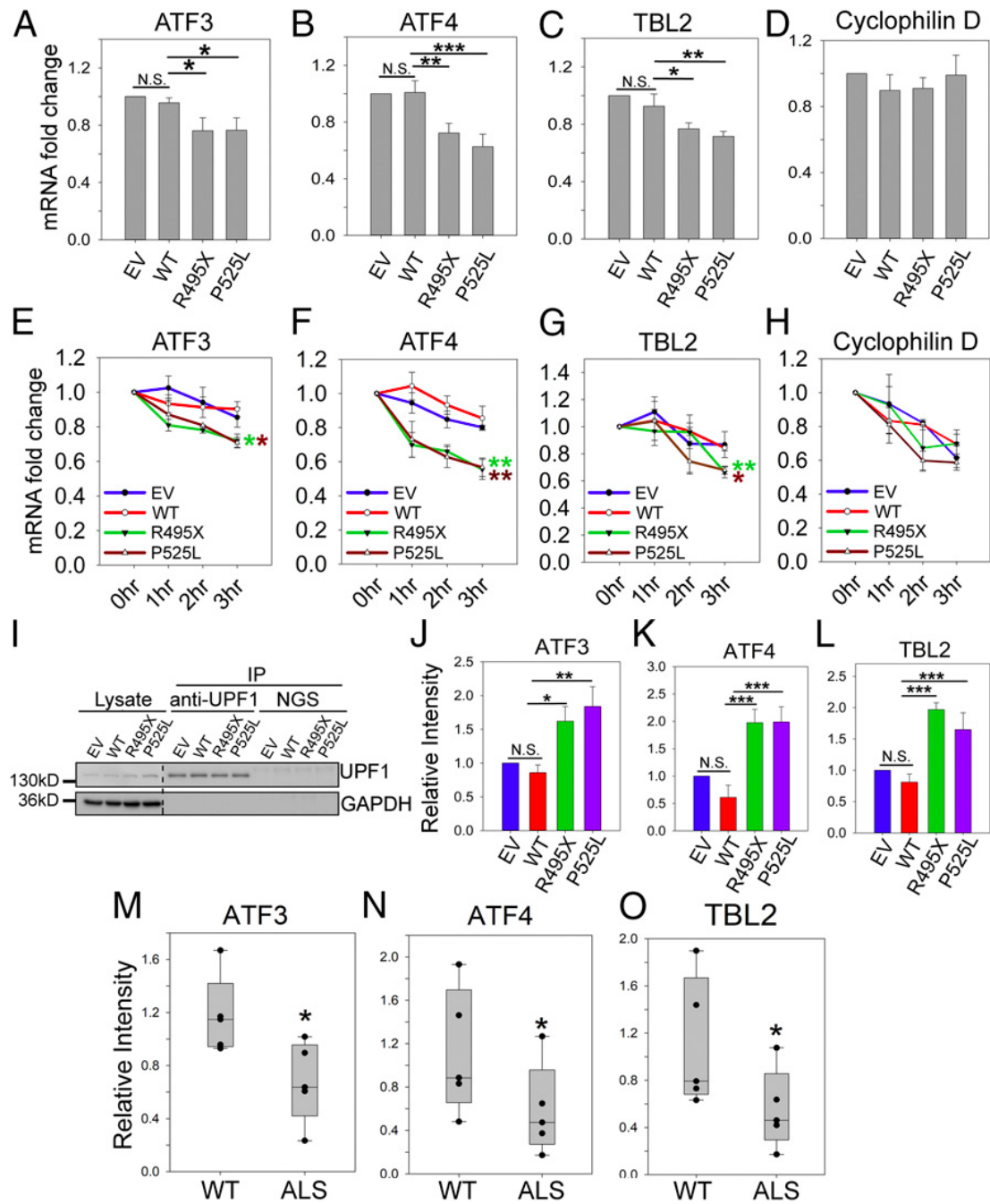


Figure 4.16

Enhanced NMD activity in the presence of mutant FUS. The mRNA levels of ATF3 (A), ATF4 (B), TBL2 (C), and cyclophilin D (D) in N2a cells transfected with EV, WT, or

Figure 4.16 Continued

mutant FUS were determined. The levels of the indicated mRNA were quantified by qPCR using the cycle threshold ( $\Delta\Delta\text{CT}$ ) method, and the fold changes compared with WT are presented. Turnover rate of ATF3 (E), ATF4 (F), TBL2 (G), and cyclophilin D (H) mRNAs in N2a cells expressing EV, WT, or mutant FUS after treatment with actinomycin or DMSO control. Individual mRNAs of interest were quantified by qPCR, normalized against RPL13a, and presented as fold change versus DMSO treatment over time. Error bars represent the SD from three replicates. (I–L) Amount of ATF3, ATF4, and TBL2 mRNA bound to the UPF1 protein. N2a cells were cotransfected with EV, WT, or mutant FUS and an NMD reporter as indicated. After UPF IP, Western blot (I) demonstrates levels of UPF1 in lysate and IP samples. The levels of ATF3 (J), ATF4 (K), and TBL2 (L) mRNA in the UPF1 IP samples were quantified by qPCR using the  $\Delta\text{CT}$  method. The fold changes normalized to WT are presented from three replicates. The mRNA levels of ATF3 (M), ATF4 (N), and TBL2 (O) in fibroblast cells derived from patients with familial ALS carrying FUS mutations and healthy WT controls are shown. \* $P \leq 0.05$ ; \*\* $P \leq 0.005$ ; \*\*\* $P \leq 0.001$ . N.S., not significant. ANOVA with a post hoc Tukey honest significant difference test was used to determine P values in A–L. A Student's t test was used to determine P values in M–O.

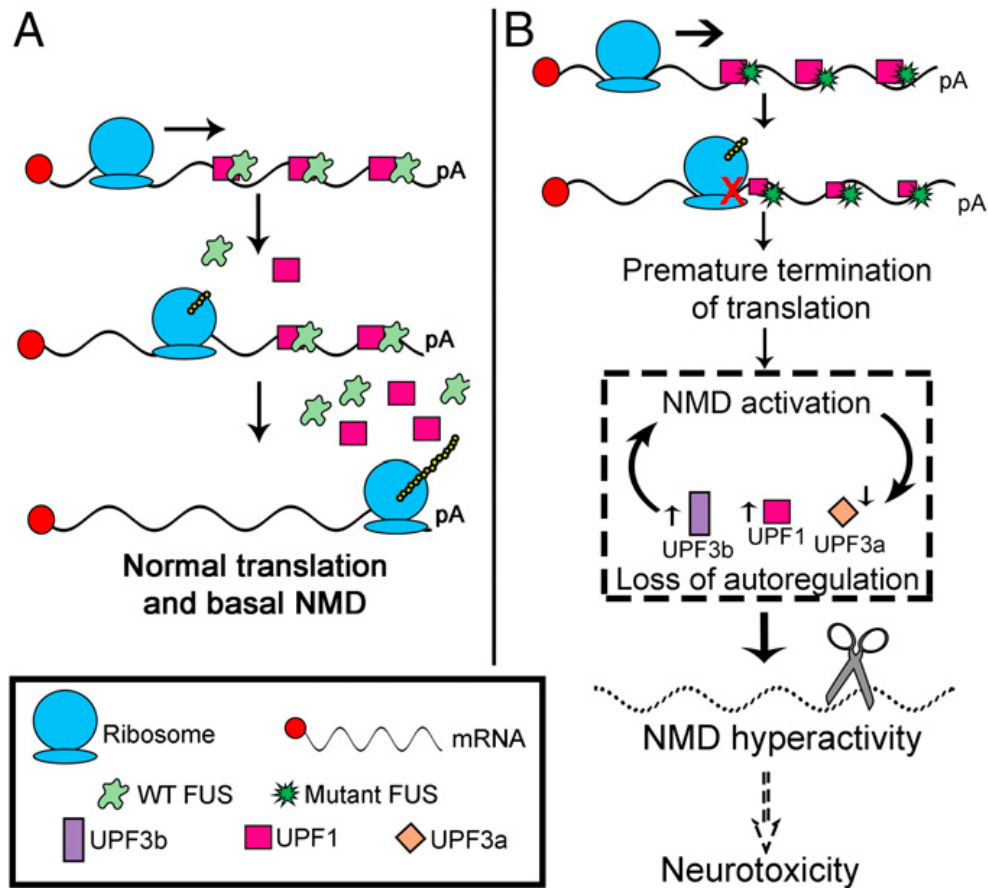


Figure 4.17

Model illustrating how mutant FUS impairs NMD regulation and suppresses protein translation. (A) Normal translation and basal NMD under physiological conditions with WT FUS. (B) Mutant FUS has greater binding ability to mRNAs and associated proteins, including UPF1, leading to ribosomal stalling, translation termination, and subsequent activation of NMD. Up-regulation of pro-NMD factors (UPF1 and UPF3b) and down-regulation of the molecular brake (UPF3a) cause the loss of autoregulation and hyperactivity of NMD. pA, poly(A) tail.

## CHAPTER 5. THE ROLE OF ENDOGENOUS FUS IN NONSENSE MEDIATED DECAY

### 5.1 Introduction

FUS is a member of the FET family of DNA- and RNA-binding proteins that are primarily localized to the nucleus. FUS forms dynamic ribonucleoprotein granules in the nucleus to maintain efficacious transcription and splicing (2, 13, 20, 21, 29, 37-39, 45, 52, 53, 113, 160, 169, 206-209). In contrast, ALS-related mutations in FUS cause its accumulation in the cytoplasm and the formation of inclusion bodies. These granules can lead to the formation of inclusion bodies and potentially contribute to neurotoxicity (2, 3, 156). However, whether the formation of these inclusions and neurotoxicity are due to loss of function or a toxic gain of function when FUS is mutated remains to be understood. To clarify the cellular consequences of FUS mutations, utilization of FUS knockout (KO) systems are critically important. FUS KO cells and mice provide a platform to observe the biochemical and physiological outcomes of the loss of FUS in a wide variety of cell types across the central nervous system.

Understanding the repercussions of FUS (KO) in a neuronal system are essential for determining FUS' major role causing ALS. While FUS KO result in embryonic lethality (210-212), conditional KO after birth does not cause motor neuron dysfunction, as homozygous mice did not exhibit an ALS phenotype (210). FUS KO has been demonstrated to have detrimental impacts on the behavior and brain structure of mice (210). Affected mice displayed hyper-activity and anxiety-like behavior but did not display defective Gem morphology previously observed (206, 207, 213). Demonstration of an FTD

phenotype without a disruption in motor function is illustrative of important transcriptome changes that may be brain-region and cell-type specific (210).

KO of FUS has been used as a cell-based tool to better understand if ALS-related mutations in FUS contribute to a gain or loss of function of the protein. FUS' role in splicing has been well defined using KO cells and animals. Splicing changes that occur when FUS is knocked out has been well described and compared in detail to changes that occur in FUS mutants (206). Overall, loss of FUS results in gross changes to the transcriptome due to loss of Gems, and therefore reduced levels of snRNPs. Reduced snRNP levels are likely to contribute to changes in gene expression. In this regard, loss of FUS greatly mimics FUS mutations, as the presence of FUS in the nucleus is required for normal splicing. RNA seq using FUS knockdown in human fibroblasts demonstrates reduction of splicing factors, as well as other important genes for neuronal function (40). These data imply that mutations in FUS result in a nuclear loss of function.

Recently, studies to examine FUS' cytoplasmic role have begun to demonstrate its importance in translation and maintenance of RNA stability (67, 214). These studies bring additional complexity as to whether mutations in FUS are a loss of function or toxic gain of function. For example, consistent changes in gene expression lead to changes in particular protein levels. WT FUS and ALS mutants have been demonstrated to interact with translation factors (214) and FUS inclusions have been demonstrated to hinder translation in both cellular and animal models (67, 214). Mechanistically, how FUS regulates and interacts with proteins within these processes has remained to be better defined, but deeper biochemical studies may yield clues as to the nature of their interaction

and how they contribute to ALS. Additionally, studies exploring mutant FUS' role in activation of mRNA degradative pathways raised the question as to whether WT FUS plays a role in maintaining the balance of nonsense mediated decay (NMD). NMD serves as a post-initiation regulatory step for protein translation and is initiated due to errors and regulatory elements within mRNA, as well as when protein translation is stalled (164).

In our exploration of how mutations in FUS initiate NMD, we observed a novel interaction between WT FUS and UPF1. However, overexpression of WT FUS does not perturb the pathway, it is possible that endogenous FUS may be important for regulation of UPF1 activity and NMD. Based on publicly available CLIP data (215), FUS has been reported to interact with UPF1 mRNA, as well as the mRNA of UPF2, UPF3a, UPF3b, SMG1, SMG5, SMG6, SMG7, and SMG8. It is worth noting that these RNA species are auto-regulated through the NMD pathway. Therefore, we hypothesized that one of FUS' endogenous functions is to aid in autoregulation of NMD. Using N2A stable FUS knockout cells (termed NCF in this chapter), we probed for basic changes in NMD regulation and function. Specifically, we examined the steady state levels of NMD factors and substrates, UPF1 interaction with effector proteins, and the stability of NMD factors.

## 5.2 Results

### 5.2.1 FUS Binds NMD Factor mRNA

The availability of large data sets through CLIPdb has allowed us to examine potential mRNA targets that FUS protein may bind (215). We initially probed the database for FUS' interaction with NMD factor mRNA that is also subject to autoregulation through

the pathway. We found that FUS has been reported to bind to UPF1, UPF2, UPF3a, UPF3b, SMG1, SMG5, SMG6, SMG7, and SMG8 mRNA. The stabilities mRNA species are autoregulated through the NMD pathway (184). Our first experimental step in understanding endogenous FUS' role in NMD was to confirm the CLIPdb FUS/mRNA interaction results (215). We selected five critical NMD factor's mRNA to examine: UPF1, UPF2, UPF3b, SMG6, and SMG7. Using a FUS RNA IP, we immunoprecipitated FUS protein and using rt-qPCR, we measured the mRNA levels of the selected RNA species bound to FUS. We demonstrated that the results found in the CLIP data base were consistent with our qPCR data, with the exception of UPF1 mRNA (data not shown), which we found did not interact with FUS. This may be due to cell type differences, however. FUS bound UPF3b (Fig. 5.1A), UPF2 (Fig. 5.1B), SMG6 (Fig. 5.1C), and SMG7 mRNA (Fig. 5.1D). These results indicate that FUS may regulate NMD factors levels through mRNA binding, with the exception of UPF1. List of additional primers used are attached in Supplemental table A.

### 5.2.2 FUS Binds NMD Substrate mRNA

In addition to using the CLIP database to identify NMD factor mRNA that binds FUS, we also probed for NMD substrates that may interact with the FUS protein. We searched CLIPdb (215) and found that FUS protein was previously published to bind ATF3, ATF4, and TBL2 mRNA. We next wanted to examine FUS' binding with natural NMD substrate mRNA: ATF3, ATF4, and TBL2 experimentally. We previously found that ALS-related mutations in FUS facilitated NMD decay these substrates (214), however the interactions between FUS and these mRNA substrates was not examined. Using a FUS

RNA immunoprecipitation, we pulled-down mRNA bound to FUS protein and used rt-qPCR to measure the levels of mRNA binding. We discovered that FUS binds all three of these mRNA species. While the levels of binding are not particularly high in ATF3 (Fig. 5.2A) and TBL2 (Fig. 5.2C), they are still significantly higher than the FUS KO (NCF) background control. FUS bound ATF4 mRNA as well (Fig. 5.3B). It should be noted that the qPCR data presented were generated from the same set as the previous set of FUS RNA IPs (Fig. 5.1) and therefore have the same western blot demonstrating effective immunoprecipitation (Fig 5.2D). We conclude that endogenous FUS binds NMD substrate mRNA, however, a more comprehensive list of substrates may be identified through RNA-Seq. Overall, we can conclude that FUS does bind these NMD substrates and therefore, may play a role in maintaining their regulation and gene expression.

### 5.2.3 FUS Knockout Downregulates Pro-NMD Factor Proteins

Following up on FUS' binding to NMD factor mRNA, we hypothesized that FUS would have an influence on the steady state levels of the selected proteins. Thus, we examined whether the steady state protein levels are changed when FUS is knocked out and whether they are rescued when FUS is re-expressed. Western blots demonstrated modest reductions of SMG1, SMG5, SMG6, SMG7 (Fig. 5.3A), UPF1, UPF3a, and UPF3b (Fig. 5.3B) protein levels. Protein levels of eIF4A3, RNPS1, and actin (Fig. 5.3C) did not change at the protein level. Interestingly, XRN1 proteins was significantly reduced in the FUS KO cells by approximately 10% (Fig. 5.3C). Western blots were quantified and represented Fig. 5.3D. We observed a rescue of protein levels when FUS was re-expressed, strongly indicating that knockout of FUS is directly responsible for reductions in protein



levels. These data imply that FUS' interaction with NMD factor mRNA (Fig. 5.1) may play a role in regulating the protein levels of NMD factors through RNA binding.

#### 5.2.4 FUS KO Reduces NMD Complex Assembly

Decreased protein levels of NMD factors led us to question if the NMD pathway activity is reduced when FUS is knocked out. A readout for the pathway activity is to examine NMD complex formation. Thus, we performed a UPF1 IP and western blotted for core NMD factors. We observed reduced interaction between UPF1 and UPF3b, SMG6, SMG7, and UPF2 (Fig. 5.4A, B) indicating that NMD complex levels in FUS KO cells are reduced as compared to WT N2A cells but rescued by re-expressing WT FUS. These data suggest two possible reasons for a reduction in complex assembly: 1) FUS protein is required for complex formation and/or 2) FUS KO's reduction in NMD factor protein levels directly translates into reduced complex formation. It appears as though NMD activity may be suppressed due to reduced levels of effector proteins and their effector complexes.

#### 5.2.5 FUS Knockout Downregulates Pro-NMD Factor mRNA

To determine if FUS KO's changes in NMD factor protein levels are due to decreased mRNA levels, we examined the steady-state levels of NMD factor mRNA. We performed rt-qPCR to examine mRNA levels of UPF1, UPF2, UPF3b, and SMG1 (Fig. 5.5A-D). We observed depressed mRNA levels of NMD factors, with modest to complete rescue by re-expression of WT FUS. Levels of XRN1, eIF4A3, and CyclophilinD mRNA (Fig. 5.5E-G) did not change. These data suggest that FUS binds NMD factor mRNA and

maintains mRNA levels, and that KO results in reduced mRNA and protein levels. We conclude that FUS is required for maintenance of NMD factor mRNA levels.

#### 5.2.6 Stability of NMD Factors is Unchanged when FUS is Knocked Out

As we observed reductions in steady state levels of NMD factor mRNA and proteins, we hypothesized that these mRNAs would have reduced stability and higher turnover in the absence of FUS. We examined the stability of UPF1, UPF3b, SMG6, and SMG7. Using an actinomycin D time course assay paired with rt-qPCR, we found that the stability of UPF1, UPF3b, SMG6, and SMG7 are unchanged (Fig. 5.6A-D), and therefore the decay of these NMD factors was not impacted by the loss of FUS. These results were unexpected but yielded very interesting information on how FUS regulates NMD. These data, in combination with the reduced steady state mRNA levels (Fig 5.5) suggest that FUS regulates NMD factor expression at the transcriptional level. Furthermore, this stability data and steady state data demonstrate that the nuclear function of FUS (e.g. transcription regulation) may impact its cytoplasmic functions and pathways (e.g. regulation of NMD or translation).

#### 5.2.7 FUS KO Reduces UPF1 Binding to NMD Factor mRNA

In previous studies we identified WT FUS as a novel binding partner for UPF1 (214). UPF1 is a dynamic protein that acts as an RNA helicase with ATPase activity that regulates its binding affinity to RNA. Additionally, it serves as a binding platform for other NMD effector proteins (162, 163). Better understanding of the dynamics between FUS and UPF1 may help us understand how FUS participates in NMD. UPF1's RNA binding ability

is critical to its function in triggering NMD (185). To understand how FUS KO impacts UPF1's RNA binding ability, we performed a UPF1 RNA IP. UPF1 protein was used as bait and was pulled down with bound RNA. We used rt-qPCR to measure the binding of the following mRNA species: UPF1, UPF3b, UPF2, SMG6, and SMG7 (Fig. 5.7A-E). FUS KO reduced UPF1 binding to all selected mRNA, including FUS mRNA itself. Moreover, re-expression of WT FUS rescued UPF1 binding to the selected mRNA. Western blot confirming UPF1 Immunoprecipitation can be found in Fig 5.9 since the same UPF1 RNA IP samples were used for both sets of experiments in Fig 5.7 and 5.9.

It is likely that FUS plays an important role in mediating UPF1/RNA interaction. Based on our selected mRNA, it is possible, that NMD autoregulation is shifted toward pathway upregulation by FUS KO. Upregulation of NMD would be logical due to splicing defects that occur when FUS is lost. However, FUS KO could also cause reduced transcription of NMD factors. Thus, the data are complex and cannot be explained simply by shifted NMD autoregulation alone.

#### 5.2.8 NMD Substrate mRNAs are Stabilized when FUS is Knocked Out

Our observation of reduced complex NMD formation (Fig 5.4) led us to question if the NMD pathway is functional when FUS is knocked out. Thus, we examined the stability of selected NMD substrates ATF3, ATF4, and TBL2 in FUS WT, KO, and re-expression cells. Using an actinomycin D time course assay paired with rt-qPCR, we found that ATF3, ATF4, and TBL2 (Fig. 5.8A-C) were stabilized when FUS is knocked out, suggesting reduced NMD activity. The stability of CyclophilinD, our control, remained consistent regardless of the presence of FUS (Fig. 5.8D). Additionally, re-expression of

FUS rescued the stabilization of these RNA species. These data suggest that FUS KO does result in reduced NMD activity. Downregulation of NMD factors and associated complexes would result in increased expression of ATF3, ATF4, and TBL2 through their stabilization.

#### 5.2.9 FUS KO Reduces UPF1 Binding to NMD Substrate mRNA

Probing into UPF1's binding ability to NMD substrates when FUS is knocked out may help us understand if FUS plays a role in target differentiation, thus we performed a UPF1 RNA IP to understand how FUS KO impacts UPF1's RNA binding ability to NMD substrate mRNAs. After UPF1 protein was pulled down we used rt-qPCR to measure the binding of the following mRNA species: ATF3, ATF4, and TBL2. FUS KO reduced UPF1 binding to all selected mRNAs (Fig. 5.9A-C), re-expression rescued UPF1 binding. It is noted that the UPF1 RNA IP in Fig 5.7 and 5.9 share the same western blot. The results suggest that the interaction between UPF1 and NMD substrates may require FUS for efficacious NMD, consistent with increased mRNA stabilities in Fig 5.8.

#### 5.2.10 Natural NMD substrate levels are influenced by FUS KO

With the reduced mRNA and protein levels of NMD factors (Fig. 5.3 and 5.5), reduced NMD complex formation (Fig. 5.4), reduced UPF1 binding to NMD substrates (Fig. 5.9), and increased mRNA stabilities of NMD substrates (Fig. 5.8), we would expect increased mRNA levels of these NMD substrates when FUS is knocked out. Thus, we measured the steady state levels of the NMD substrates previously published (214): ATF3, ATF4, and TBL2, as well as ATF6 and GADD45B (186). Surprisingly, the steady state

mRNA levels appear to be complex. For ATF3 (Fig. 5.10A), there was a modest, but insignificant increase in mRNA levels and reduction when FUS was re-expressed. While this followed the proposed trend, it was not statistically significant. ATF4 and TBL2 (Fig. 5.10B, D) saw increased mRNA levels when FUS was knocked out, but upon re-expression mRNA levels increased further. ATF6 levels decreased following FUS KO and transcript levels partially recovered following rescue (Fig. 5.10C). GADD45B (Fig. 5.10E) demonstrated reduction of mRNA levels when FUS was knocked out and then further reductions when FUS was re-expressed. These results obviously are inconsistent with the above hypothesis solely based on NMD alone. The results suggest that FUS' influence over the expression specific genes is more complicated than regulation of mRNA stability through NMD alone. It is likely that FUS' ability to regulate gene expression is a gene-specific mixture of its function in transcription, RNA splicing, RNA export, translation, and stability.

### 5.3 Conclusions and Future Directions for FUS KO/ NMD Study

Overall, the results of this small study are promising, however, more work needs to be done to fully develop a mechanism by which endogenous FUS regulates NMD factor expression and its impact on downstream substrate stability. In our preliminary examination of FUS' role, we aimed to demonstrate its function in modulating the expression NMD factor genes through the NMD pathways autoregulation. However, FUS' cellular function is complex and encompasses nearly every aspect of canonical gene expression: transcription, splicing, translation, and mRNA stabilization. We were able to establish that FUS likely controls the expression of major NMD factors through

transcription, as KO of FUS does not impact the stability of their mRNA but reduces the steady levels of mRNA and proteins. We observed increased stability of endogenous NMD substrate, however, steady state levels of these mRNAs indicate that FUS may play a more intricate role in their expression as well.

Future studies to expand on these data should include both quantitative LC MS/MS and RNA-seq studies to examine changes in the protein and mRNA repertoire that occur when FUS is knocked out. Recently, studies exploring why motor neurons are uniquely susceptible to degeneration demonstrated vast differences in the proteome compared to oculomotor neurons, a subtype of motor neurons unaffected by disease. Downregulation of “supersaturated” proteins, including ion channels and proteins related to RNA metabolism contribute to neuronal dysfunction (216). Comparison of proteins and mRNA lost upon FUS KO to those known to be supersaturated may provide important clues as to which proteins are most heavily impacted. Functional and mechanistic experiments following up these large-omic studies may include deeper dives into molecular pathways negatively impacted by both loss of FUS and ALS.

Additionally, studies exploring the biochemical and molecular interaction between UPF1 and FUS will be critical for understanding UPF1’s newly described role in the nucleus and in ALS(217). A recently published study illustrates a novel aspect of UPF1 function in the nucleus that seems to mirror FUS’. Like FUS, UPF1 has been demonstrated to cluster with nascent transcripts, and RNAP II and III (14, 106, 217). Similarly, UPF1 demonstrated to be important for efficient polyadenylation and release of new transcripts, RNP assembly, and RNA export. Deeper exploration into the interactions between UPF1

and WT or mutant FUS (214) (Fig 5.9D) will likely yield important information as to how FUS directly plays a role in NMD and how mutants disturb the pathway.

We conclude that endogenous FUS plays an important role in mediating NMD activity through transcriptional regulation of NMD factors (Fig 5.3, 5.5, and 5.6). This is supported by the stabilization of endogenous NMD substrates ATF3, ATF4, and TBL2 when FUS is knocked out (Fig 5.8). In addition, FUS appears to regulate mRNA levels at different levels in fine tuning the final mRNA and protein levels of these genes.

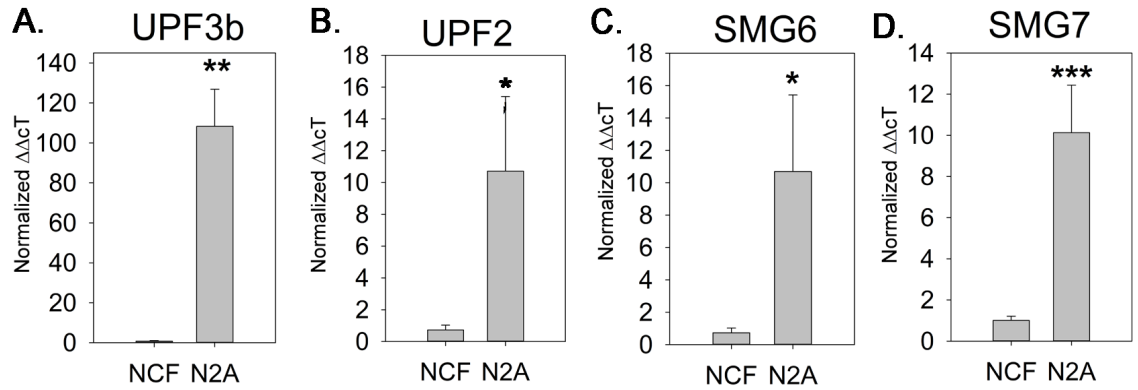


Figure 5.1 Endogenous FUS binds key NMD factor mRNA

Wild type N2a cells and N2a FUS knockout (NCF) cells were lysed and FUS was immunoprecipitated. mRNA bound to endogenous FUS was measured using rt-qPCR (A-D). The levels of the indicated mRNA were quantified by qPCR using the cycle threshold ( $\Delta\Delta Ct$ ) method, and the fold changes compared with NCF are presented. \* $P \leq 0.05$ ; \*\*\* $P \leq 0.001$ . A Student's t test was used to determine P values.



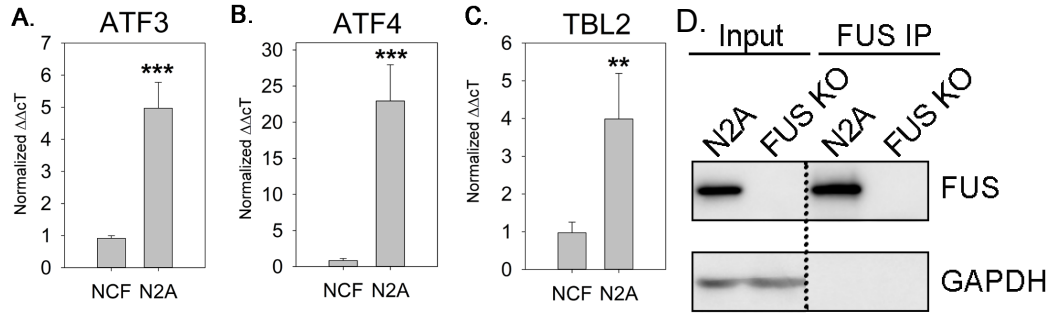


Figure 5.2 Endogenous FUS binds NMD substrate mRNA

Wild type N2a cells and N2a FUS knockout (NCF) cells were lysed and FUS was immunoprecipitated. mRNA bound to endogenous FUS was measured using rt-qPCR (A-C). The levels of the indicated mRNA were quantified by qPCR using the cycle threshold ( $\Delta\Delta CT$ ) method, and the fold changes compared with NCF are presented. \* $P \leq 0.05$ ; \*\* $P \leq 0.005$ ; \*\*\* $P \leq 0.001$ . A Student's t test was used to determine P values.

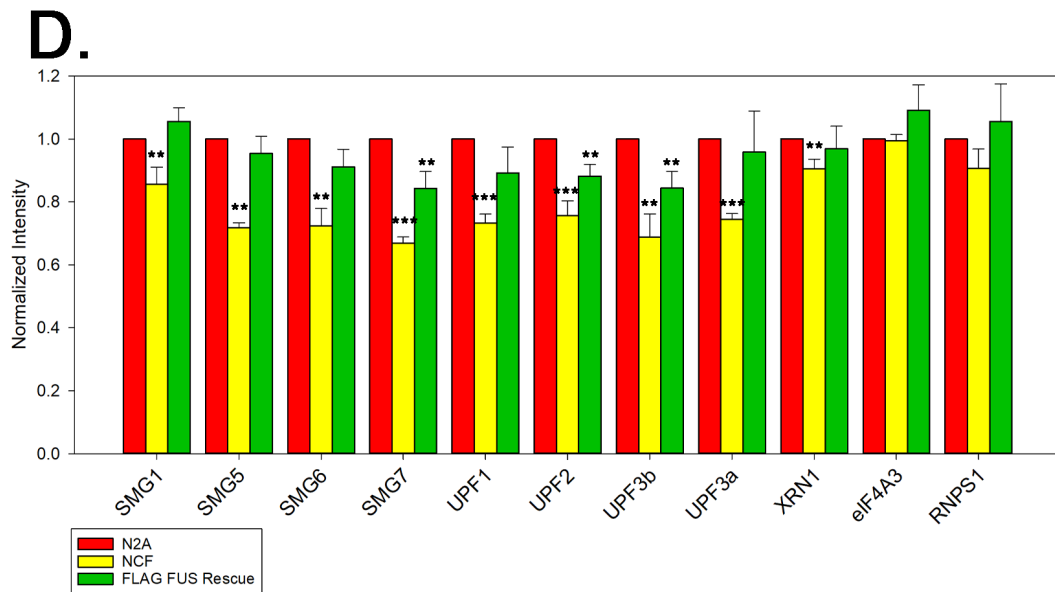
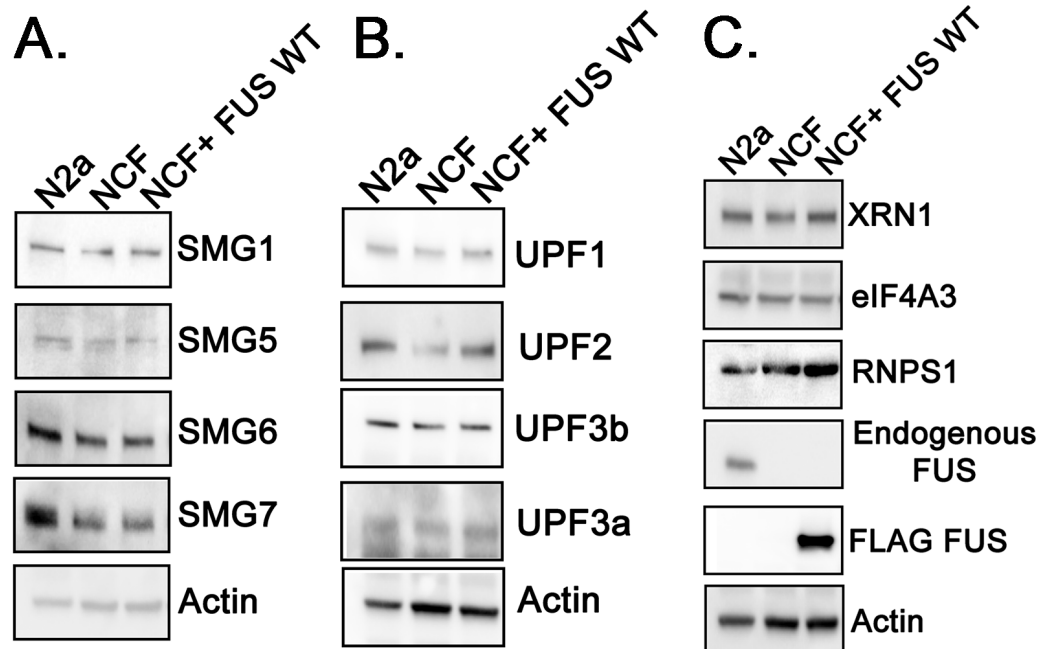


Figure 5.3 Endogenous FUS is required for normal expression of NMD factor protein

NMD factors were blotted for in WT N2a, NCF, and FLAG FUS rescue cells to examine their steady state levels. Immunoblots of the following proteins are shown: SMG1, SMG5, SMG6, and SMG7 (A), UPF1, UPF2, UPF3b, and UPF3a (B), and XRN1, eIF4A3,

Figure 5.3 continued

RNPS1, endogenous FUS, FLAG FUS, and Actin (C). Quantitative results are shown in D. Protein intensities were normalized to actin and compared with N2a. \*P ≤ 0.05; \*\*P ≤ 0.005; \*\*\*P ≤ 0.001. A Student's t test was used to determine P values.

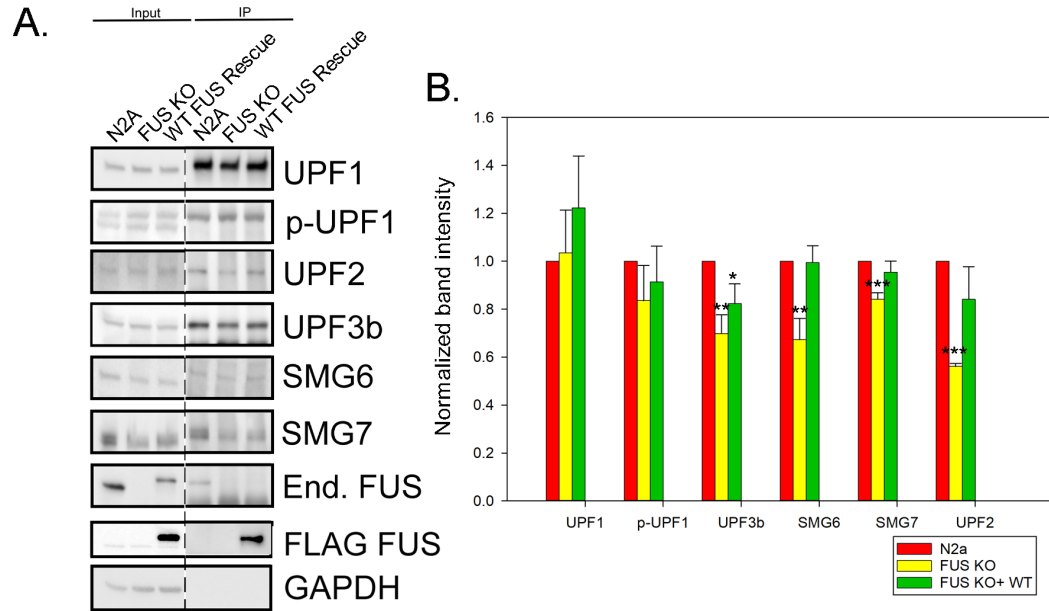


Figure 5.4 Endogenous FUS is required for assembly of NMD factor complexes

NMD factors coprecipitated with endogenous UPF1 from WT N2a, NCF, and FLAG FUS rescue cells. Immunoblots of UPF1, p-UPF1, UPF3b, SMG6, SMG7, endogenous FUS, FLAG-FUS, and GAPDH are shown in A, and quantitative results are shown in B. Protein intensities were normalized to corresponding UPF1 bands and compared with N2a. \* $P \leq 0.05$ ; \*\* $P \leq 0.005$ ; \*\*\* $P \leq 0.001$ . A Student's t test was used to determine P values.

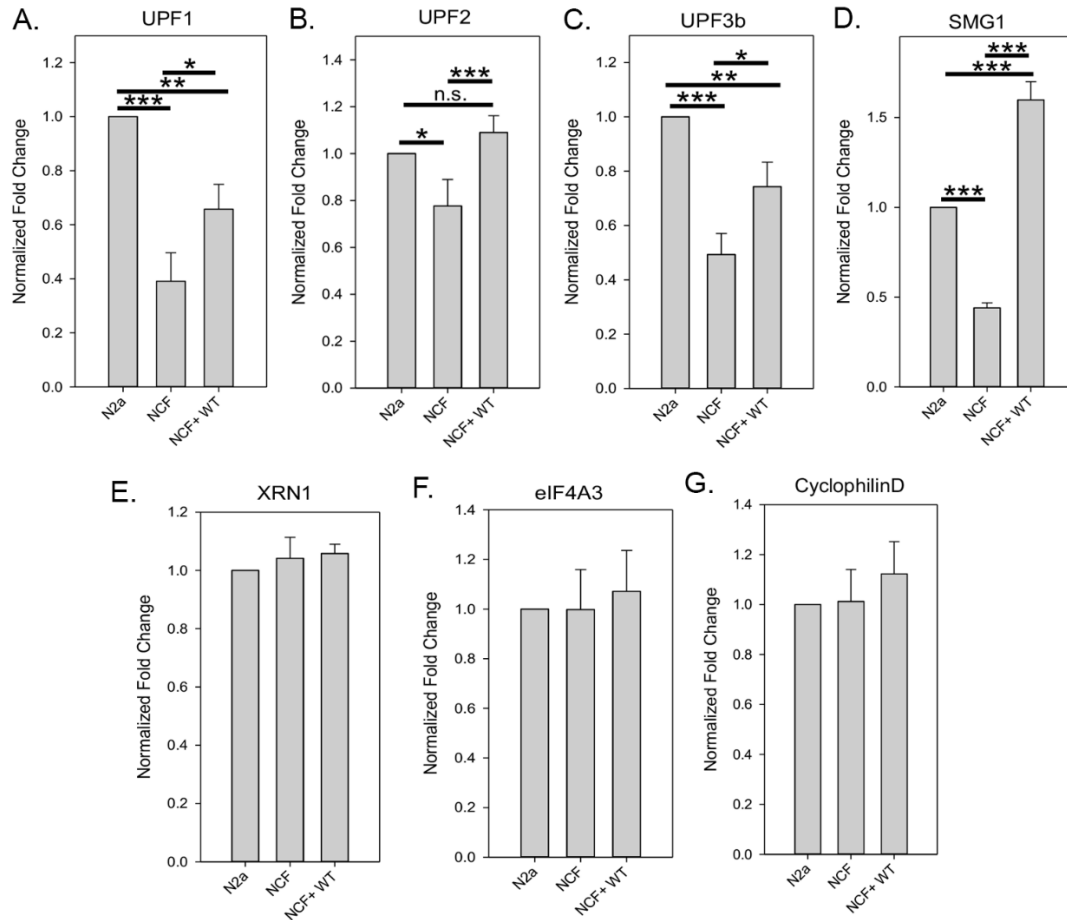


Figure 5.5 Endogenous FUS is required for normal expression of NMD factor mRNA

mRNA from WT N2a, NCF, and FLAG FUS rescue cells were collected and steady state levels measured using rt-qPCR (A-G). The levels of the indicated mRNA were quantified by qPCR using the cycle threshold ( $\Delta\Delta CT$ ) method, and the fold changes compared with N2a are presented. \* $P \leq 0.05$ ; \*\* $P \leq 0.005$ ; \*\*\* $P \leq 0.001$ . A Student's t test was used to determine P values.

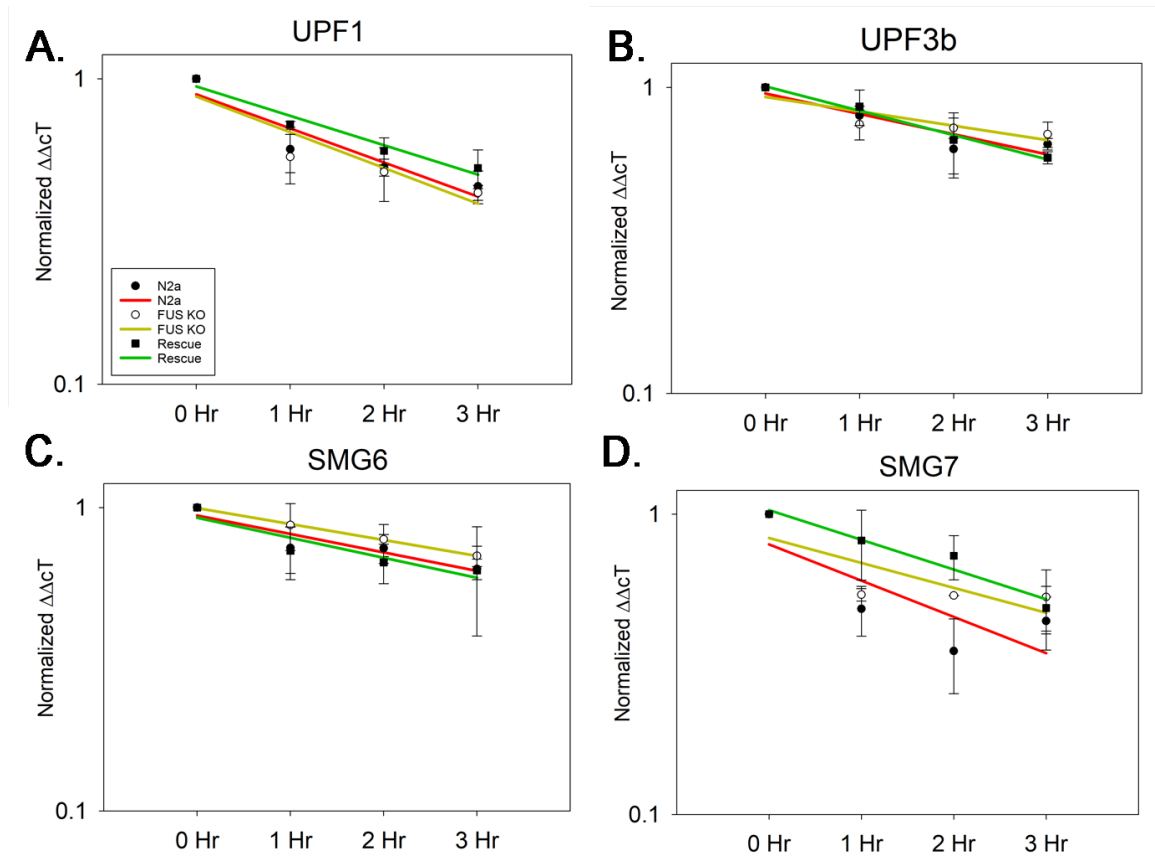


Figure 5.6 NMD factor mRNA stability is unchanged when FUS is Knocked Out

Turnover rates of UPF1 (A), UPF3b (B), SMG6 (C), and SMG7 (D) mRNAs in WT N2a, NCF, or FLAG FUS rescue cells. Actinomycin D or DMSO control was added 1, 2, or 3 hr before harvesting for RNA isolation. Individual mRNAs of interest were quantified by qPCR, normalized against RPL13a, and presented as fold change versus DMSO treatment over time. Error bars represent the SD from three replicates. ANOVA with a post hoc Tukey honest significant difference test was used.

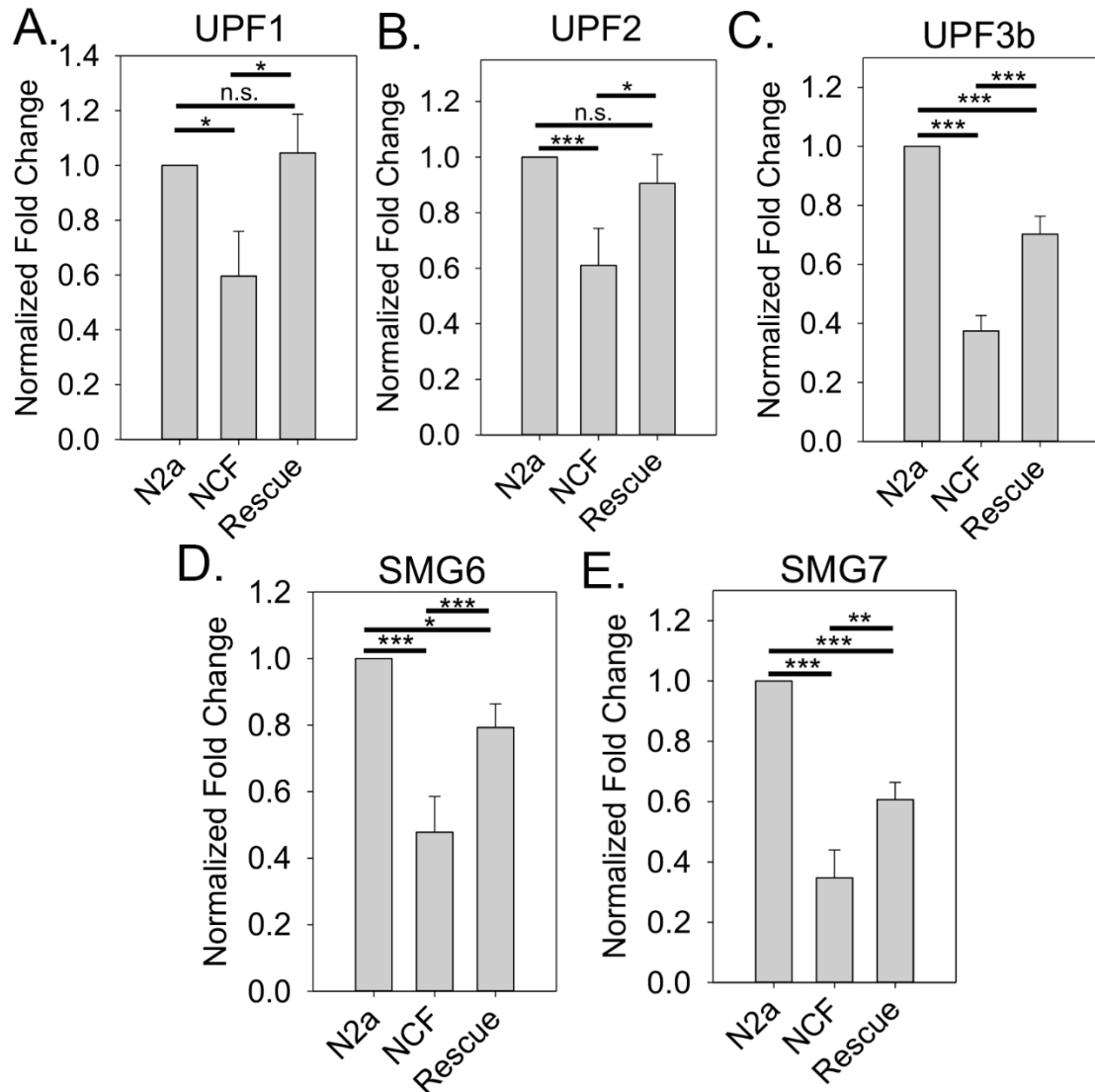


Figure 5.7 FUS KO Reduces UPF1 Binding to NMD Factor mRNA

WT N2a, NCF, or FLAG FUS rescue cells lysate was subjected to IP using normal goat serum (NGS) or goat anti-UPF1 antibody. The IP samples were aliquoted for Western blot and qPCR quantification comparing RNA coprecipitated with UPF1 protein versus NGS control. UPF1 IP from WT N2a, NCF, or FLAG FUS rescue cells was performed, followed by Western blot (Fig. 5.10) and qPCR measurement of UPF1 (A), UPF2 (B), UPF3b (C),

Figure 5.7 continued

SMG6 (D), and SMG7 (E) mRNAs. The levels of the indicated mRNA were quantified by qPCR using the cycle threshold ( $\Delta\Delta CT$ ) method, and the fold changes compared with N2a are presented. \* $P \leq 0.05$ ; \*\* $P \leq 0.005$ ; \*\*\* $P \leq 0.001$ . N.S., not significant. ANOVA with a post hoc Tukey honest significant difference test was used to determine P values.



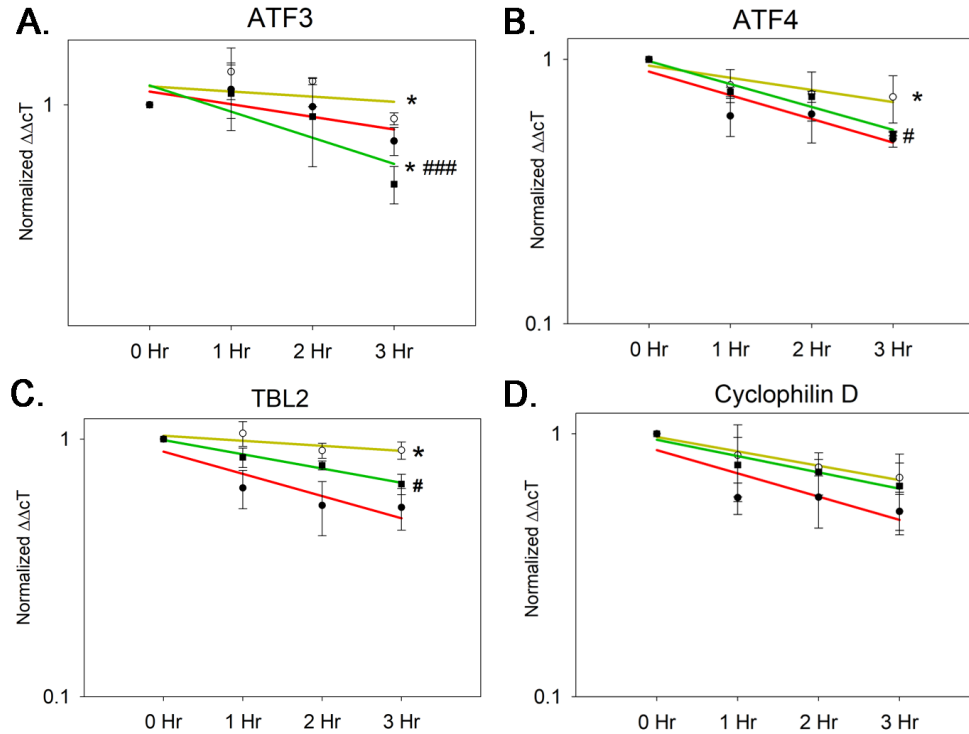


Figure 5.8 NMD substrate mRNA is stabilized when FUS is Knocked Out

Turnover rates of ATF3 (A), ATF4 (B), TBL2 (C), and CyclophilinD (D) mRNAs in WT N2a, NCF, or FLAG FUS rescue cells. Actinomycin D or DMSO control was added 1, 2, or 3 hr before harvesting for RNA isolation. Individual mRNAs of interest were quantified by qPCR, normalized against RPL13a, and presented as fold change versus DMSO treatment over time. Error bars represent the SD from three replicates. \*, #  $P \leq 0.05$ ; \*\*, ##  $P \leq 0.005$ ; \*\*\*, ###  $P \leq 0.001$ . A Student's t test was used to determine P values. \* represent significance compared to N2a, # represent significance compared to NCF.

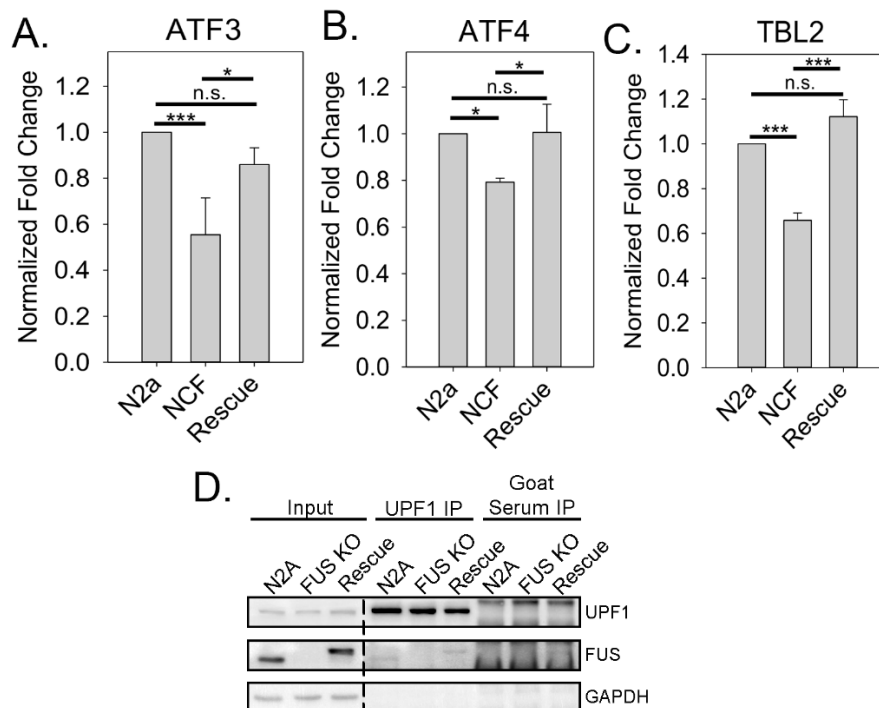


Figure 5.9 UPF1 Binding to NMD Substrate mRNA is Reduced When FUS is Knocked Out

WT N2a, NCF, or FLAG FUS rescue cells lysate was subjected to IP using normal goat serum (NGS) or goat anti-UPF1 antibody. The IP samples were aliquoted for Western blot and qPCR quantification comparing RNA coprecipitated with UPF1 protein versus NGS control. UPF1 IP from WT N2a, NCF, or FLAG FUS rescue cells was performed, followed by Western blot (Fig. 5.10) and qPCR measurement of ATF3 (A), ATF4 (B), and TBL2 mRNAs. UPF1, FUS, and GAPDH were assessed by Western blot, as shown in D. The levels of the indicated mRNA were quantified by qPCR using the cycle threshold ( $\Delta\Delta CT$ ) method, and the fold changes compared with N2a are presented. \* $P \leq 0.05$ ; \*\* $P \leq 0.005$ ;

Figure 5.9 continued

\*\*\* $P \leq 0.001$ . N.S., not significant. ANOVA with a post hoc Tukey honest significant difference test was used to determine P values.

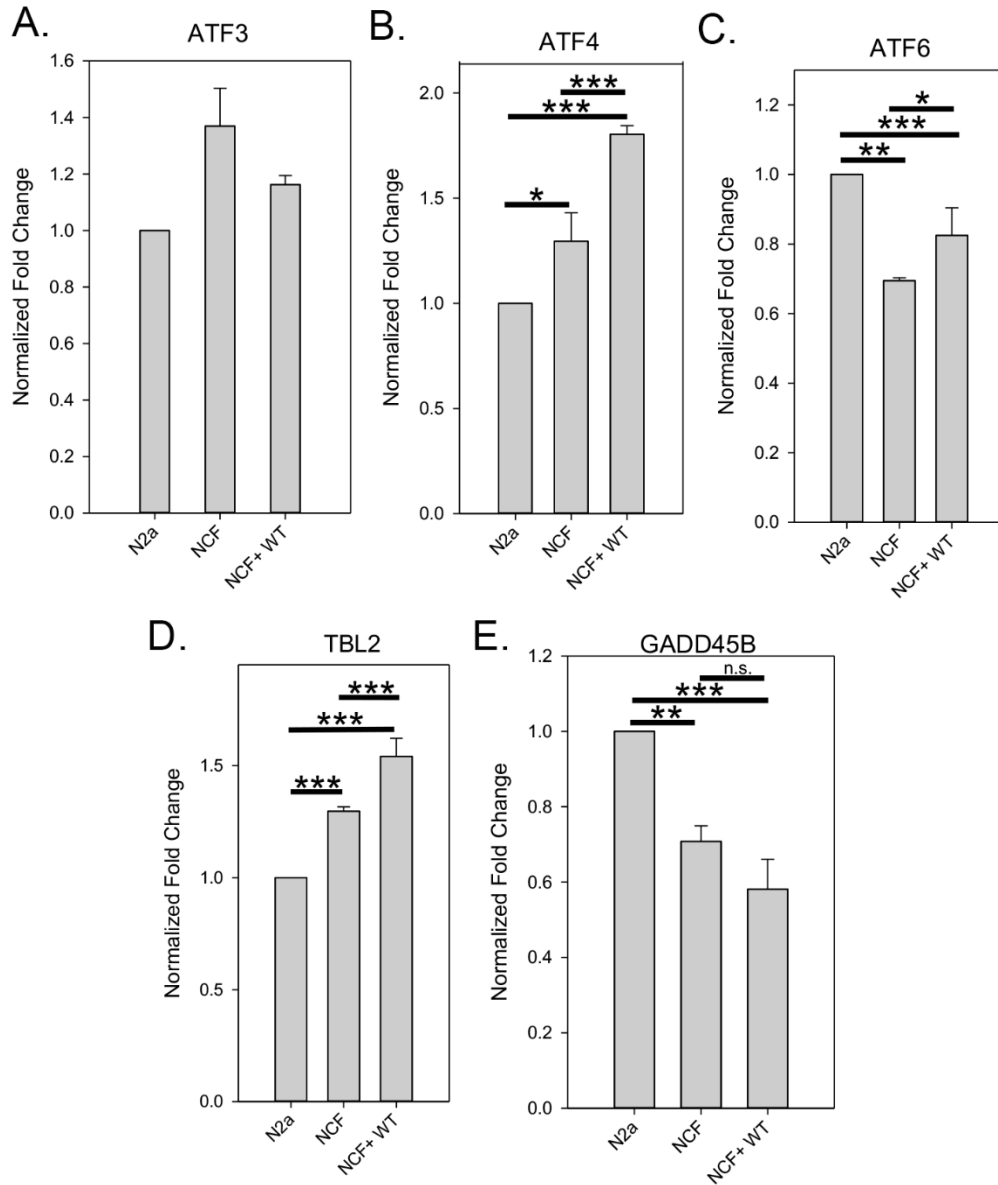


Figure 5.10 Natural NMD substrate levels are influenced by FUS KO

mRNA from WT N2a, NCF, and FLAG FUS rescue cells were collected and steady state levels measured using rt-qPCR (A-E). The levels of the indicated mRNA were quantified by qPCR using the cycle threshold ( $\Delta\Delta CT$ ) method, and the fold changes compared with

Figure 5.10 continued

N2a are presented. \* $P \leq 0.05$ ; \*\* $P \leq 0.005$ ; \*\*\* $P \leq 0.001$ . N.S., not significant. ANOVA with a post hoc Tukey honest significant difference test was used to determine P values.

## REFERENCES

1. Hardiman O, Al-Chalabi A, Chio A, Corr EM, Logroscino G, Robberecht W, Shaw PJ, Simmons Z, van den Berg LH. Amyotrophic lateral sclerosis. *Nature Reviews Disease Primers*. 2017;3:17071.
2. Vance C, Rogelj B, Hortobagyi T, De Vos KJ, Nishimura AL, Sreedharan J, Hu X, Smith B, Ruddy D, Wright P, Ganesalingam J, Williams KL, Tripathi V, Al-Saraj S, Al-Chalabi A, Leigh PN, Blair IP, Nicholson G, de Bellerocche J, Gallo JM, Miller CC, Shaw CE. Mutations in FUS, an RNA processing protein, cause familial amyotrophic lateral sclerosis type 6. *Science (New York, NY)*. 2009;323(5918):1208-11. Epub 2009/03/03. doi: 10.1126/science.1165942. PubMed PMID: 19251628; PMCID: PMC4516382.
3. Kwiatkowski TJ, Jr., Bosco DA, Leclerc AL, Tamrazian E, Vanderburg CR, Russ C, Davis A, Gilchrist J, Kasarskis EJ, Munsat T, Valdmanis P, Rouleau GA, Hosler BA, Cortelli P, de Jong PJ, Yoshinaga Y, Haines JL, Pericak-Vance MA, Yan J, Ticozzi N, Siddique T, McKenna-Yasek D, Sapp PC, Horvitz HR, Landers JE, Brown RH, Jr. Mutations in the FUS/TLS gene on chromosome 16 cause familial amyotrophic lateral sclerosis. *Science (New York, NY)*. 2009;323(5918):1205-8. Epub 2009/03/03. doi: 10.1126/science.1166066. PubMed PMID: 19251627.
4. Testa D, Lovati R, Ferrarini M, Salmoiraghi F, Filippini G. Survival of 793 patients with amyotrophic lateral sclerosis diagnosed over a 28-year period. *Amyotrophic lateral sclerosis and other motor neuron disorders : official publication of the World Federation of Neurology, Research Group on Motor Neuron Diseases*. 2004;5(4):208-12. Epub 2005/04/01. PubMed PMID: 15799548.
5. Shang Y, Huang EJ. Mechanisms of FUS Mutations in Familial Amyotrophic Lateral Sclerosis. *Brain research*. 2016;1647:65-78. doi: 10.1016/j.brainres.2016.03.036. PubMed PMID: PMC5003642.
6. Huang EJ, Zhang J, Geser F, Trojanowski JQ, Strober JB, Dickson DW, Brown RH, Jr., Shapiro BE, Lomen-Hoerth C. Extensive FUS-immunoreactive pathology in juvenile amyotrophic lateral sclerosis with basophilic inclusions. *Brain pathology (Zurich, Switzerland)*. 2010;20(6):1069-76. Epub 2010/06/29. doi: 10.1111/j.1750-3639.2010.00413.x. PubMed PMID: 20579074; PMCID: PMC2951498.
7. Baumer D, Hilton D, Paine SM, Turner MR, Lowe J, Talbot K, Ansorge O. Juvenile ALS with basophilic inclusions is a FUS proteinopathy with FUS mutations. *Neurology*. 2010;75(7):611-8. Epub 2010/07/30. doi: 10.1212/WNL.0b013e3181ed9cde. PubMed PMID: 20668261; PMCID: PMC2931770.
8. Murray DT, Kato M, Lin Y, Thurber KR, Hung I, McKnight SL, Tycko R. Structure of FUS Protein Fibrils and Its Relevance to Self-Assembly and Phase Separation of Low-Complexity Domains. *Cell*. 2017;171(3):615-27.e16. Epub 2017/09/26. doi: 10.1016/j.cell.2017.08.048. PubMed PMID: 28942918; PMCID: PMC5650524.
9. Monahan Z, Ryan VH, Janke AM, Burke KA, Rhoads SN, Zerze GH, O'Meally R, Dignon GL, Conicella AE, Zheng W, Best RB, Cole RN, Mittal J, Shewmaker F, Fawzi NL. Phosphorylation of the FUS low-complexity domain disrupts phase separation, aggregation, and toxicity. *The EMBO journal*. 2017;36(20):2951-67. Epub 2017/08/10. doi: 10.15252/embj.201696394. PubMed PMID: 28790177; PMCID: PMC5641905.
10. Baron DM, Kaushansky LJ, Ward CL, Sama R, Chian R-J, Boggio KJ, Quaresima AJC, Nickerson JA, Bosco DA. Amyotrophic lateral sclerosis-linked FUS/TLS

- alters stress granule assembly and dynamics. *Molecular Neurodegeneration*. 2013;8(1):30. doi: 10.1186/1750-1326-8-30.
11. Daigle JG, Lanson JNA, Smith RB, Casci I, Maltare A, Monaghan J, Nichols CD, Kryndushkin D, Shewmaker F, Pandey UB. RNA-binding ability of FUS regulates neurodegeneration, cytoplasmic mislocalization and incorporation into stress granules associated with FUS carrying ALS-linked mutations. *Human Molecular Genetics*. 2013;22(6):1193-205. doi: 10.1093/hmg/dd526.
  12. Bosco DA, Lemay N, Ko HK, Zhou H, Burke C, Kwiatkowski TJ, Jr., Sapp P, McKenna-Yasek D, Brown RH, Jr., Hayward LJ. Mutant FUS proteins that cause amyotrophic lateral sclerosis incorporate into stress granules. *Hum Mol Genet*. 2010;19(21):4160-75. Epub 2010/08/12. doi: 10.1093/hmg/ddq335. PubMed PMID: 20699327; PMCID: PMC2981014.
  13. Schwartz JC, Ebmeier CC, Podell ER, Heimiller J, Taatjes DJ, Cech TR. FUS binds the CTD of RNA polymerase II and regulates its phosphorylation at Ser2. *Genes & development*. 2012;26(24):2690-5. Epub 2012/12/20. doi: 10.1101/gad.204602.112. PubMed PMID: 23249733; PMCID: PMC3533074.
  14. Schwartz JC, Ebmeier CC, Podell ER, Heimiller J, Taatjes DJ, Cech TR. FUS binds the CTD of RNA polymerase II and regulates its phosphorylation at Ser2. *Genes & development*. 2012;26(24):2690-5.
  15. Han TW, Kato M, Xie S, Wu LC, Mirzaei H, Pei J, Chen M, Xie Y, Allen J, Xiao G, McKnight SL. Cell-free formation of RNA granules: bound RNAs identify features and components of cellular assemblies. *Cell*. 2012;149(4):768-79. Epub 2012/05/15. doi: 10.1016/j.cell.2012.04.016. PubMed PMID: 22579282.
  16. Kato M, Han Tina W, Xie S, Shi K, Du X, Wu Leeju C, Mirzaei H, Goldsmith Elizabeth J, Longgood J, Pei J, Grishin Nick V, Frantz Douglas E, Schneider Jay W, Chen S, Li L, Sawaya Michael R, Eisenberg D, Tycko R, McKnight Steven L. Cell-free Formation of RNA Granules: Low Complexity Sequence Domains Form Dynamic Fibers within Hydrogels. *Cell*. 149(4):753-67. doi: 10.1016/j.cell.2012.04.017.
  17. Qamar S, Wang G, Randle SJ, Ruggeri FS, Varela JA, Lin JQ, Phillips EC, Miyashita A, Williams D, Ströhl F, Meadows W, Ferry R, Dardov VJ, Tartaglia GG, Farrer LA, Kaminski Schierle GS, Kaminski CF, Holt CE, Fraser PE, Schmitt-Ulms G, Klenerman D, Knowles T, Vendruscolo M, St George-Hyslop P. FUS Phase Separation Is Modulated by a Molecular Chaperone and Methylation of Arginine Cation- $\pi$  Interactions. *Cell*. 2018;173(3):720-34.e15. doi: <https://doi.org/10.1016/j.cell.2018.03.056>.
  18. Hofweber M, Hutten S, Bourgeois B, Spreitzer E, Niedner-Boblenz A, Schifferer M, Ruepp M-D, Simons M, Niessing D, Madl T, Dormann D. Phase Separation of FUS Is Suppressed by Its Nuclear Import Receptor and Arginine Methylation. *Cell*. 2018;173(3):706-19.e13. doi: <https://doi.org/10.1016/j.cell.2018.03.004>.
  19. Dormann D, Haass C. TDP-43 and FUS: a nuclear affair. *Trends in Neurosciences*. 2011;34(7):339-48. doi: <https://doi.org/10.1016/j.tins.2011.05.002>.
  20. Yang L, Gal J, Chen J, Zhu H. Self-assembled FUS binds active chromatin and regulates gene transcription. *Proceedings of the National Academy of Sciences*. 2014;111(50):17809-14. doi: 10.1073/pnas.1414004111.
  21. Lagier-Tourenne C, Polymenidou M, Hutt KR, Vu AQ, Baughn M, Huelga SC, Clutario KM, Ling SC, Liang TY, Mazur C, Wancewicz E, Kim AS, Watt A, Freier S,

- Hicks GG, Donohue JP, Shiue L, Bennett CF, Ravits J, Cleveland DW, Yeo GW. Divergent roles of ALS-linked proteins FUS/TLS and TDP-43 intersect in processing long pre-mRNAs. *Nature neuroscience*. 2012;15(11):1488-97. Epub 2012/10/02. doi: 10.1038/nn.3230. PubMed PMID: 23023293; PMCID: PMC3586380.
22. Yang L, Zhang J, Kamelgarn M, Niu C, Gal J, Gong W, Zhu H. Subcellular localization and RNAs determine FUS architecture in different cellular compartments. *Human Molecular Genetics*. 2015;24(18):5174-83. doi: 10.1093/hmg/ddv239. PubMed PMID: PMC4643640.
23. Schwartz JC, Podell ER, Han SSW, Berry JD, Eggan KC, Cech TR. FUS is sequestered in nuclear aggregates in ALS patient fibroblasts. *Molecular Biology of the Cell*. 2014;25(17):2571-8. doi: 10.1091/mbc.E14-05-1007. PubMed PMID: PMC4148247.
24. Kim H, Erickson B, Luo W, Seward D, Graber JH, Pollock DD, Megee PC, Bentley DL. Gene-specific RNA polymerase II phosphorylation and the CTD code. *Nature structural & molecular biology*. 2010;17(10):1279-86.
25. Ahn SH, Kim M, Buratowski S. Phosphorylation of serine 2 within the RNA polymerase II C-terminal domain couples transcription and 3' end processing. *Molecular cell*. 2004;13(1):67-76.
26. Kwon I, Kato M, Xiang S, Wu L, Theodoropoulos P, Mirzaei H, Han T, Xie S, Corden JL, McKnight SL. Phosphorylation-regulated Binding of RNA Polymerase II to Fibrous Polymers of Low Complexity Domains. *Cell*. 2013;155(5):1049-60. doi: 10.1016/j.cell.2013.10.033. PubMed PMID: PMC4010232.
27. Das R, Yu J, Zhang Z, Gygi MP, Krainer AR, Gygi SP, Reed R. SR proteins function in coupling RNAP II transcription to pre-mRNA splicing. *Molecular cell*. 2007;26(6):867-81.
28. Kaida D, Berg MG, Younis I, Kasim M, Singh LN, Wan L, Dreyfuss G. U1 snRNP protects pre-mRNAs from premature cleavage and polyadenylation. *Nature*. 2010;468(7324):664-8. Epub 2010/10/01. doi: 10.1038/nature09479. PubMed PMID: 20881964; PMCID: PMC2996489.
29. Berg MG, Singh LN, Younis I, Liu Q, Pinto AM, Kaida D, Zhang Z, Cho S, Sherrill-Mix S, Wan L, Dreyfuss G. U1 snRNP determines mRNA length and regulates isoform expression. *Cell*. 2012;150(1):53-64. Epub 2012/07/10. doi: 10.1016/j.cell.2012.05.029. PubMed PMID: 22770214; PMCID: PMC3412174.
30. Masuda A, Takeda J-i, Okuno T, Okamoto T, Ohkawara B, Ito M, Ishigaki S, Sobue G, Ohno K. Position-specific binding of FUS to nascent RNA regulates mRNA length. *Genes & development*. 2015;29(10):1045-57. doi: 10.1101/gad.255737.114. PubMed PMID: PMC4441052.
31. Wahle E. Poly(A) tail length control is caused by termination of processive synthesis. *The Journal of biological chemistry*. 1995;270(6):2800-8. Epub 1995/02/10. doi: 10.1074/jbc.270.6.2800. PubMed PMID: 7852352.
32. Voisinet-Hakil F, Viphakone N, Minvielle-Sebastia L. Molecular dissection of mRNA poly(A) tail length control in yeast. *Nucleic Acids Research*. 2008;36(7):2418-33. doi: 10.1093/nar/gkn080.
33. Fujioka Y, Ishigaki S, Masuda A, Iguchi Y, Udagawa T, Watanabe H, Katsuno M, Ohno K, Sobue G. FUS-regulated region- and cell-type-specific transcriptome is associated



- with cell selectivity in ALS/FTLD. *Scientific reports*. 2013;3:2388. Epub 2013/08/09. doi: 10.1038/srep02388. PubMed PMID: 23925123; PMCID: PMC3737506.
34. Lerga A, Hallier M, Delva L, Orvain C, Gallais I, Marie J, Moreau-Gachelin F. Identification of an RNA binding specificity for the potential splicing factor TLS. *The Journal of biological chemistry*. 2001;276(9):6807-16. Epub 2000/12/01. doi: 10.1074/jbc.M008304200. PubMed PMID: 11098054.
35. Nakaya T, Alexiou P, Maragkakis M, Chang A, Mourelatos Z. FUS regulates genes coding for RNA-binding proteins in neurons by binding to their highly conserved introns. *RNA (New York, NY)*. 2013;19(4):498-509. Epub 2013/02/08. doi: 10.1261/rna.037804.112. PubMed PMID: 23389473; PMCID: PMC3677260.
36. Hoell JI, Larsson E, Runge S, Nusbaum JD, Duggimpudi S, Farazi TA, Hafner M, Borkhardt A, Sander C, Tuschl T. RNA targets of wild-type and mutant FET family proteins. *Nat Struct Mol Biol*. 2011;18(12):1428-31. Epub 2011/11/15. doi: 10.1038/nsmb.2163. PubMed PMID: 22081015; PMCID: PMC3230689.
37. Ishigaki S, Masuda A, Fujioka Y, Iguchi Y, Katsuno M, Shibata A, Urano F, Sobue G, Ohno K. Position-dependent FUS-RNA interactions regulate alternative splicing events and transcriptions. *Scientific reports*. 2012;2:529. Epub 2012/07/26. doi: 10.1038/srep00529. PubMed PMID: 22829983; PMCID: PMC3402842.
38. Rogelj B, Easton LE, Bogu GK, Stanton LW, Rot G, Curk T, Zupan B, Sugimoto Y, Modic M, Haberman N, Tollervey J, Fujii R, Takumi T, Shaw CE, Ule J. Widespread binding of FUS along nascent RNA regulates alternative splicing in the brain. *Scientific reports*. 2012;2:603. Epub 2012/08/31. doi: 10.1038/srep00603. PubMed PMID: 22934129; PMCID: PMC3429604.
39. Zhou Y, Liu S, Liu G, Öztürk A, Hicks GG. ALS-associated FUS mutations result in compromised FUS alternative splicing and autoregulation. *PLoS genetics*. 2013;9(10):e1003895.
40. Sun S, Ling S-C, Qiu J, Albuquerque CP, Zhou Y, Tokunaga S, Li H, Qiu H, Bui A, Yeo GW. ALS-causative mutations in FUS/TLS confer gain and loss of function by altered association with SMN and U1-snRNP. *Nature communications*. 2015;6:6171.
41. Yu Y, Chi B, Xia W, Gangopadhyay J, Yamazaki T, Winkelbauer-Hurt ME, Yin S, Eliasse Y, Adams E, Shaw CE. U1 snRNP is mislocalized in ALS patient fibroblasts bearing NLS mutations in FUS and is required for motor neuron outgrowth in zebrafish. *Nucleic acids research*. 2015;43(6):3208-18.
42. Yamazaki T, Chen S, Yu Y, Yan B, Haertlein TC, Carrasco MA, Tapia JC, Zhai B, Das R, Lalancette-Hebert M. FUS-SMN protein interactions link the motor neuron diseases ALS and SMA. *Cell reports*. 2012;2(4):799-806.
43. Gerbino V, Carri MT, Cozzolino M, Achsel T. Mislocalised FUS mutants stall spliceosomal snRNPs in the cytoplasm. *Neurobiology of disease*. 2013;55:120-8.
44. Eperon IC, Makarova OV, Mayeda A, Munroe SH, Cáceres JF, Hayward DG, Krainer AR. Selection of alternative 5' splice sites: role of U1 snRNP and models for the antagonistic effects of SF2/ASF and hnRNP A1. *Molecular and cellular biology*. 2000;20(22):8303-18.
45. Yu Y, Reed R. FUS functions in coupling transcription to splicing by mediating an interaction between RNAP II and U1 snRNP. *Proc Natl Acad Sci U S A*.

- 2015;112(28):8608-13. Epub 2015/07/01. doi: 10.1073/pnas.1506282112. PubMed PMID: 26124092; PMCID: PMC4507187.
46. Battle DJ, Kasim M, Yong J, Lotti F, Lau CK, Mouaikel J, Zhang Z, Han K, Wan L, Dreyfuss G. The SMN complex: an assembly machine for RNPs. *Cold Spring Harbor symposia on quantitative biology*. 2006;71:313-20. Epub 2007/03/27. doi: 10.1101/sqb.2006.71.001. PubMed PMID: 17381311.
47. Burghes AH, Beattie CE. Spinal muscular atrophy: why do low levels of survival motor neuron protein make motor neurons sick? *Nature Reviews Neuroscience*. 2009;10(8):597.
48. Terns MP, Terns RM. Macromolecular complexes: SMN—the master assembler. *Current biology*. 2001;11(21):R862-R4.
49. Clelland AK, Kinnear NP, Oram L, Burza J, Sleeman JE. The SMN protein is a key regulator of nuclear architecture in differentiating neuroblastoma cells. *Traffic (Copenhagen, Denmark)*. 2009;10(11):1585-98. Epub 2009/09/04. doi: 10.1111/j.1600-0854.2009.00972.x. PubMed PMID: 19735367.
50. Groen EJ, Fumoto K, Blokhuis AM, Engelen-Lee J, Zhou Y, van den Heuvel DM, Koppers M, van Diggelen F, van Heest J, Demmers JA. ALS-associated mutations in FUS disrupt the axonal distribution and function of SMN. *Human molecular genetics*. 2013;22(18):3690-704.
51. Yu Y, Reed R. FUS functions in coupling transcription to splicing by mediating an interaction between RNAP II and U1 snRNP. *Proceedings of the National Academy of Sciences of the United States of America*. 2015;112(28):8608-13. doi: 10.1073/pnas.1506282112. PubMed PMID: PMC4507187.
52. Ishigaki S, Masuda A, Fujioka Y, Iguchi Y, Katsuno M, Shibata A, Urano F, Sobue G, Ohno K. Position-dependent FUS-RNA interactions regulate alternative splicing events and transcriptions. *Scientific reports*. 2012;2:529.
53. Reber S, Stettler J, Filosa G, Colombo M, Jutzi D, Lenzken SC, Schweingruber C, Bruggmann R, Bachi A, Barabino SM, Muhlemann O, Ruepp MD. Minor intron splicing is regulated by FUS and affected by ALS-associated FUS mutants. *The EMBO journal*. 2016;35(14):1504-21. Epub 2016/06/03. doi: 10.15252/embj.201593791. PubMed PMID: 27252488; PMCID: PMC4946139.
54. Jurkat-Rott K, Holzherr B, Fauler M, Lehmann-Horn F. Sodium channelopathies of skeletal muscle result from gain or loss of function. *Pflugers Archiv : European journal of physiology*. 2010;460(2):239-48. Epub 2010/03/20. doi: 10.1007/s00424-010-0814-4. PubMed PMID: 20237798; PMCID: PMC2883924.
55. Porter JD, Goldstein LA, Kasarskis EJ, Brueckner JK, Spear BT. The neuronal voltage-gated sodium channel, Scn8a, is essential for postnatal maturation of spinal, but not oculomotor, motor units. *Experimental neurology*. 1996;139(2):328-34. Epub 1996/06/01. doi: 10.1006/exnr.1996.0107. PubMed PMID: 8654536.
56. Starke S, Jost I, Roszbach O, Schneider T, Schreiner S, Hung LH, Bindereif A. Exon circularization requires canonical splice signals. *Cell Rep*. 2015;10(1):103-11. Epub 2014/12/30. doi: 10.1016/j.celrep.2014.12.002. PubMed PMID: 25543144.
57. Salzman J, Gawad C, Wang PL, Lacayo N, Brown PO. Circular RNAs are the predominant transcript isoform from hundreds of human genes in diverse cell types. *PloS one*. 2012;7(2):e30733-e. doi: 10.1371/journal.pone.0030733. PubMed PMID: 22319583.

58. Errichelli L, Modigliani SD, Laneve P, Colantoni A, Legnini I, Capauto D, Rosa A, De Santis R, Scarfo R, Peruzzi G. FUS affects circular RNA expression in murine embryonic stem cell-derived motor neurons. *Nature communications*. 2017;8:14741.
59. Lee BJ, Cansizoglu AE, Suel KE, Louis TH, Zhang Z, Chook YM. Rules for nuclear localization sequence recognition by karyopherin beta 2. *Cell*. 2006;126(3):543-58. Epub 2006/08/12. doi: 10.1016/j.cell.2006.05.049. PubMed PMID: 16901787; PMCID: PMC3442361.
60. Zhang ZC, Chook YM. Structural and energetic basis of ALS-causing mutations in the atypical proline-tyrosine nuclear localization signal of the Fused in Sarcoma protein (FUS). *Proc Natl Acad Sci U S A*. 2012;109(30):12017-21. Epub 2012/07/11. doi: 10.1073/pnas.1207247109. PubMed PMID: 22778397; PMCID: PMC3409756.
61. Du K, Arai S, Kawamura T, Matsushita A, Kurokawa R. TLS and PRMT1 synergistically coactivate transcription at the survivin promoter through TLS arginine methylation. *Biochemical and biophysical research communications*. 2011;404(4):991-6. Epub 2010/12/29. doi: 10.1016/j.bbrc.2010.12.097. PubMed PMID: 21187067.
62. Dormann D, Rodde R, Edbauer D, Bentmann E, Fischer I, Hruscha A, Than ME, Mackenzie IRA, Capell A, Schmid B, Neumann M, Haass C. ALS-associated fused in sarcoma (FUS) mutations disrupt Transportin-mediated nuclear import. *The EMBO journal*. 2010;29(16):2841-57. Epub 2010/07/06. doi: 10.1038/emboj.2010.143. PubMed PMID: 20606625.
63. Ito D, Seki M, Tsunoda Y, Uchiyama H, Suzuki N. Nuclear transport impairment of amyotrophic lateral sclerosis-linked mutations in FUS/TLS. *Annals of neurology*. 2011;69(1):152-62. Epub 2011/02/01. doi: 10.1002/ana.22246. PubMed PMID: 21280085.
64. Suarez-Calvet M, Neumann M, Arzberger T, Abou-Ajram C, Funk E, Hartmann H, Edbauer D, Kremmer E, Gobl C, Resch M, Bourgeois B, Madl T, Reber S, Jutzi D, Ruepp MD, Mackenzie IR, Ansorge O, Dormann D, Haass C. Monomethylated and unmethylated FUS exhibit increased binding to Transportin and distinguish FTLD-FUS from ALS-FUS. *Acta neuropathologica*. 2016;131(4):587-604. Epub 2016/02/20. doi: 10.1007/s00401-016-1544-2. PubMed PMID: 26895297.
65. Yoshizawa T, Ali R, Jiou J, Fung HYJ, Burke KA, Kim SJ, Lin Y, Peeples WB, Saltzberg D, Soniat M. Nuclear import receptor inhibits phase separation of FUS through binding to multiple sites. *Cell*. 2018;173(3):693-705. e22.
66. Yasuda K, Zhang H, Loisel D, Haystead T, Macara IG, Mili S. The RNA-binding protein Fus directs translation of localized mRNAs in APC-RNP granules. *The Journal of cell biology*. 2013;203(5):737-46. doi: 10.1083/jcb.201306058. PubMed PMID: 24297750.
67. Lopez-Erauskin J, Tadokoro T, Baughn MW, Myers B, McAlonis-Downes M, Chillon-Marinhas C, Asiaban JN, Artates J, Bui AT, Vetto AP, Lee SK, Le AV, Sun Y, Jambeau M, Boubaker J, Swing D, Qiu J, Hicks GG, Ouyang Z, Fu XD, Tessarollo L, Ling SC, Parone PA, Shaw CE, Marsala M, Lagier-Tourenne C, Cleveland DW, Da Cruz S. ALS/FTD-Linked Mutation in FUS Suppresses Intra-axonal Protein Synthesis and Drives Disease Without Nuclear Loss-of-Function of FUS. *Neuron*. 2018. Epub 2018/10/23. doi: 10.1016/j.neuron.2018.09.044. PubMed PMID: 30344044.
68. Udagawa T, Fujioka Y, Tanaka M, Honda D, Yokoi S, Riku Y, Ibi D, Nagai T, Yamada K, Watanabe H. FUS regulates AMPA receptor function and FTLD/ALS-

- associated behaviour via GluA1 mRNA stabilization. *Nature communications*. 2015;6:7098.
69. Blechingberg J, Luo Y, Bolund L, Damgaard CK, Nielsen AL. Gene expression responses to FUS, EWS, and TAF15 reduction and stress granule sequestration analyses identifies FET-protein non-redundant functions. *PloS one*. 2012;7(9):e46251-e. doi: 10.1371/journal.pone.0046251. PubMed PMID: 23049996.
70. Mackenzie IR, Nicholson AM, Sarkar M, Messing J, Purice MD, Pottier C, Annu K, Baker M, Perkerson RB, Kurti A. TIA1 mutations in amyotrophic lateral sclerosis and frontotemporal dementia promote phase separation and alter stress granule dynamics. *Neuron*. 2017;95(4):808-16. e9.
71. Gal J, Kuang L, Barnett KR, Zhu BZ, Shissler SC, Korotkov KV, Hayward LJ, Kasarskis EJ, Zhu H. ALS mutant SOD1 interacts with G3BP1 and affects stress granule dynamics. *Acta neuropathologica*. 2016;132(4):563-76. Epub 2016/08/03. doi: 10.1007/s00401-016-1601-x. PubMed PMID: 27481264; PMCID: PMC5023729.
72. Gal J, Zhang J, Kwinter DM, Zhai J, Jia H, Jia J, Zhu H. Nuclear localization sequence of FUS and induction of stress granules by ALS mutants. *Neurobiology of aging*. 2011;32(12):2323.e27-.e2.323E40. Epub 2010/07/31. doi: 10.1016/j.neurobiolaging.2010.06.010. PubMed PMID: 20674093.
73. Aulas A, Stabile S, Vande Velde C. Endogenous TDP-43, but not FUS, contributes to stress granule assembly via G3BP. *Molecular neurodegeneration*. 2012;7:54-. doi: 10.1186/1750-1326-7-54. PubMed PMID: 23092511.
74. Solomon S, Xu Y, Wang B, David M, Schubert P, Kennedy D, Schrader J. 558 2007. Distinct structural features of caprin-1 mediate its interaction with G3BP-1 and its 559 induction of phosphorylation of eukaryotic translation initiation factor 2alpha, entry to 560 cytoplasmic stress granules, and selective interaction with a subset of mRNAs. *Mol Cell Biol*.561(27):2324-42.
75. Daigle JG, Krishnamurthy K, Ramesh N, Casci I, Monaghan J, McAvoy K, Godfrey EW, Daniel DC, Johnson EM, Monahan Z, Shewmaker F, Pasinelli P, Pandey UB. Pur-alpha regulates cytoplasmic stress granule dynamics and ameliorates FUS toxicity. *Acta neuropathologica*. 2016;131(4):605-20. Epub 2016/01/04. doi: 10.1007/s00401-015-1530-0. PubMed PMID: 26728149.
76. Di Salvio M, Piccinni V, Gerbino V, Mantoni F, Camerini S, Lenzi J, Rosa A, Chellini L, Loreni F, Carri MT, Bozzoni I, Cozzolino M, Cestra G. Pur-alpha functionally interacts with FUS carrying ALS-associated mutations. *Cell death & disease*. 2015;6:e1943. Epub 2015/10/23. doi: 10.1038/cddis.2015.295. PubMed PMID: 26492376; PMCID: PMC4632316.
77. Acosta JR, Goldsbury C, Winnick C, Badrock AP, Fraser ST, Laird AS, Hall TE, Don EK, Fifita JA, Blair IP, Nicholson GA, Cole NJ. Mutant human FUS Is ubiquitously mislocalized and generates persistent stress granules in primary cultured transgenic zebrafish cells. *PLoS One*. 2014;9(6):e90572. Epub 2014/06/10. doi: 10.1371/journal.pone.0090572. PubMed PMID: 24912067; PMCID: PMC4049593.
78. Morlando M, Dini Modigliani S, Torrelli G, Rosa A, Di Carlo V, Caffarelli E, Bozzoni I. FUS stimulates microRNA biogenesis by facilitating co-transcriptional Drosha recruitment. *The EMBO journal*. 2012;31(24):4502-10. doi: 10.1038/emboj.2012.319. PubMed PMID: 23232809.

79. Filippov V, Solovyev V, Filippova M, Gill SS. A novel type of RNase III family proteins in eukaryotes. *Gene*. 2000;245(1):213-21. Epub 2000/03/14. PubMed PMID: 10713462.
80. Caputo D, Colantoni A, Lu L, Santini T, Peruzzi G, Biscarini S, Morlando M, Shneider NA, Caffarelli E, Laneve P, Bozzoni I. A Regulatory Circuitry Between Gria2, miR-409, and miR-495 Is Affected by ALS FUS Mutation in ESC-Derived Motor Neurons. *Molecular neurobiology*. 2018;55(10):7635-51. Epub 2018/02/13. doi: 10.1007/s12035-018-0884-4. PubMed PMID: 29430619; PMCID: PMC6132778.
81. Hawley ZCE, Campos-Melo D, Strong MJ. Novel miR-b2122 regulates several ALS-related RNA-binding proteins. *Molecular brain*. 2017;10(1):46-. doi: 10.1186/s13041-017-0326-7. PubMed PMID: 28969660.
82. Ju S, Tardiff DF, Han H, Divya K, Zhong Q, Maquat LE, Bosco DA, Hayward LJ, Brown Jr RH, Lindquist S. A yeast model of FUS/TLS-dependent cytotoxicity. *PLoS biology*. 2011;9(4):e1001052.
83. Barmada SJ, Ju S, Arjun A, Batarse A, Archbold HC, Peisach D, Li X, Zhang Y, Tank EMH, Qiu H, Huang EJ, Ringe D, Petsko GA, Finkbeiner S. Amelioration of toxicity in neuronal models of amyotrophic lateral sclerosis by hUPF1. *Proceedings of the National Academy of Sciences of the United States of America*. 2015;112(25):7821-6. doi: 10.1073/pnas.1509744112. PubMed PMID: PMC4485101.
84. Choo AY, Yoon S-O, Kim SG, Roux PP, Blenis J. Rapamycin differentially inhibits S6Ks and 4E-BP1 to mediate cell-type-specific repression of mRNA translation. *Proceedings of the National Academy of Sciences*. 2008;105(45):17414-9.
85. Abisambra J, Jinwal UK, Miyata Y, Rogers J, Blair L, Li X, Seguin SP, Wang L, Jin Y, Bacon J. Allosteric heat shock protein 70 inhibitors rapidly rescue synaptic plasticity deficits by reducing aberrant tau. *Biological psychiatry*. 2013;74(5):367-74.
86. Tanaka M, Gupta R, Mayer BJ. Differential inhibition of signaling pathways by dominant-negative SH2/SH3 adapter proteins. *Molecular and cellular biology*. 1995;15(12):6829-37.
87. Zhai J, Ström AL, Kilty R, Venkatakrisnan P, White J, Everson WV, Smart EJ, Zhu H. Proteomic characterization of lipid raft proteins in amyotrophic lateral sclerosis mouse spinal cord. *The FEBS journal*. 2009;276(12):3308-23.
88. Consortium U. UniProt: a hub for protein information. *Nucleic acids research*. 2014;43(D1):D204-D12.
89. Kuang L, Kamelgarn M, Arenas A, Gal J, Taylor D, Gong W, Brown M, St Clair D, Kasarskis EJ, Zhu H. Clinical and experimental studies of a novel P525R FUS mutation in amyotrophic lateral sclerosis. *Neurology Genetics*. 2017;3(4):e172. Epub 2017/08/16. doi: 10.1212/nxg.0000000000000172. PubMed PMID: 28812062; PMCID: PMC5546284.
90. Kuleshov MV, Jones MR, Rouillard AD, Fernandez NF, Duan Q, Wang Z, Koplev S, Jenkins SL, Jagodnik KM, Lachmann A. Enrichr: a comprehensive gene set enrichment analysis web server 2016 update. *Nucleic acids research*. 2016;44(W1):W90-W7.
91. Chen EY, Tan CM, Kou Y, Duan Q, Wang Z, Meirelles GV, Clark NR, Ma'ayan A. Enrichr: interactive and collaborative HTML5 gene list enrichment analysis tool. *BMC bioinformatics*. 2013;14(1):128.
92. Consortium GO. Expansion of the Gene Ontology knowledgebase and resources. *Nucleic acids research*. 2016;45(D1):D331-D8.

93. Ashburner M, Ball CA, Blake JA, Botstein D, Butler H, Cherry JM, Davis AP, Dolinski K, Dwight SS, Eppig JT. Gene Ontology: tool for the unification of biology. *Nature genetics*. 2000;25(1):25.
94. Pletscher-Frankild S, Pallejà A, Tsafou K, Binder JX, Jensen LJ. DISEASES: Text mining and data integration of disease–gene associations. *Methods*. 2015;74:83-9.
95. Walling AD. Amyotrophic lateral sclerosis: Lou Gehrig's disease. *American family physician*. 1999;59(6):1489-96.
96. Wijesekera LC, Nigel Leigh P. Amyotrophic lateral sclerosis. *Orphanet Journal of Rare Diseases*. 2009;4(1):3. doi: 10.1186/1750-1172-4-3.
97. DeJesus-Hernandez M, Kocerha J, Finch N, Crook R, Baker M, Desaro P, Johnston A, Rutherford N, Wojtas A, Kennelly K. De novo truncating FUS gene mutation as a cause of sporadic amyotrophic lateral sclerosis. *Human mutation*. 2010;31(5):E1377-E89.
98. Belzil V, Valdmanis P, Dion P, Daoud H, Kabashi E, Noreau A, Gauthier J, Hince P, Desjarlais A, Bouchard J-P. Mutations in FUS cause FALS and SALS in French and French Canadian populations. *Neurology*. 2009;73(15):1176-9.
99. Corrado L, Del Bo R, Castellotti B, Ratti A, Cereda C, Penco S, Sorarù G, Carlomagno Y, Ghezzi S, Pensato V. Mutations of FUS gene in sporadic amyotrophic lateral sclerosis. *Journal of medical genetics*. 2010;47(3):190-4.
100. Andersson MK, Ståhlberg A, Arvidsson Y, Olofsson A, Semb H, Stenman G, Nilsson O, Åman P. The multifunctional FUS, EWS and TAF15 proto-oncoproteins show cell type-specific expression patterns and involvement in cell spreading and stress response. *BMC cell biology*. 2008;9(1):37.
101. Zinszner H, Sok J, Immanuel D, Yin Y, Ron D. TLS (FUS) binds RNA in vivo and engages in nucleo-cytoplasmic shuttling. *Journal of cell science*. 1997;110(15):1741-50.
102. Baechtold H, Kuroda M, Sok J, Ron D, Lopez BS, Akhmedov AT. Human 75-kDa DNA-pairing protein is identical to the pro-oncoprotein TLS/FUS and is able to promote D-loop formation. *Journal of Biological Chemistry*. 1999;274(48):34337-42.
103. Mastrocola AS, Kim SH, Trinh AT, Rodenkirch LA, Tibbetts RS. The RNA binding protein fused in sarcoma (FUS) functions downstream of PARP in response to DNA damage. *Journal of Biological Chemistry*. 2013;jbc. M113. 497974.
104. Wang W-Y, Pan L, Su SC, Quinn EJ, Sasaki M, Jimenez JC, Mackenzie IR, Huang EJ, Tsai L-H. Interaction of FUS and HDAC1 regulates DNA damage response and repair in neurons. *Nature neuroscience*. 2013;16(10):1383.
105. Wang X, Arai S, Song X, Reichart D, Du K, Pascual G, Tempst P, Rosenfeld MG, Glass CK, Kurokawa R. Induced ncRNAs allosterically modify RNA-binding proteins in cis to inhibit transcription. *Nature*. 2008;454(7200):126.
106. Tan AY, Manley JL. TLS inhibits RNA polymerase III transcription. *Molecular and cellular biology*. 2010;30(1):186-96.
107. Haile S, Lal A, Myung J-K, Sadar MD. FUS/TLS is a co-activator of androgen receptor in prostate cancer cells. *PloS one*. 2011;6(9):e24197.
108. Tan AY, Riley TR, Coady T, Bussemaker HJ, Manley JL. TLS/FUS (translocated in liposarcoma/fused in sarcoma) regulates target gene transcription via single-stranded DNA response elements. *Proceedings of the National Academy of Sciences*. 2012;109(16):6030-5.

109. Bronisz A, Carey HA, Godlewski J, Sif S, Ostrowski MC, Sharma SM. The multifunctional protein fused in sarcoma (FUS) is a coactivator of microphthalmia-associated transcription factor (MITF). *Journal of Biological Chemistry*. 2014;289(1):326-34.
110. Dhar SK, Zhang J, Gal J, Xu Y, Miao L, Lynn BC, Zhu H, Kasarskis EJ, St. Clair DK. FUsed in sarcoma is a novel regulator of manganese superoxide dismutase gene transcription. *Antioxidants & redox signaling*. 2014;20(10):1550-66.
111. Uranishi H, Tetsuka T, Yamashita M, Asamitsu K, Shimizu M, Itoh M, Okamoto T. Involvement of the Pro-oncoprotein TLS (Translocated in Liposarcoma) in the NF-kappaB p65-mediated transcription as a coactivator. *Journal of Biological Chemistry*. 2001.
112. Yang L, Embree LJ, Tsai S, Hickstein DD. Oncoprotein TLS interacts with serine-arginine proteins involved in RNA splicing. *Journal of Biological Chemistry*. 1998;273(43):27761-4.
113. Dichmann DS, Harland RM. fus/TLS orchestrates splicing of developmental regulators during gastrulation. *Genes & development*. 2012;26(12):1351-63.
114. Fujii R, Takumi T. TLS facilitates transport of mRNA encoding an actin-stabilizing protein to dendritic spines. *Journal of cell science*. 2005;118(24):5755-65.
115. Fujii R, Okabe S, Urushido T, Inoue K, Yoshimura A, Tachibana T, Nishikawa T, Hicks GG, Takumi T. The RNA binding protein TLS is translocated to dendritic spines by mGluR5 activation and regulates spine morphology. *Current Biology*. 2005;15(6):587-93.
116. Sephton CF, Tang AA, Kulkarni A, West J, Brooks M, Stubblefield JJ, Liu Y, Zhang MQ, Green CB, Huber KM. Activity-dependent FUS dysregulation disrupts synaptic homeostasis. *Proceedings of the National Academy of Sciences*. 2014;111(44):E4769-E78.
117. Modigliani SD, Morlando M, Errichelli L, Sabatelli M, Bozzoni I. An ALS-associated mutation in the FUS 3'-UTR disrupts a microRNA-FUS regulatory circuitry. *Nature communications*. 2014;5:4335.
118. Urwin H, Josephs KA, Rohrer JD, Mackenzie IR, Neumann M, Authier A, Seelaar H, Van Swieten JC, Brown JM, Johannsen P. FUS pathology defines the majority of tau- and TDP-43-negative frontotemporal lobar degeneration. *Acta neuropathologica*. 2010;120(1):33-41.
119. Neumann M, Rademakers R, Roeber S, Baker M, Kretzschmar HA, Mackenzie IR. A new subtype of frontotemporal lobar degeneration with FUS pathology. *Brain*. 2009;132(11):2922-31.
120. Armstrong GA, Drapeau P. Loss and gain of FUS function impair neuromuscular synaptic transmission in a genetic model of ALS. *Human molecular genetics*. 2013;22(21):4282-92.
121. Kim HJ, Kim NC, Wang Y-D, Scarborough EA, Moore J, Diaz Z, MacLea KS, Freibaum B, Li S, Molliex A. Mutations in prion-like domains in hnRNPA2B1 and hnRNPA1 cause multisystem proteinopathy and ALS. *Nature*. 2013;495(7442):467.
122. Johnson JO, Piore EP, Boehringer A, Chia R, Feit H, Renton AE, Pliner HA, Abramzon Y, Marangi G, Winborn BJ. Mutations in the Matrin 3 gene cause familial amyotrophic lateral sclerosis. *Nature neuroscience*. 2014;17(5):664.

123. Szklarczyk D, Franceschini A, Wyder S, Forslund K, Heller D, Huerta-Cepas J, Simonovic M, Roth A, Santos A, Tsafou KP. STRING v10: protein–protein interaction networks, integrated over the tree of life. *Nucleic acids research*. 2014;43(D1):D447-D52.
124. Franceschini A, Szklarczyk D, Frankild S, Kuhn M, Simonovic M, Roth A, Lin J, Minguez P, Bork P, Von Mering C. STRING v9. 1: protein-protein interaction networks, with increased coverage and integration. *Nucleic acids research*. 2012;41(D1):D808-D15.
125. Jurica MS, Licklider LJ, GYGI SP, Grigorieff N, Moore MJ. Purification and characterization of native spliceosomes suitable for three-dimensional structural analysis. *RNA (New York, NY)*. 2002;8(4):426-39.
126. Will CL, Urlaub H, Achsel T, Gentzel M, Wilm M, Lührmann R. Characterization of novel SF3b and 17S U2 snRNP proteins, including a human Prp5p homologue and an SF3b DEAD-box protein. *The EMBO journal*. 2002;21(18):4978-88.
127. WILL CL, SCHNEIDER C, HOSSBACH M, URLAUB H, RAUHUT R, ELBASHIR S, TUSCHL T, LÜHRMANN R. The human 18S U11/U12 snRNP contains a set of novel proteins not found in the U2-dependent spliceosome. *RNA (New York, NY)*. 2004;10(6):929-41.
128. Popow J, Englert M, Weitzer S, Schleiffer A, Mierzwa B, Mechtler K, Trowitzsch S, Will CL, Lührmann R, Söll D. HSPC117 is the essential subunit of a human tRNA splicing ligase complex. *Science (New York, NY)*. 2011;331(6018):760-4.
129. Jønson L, Vikesaa J, Krogh A, Nielsen LK, Borup R, Johnsen AH, Christiansen J, Nielsen FC. Molecular composition of IMP1 ribonucleoprotein granules. *Molecular & cellular proteomics*. 2007;6(5):798-811.
130. Weidensdorfer D, Stöhr N, Baude A, Lederer M, Köhn M, Schierhorn A, Buchmeier S, Wahle E, Hüttelmaier S. Control of c-myc mRNA stability by IGF2BP1-associated cytoplasmic RNPs. *RNA (New York, NY)*. 2009;15(1):104-15.
131. Kanai Y, Dohmae N, Hirokawa N. Kinesin transports RNA: isolation and characterization of an RNA-transporting granule. *Neuron*. 2004;43(4):513-25.
132. Brendel C, Rehbein M, Kreienkamp H-J, Friedrich B, Richter D, Kindler S. Characterization of Staufen 1 ribonucleoprotein complexes. *Biochemical Journal*. 2004;384(2):239-46.
133. Villacé P, Marión RM, Ortín J. The composition of Staufen-containing RNA granules from human cells indicates their role in the regulated transport and translation of messenger RNAs. *Nucleic acids research*. 2004;32(8):2411-20.
134. Hoek KS, Kidd GJ, Carson JH, Smith R. hnRNP A2 selectively binds the cytoplasmic transport sequence of myelin basic protein mRNA. *Biochemistry*. 1998;37(19):7021-9.
135. Burgess HM, Richardson WA, Anderson RC, Salaun C, Graham SV, Gray NK. Nuclear relocation of cytoplasmic poly (A)-binding proteins PABP1 and PABP4 in response to UV irradiation reveals mRNA-dependent export of metazoan PABPs. *J Cell Sci*. 2011;124(19):3344-55.
136. Wilczynska A, Aigueperse C, Kress M, Dautry F, Weil D. The translational regulator CPEB1 provides a link between dcp1 bodies and stress granules. *J Cell Sci*. 2005;118(5):981-92.



137. Meister G, Landthaler M, Peters L, Chen PY, Urlaub H, Lührmann R, Tuschl T. Identification of novel argonaute-associated proteins. *Current biology*. 2005;15(23):2149-55.
138. Aulas A, Vande Velde C. Alterations in stress granule dynamics driven by TDP-43 and FUS: a link to pathological inclusions in ALS? *Frontiers in cellular neuroscience*. 2015;9:423.
139. Kedersha N, Stoecklin G, Ayodele M, Yacono P, Lykke-Andersen J, Fritzler MJ, Scheuner D, Kaufman RJ, Golan DE, Anderson P. Stress granules and processing bodies are dynamically linked sites of mRNP remodeling. *J Cell Biol*. 2005;169(6):871-84.
140. Borggrefe T, Wabl M, Akhmedov AT, Jessberger R. A B-cell-specific DNA recombination complex. *Journal of Biological Chemistry*. 1998;273(27):17025-35.
141. Guil S, Long JC, Cáceres JF. hnRNP A1 relocalization to the stress granules reflects a role in the stress response. *Molecular and cellular biology*. 2006;26(15):5744-58.
142. Sama R, Ward CL, Kaushansky LJ, Lemay N, Ishigaki S, Urano F, Bosco DA. FUS/TLS assembles into stress granules and is a prosurvival factor during hyperosmolar stress. *Journal of cellular physiology*. 2013;228(11):2222-31.
143. Pokrishevsky E, Grad LI, Cashman NR. TDP-43 or FUS-induced misfolded human wild-type SOD1 can propagate intercellularly in a prion-like fashion. *Scientific reports*. 2016;6:22155.
144. Ting NS, Kao PN, Chan DW, Lintott LG, Lees-Miller SP. DNA-dependent protein kinase interacts with antigen receptor response element binding proteins NF90 and NF45. *Journal of Biological Chemistry*. 1998;273(4):2136-45.
145. Deng Q, Holler CJ, Taylor G, Hudson KF, Watkins W, Gearing M, Ito D, Murray ME, Dickson DW, Seyfried NT. FUS is phosphorylated by DNA-PK and accumulates in the cytoplasm after DNA damage. *Journal of Neuroscience*. 2014;34(23):7802-13.
146. Pérez-González A, Pazo A, Navajas R, Ciordia S, Rodríguez-Frandsen A, Nieto A. hCLE/C14orf166 associates with DDX1-HSPC117-FAM98B in a novel transcription-dependent shuttling RNA-transporting complex. *PloS one*. 2014;9(3):e90957.
147. Nielsen J, Christiansen J, Lykke-Andersen J, Johnsen AH, Wewer UM, Nielsen FC. A family of insulin-like growth factor II mRNA-binding proteins represses translation in late development. *Molecular and cellular biology*. 1999;19(2):1262-70.
148. Patel GP, Ma S, Bag J. The autoregulatory translational control element of poly (A)-binding protein mRNA forms a heteromeric ribonucleoprotein complex. *Nucleic acids research*. 2005;33(22):7074-89.
149. Prokipcak R, Herrick D, Ross J. Purification and properties of a protein that binds to the C-terminal coding region of human c-myc mRNA. *Journal of Biological Chemistry*. 1994;269(12):9261-9.
150. Donnelly CJ, Willis DE, Xu M, Tep C, Jiang C, Yoo S, Schanen NC, Kirn-Safran CB, Van Minnen J, English A. Limited availability of ZBP1 restricts axonal mRNA localization and nerve regeneration capacity. *The EMBO journal*. 2011;30(22):4665-77.
151. Kedersha N, Anderson P. Mammalian stress granules and processing bodies. *Methods in enzymology*. 2007;431:61-81.
152. Sheth U, Parker R. Decapping and decay of messenger RNA occur in cytoplasmic processing bodies. *Science (New York, NY)*. 2003;300(5620):805-8.

153. Li YR, King OD, Shorter J, Gitler AD. Stress granules as crucibles of ALS pathogenesis. *J Cell Biol.* 2013;201(3):361-72.
154. Bentmann E, Haass C, Dormann D. Stress granules in neurodegeneration—lessons learnt from TAR DNA binding protein of 43 kDa and fused in sarcoma. *The FEBS journal.* 2013;280(18):4348-70.
155. Blokhuis AM, Koppers M, Groen EJ, van den Heuvel DM, Modigliani SD, Anink JJ, Fumoto K, van Diggelen F, Snelting A, Sooda P. Comparative interactomics analysis of different ALS-associated proteins identifies converging molecular pathways. *Acta neuropathologica.* 2016;132(2):175-96.
156. Murakami T, Qamar S, Lin JQ, Schierle GS, Rees E, Miyashita A, Costa AR, Dodd RB, Chan FT, Michel CH, Kronenberg-Versteeg D, Li Y, Yang SP, Wakutani Y, Meadows W, Ferry RR, Dong L, Tartaglia GG, Favrin G, Lin WL, Dickson DW, Zhen M, Ron D, Schmitt-Ulms G, Fraser PE, Shneider NA, Holt C, Vendruscolo M, Kaminski CF, St George-Hyslop P. ALS/FTD Mutation-Induced Phase Transition of FUS Liquid Droplets and Reversible Hydrogels into Irreversible Hydrogels Impairs RNP Granule Function. *Neuron.* 2015;88(4):678-90. Epub 2015/11/04. doi: 10.1016/j.neuron.2015.10.030. PubMed PMID: 26526393; PMCID: PMC4660210.
157. Patel A, Lee HO, Jawerth L, Maharana S, Jahnel M, Hein MY, Stoykov S, Mahamid J, Saha S, Franzmann TM, Poznaniakowski A, Poser I, Maghelli N, Royer LA, Weigert M, Myers EW, Grill S, Drechsel D, Hyman AA, Alberti S. A Liquid-to-Solid Phase Transition of the ALS Protein FUS Accelerated by Disease Mutation. *Cell.* 2015;162(5):1066-77. Epub 2015/09/01. doi: 10.1016/j.cell.2015.07.047. PubMed PMID: 26317470.
158. Molliex A, Temirov J, Lee J, Coughlin M, Kanagaraj AP, Kim HJ, Mittag T, Taylor JP. Phase separation by low complexity domains promotes stress granule assembly and drives pathological fibrillization. *Cell.* 2015;163(1):123-33.
159. Boeynaems S, Bogaert E, Kovacs D, Konijnenberg A, Timmerman E, Volkov A, Guharoy M, De Decker M, Jaspers T, Ryan VH. Phase separation of C9orf72 dipeptide repeats perturbs stress granule dynamics. *Molecular cell.* 2017;65(6):1044-55. e5.
160. Svetoni F, Frisone P, Paronetto MP. Role of FET proteins in neurodegenerative disorders. *RNA Biology.* 2016;13(11):1089-102. doi: 10.1080/15476286.2016.1211225. PubMed PMID: PMC5100351.
161. Karam R, Wengrod J, Gardner LB, Wilkinson MF. Regulation of nonsense-mediated mRNA decay: implications for physiology and disease. *Biochimica et biophysica acta.* 2013;1829(6-7):624-33. Epub 2013/03/19. doi: 10.1016/j.bbagr.2013.03.002. PubMed PMID: 23500037; PMCID: PMC3660545.
162. Celik A, He F, Jacobson A. NMD monitors translational fidelity 24/7. *Current genetics.* 2017;63(6):1007-10. Epub 2017/05/26. doi: 10.1007/s00294-017-0709-4. PubMed PMID: 28536849; PMCID: PMC5668330.
163. Serdar LD, Whiteside DL, Baker KE. ATP hydrolysis by UPF1 is required for efficient translation termination at premature stop codons. *Nat Commun.* 2016;7:14021. Epub 2016/12/23. doi: 10.1038/ncomms14021. PubMed PMID: 28008922; PMCID: PMC5196439.

164. Karousis ED, Muhlemann O. Nonsense-Mediated mRNA Decay Begins Where Translation Ends. *Cold Spring Harbor perspectives in biology*. 2018. Epub 2018/06/13. doi: 10.1101/cshperspect.a032862. PubMed PMID: 29891560.
165. Chan WK, Bhalla AD, Le Hir H, Nguyen LS, Huang L, Gecz J, Wilkinson MF. A UPF3-mediated regulatory switch that maintains RNA surveillance. *Nat Struct Mol Biol*. 2009;16(7):747-53. Epub 2009/06/09. doi: 10.1038/nsmb.1612. PubMed PMID: 19503078.
166. Franks TM, Singh G, Lykke-Andersen J. Upf1 ATPase-dependent mRNP disassembly is required for completion of nonsense-mediated mRNA decay. *Cell*. 2010;143(6):938-50. Epub 2010/12/15. doi: 10.1016/j.cell.2010.11.043. PubMed PMID: 21145460; PMCID: PMC3357093.
167. Shum EY, Jones SH, Shao A, Dumdie J, Krause MD, Chan WK, Lou CH, Espinoza JL, Song HW, Phan MH, Ramaiah M, Huang L, McCarrey JR, Peterson KJ, De Rooij DG, Cook-Andersen H, Wilkinson MF. The Antagonistic Gene Paralogs Upf3a and Upf3b Govern Nonsense-Mediated RNA Decay. *Cell*. 2016;165(2):382-95. Epub 2016/04/05. doi: 10.1016/j.cell.2016.02.046. PubMed PMID: 27040500; PMCID: PMC4826573.
168. Gal J, Chen J, Barnett KR, Yang L, Brumley E, Zhu H. HDAC6 regulates mutant SOD1 aggregation through two SMIR motifs and tubulin acetylation. *The Journal of biological chemistry*. 2013;288(21):15035-45. Epub 2013/04/13. doi: 10.1074/jbc.M112.431957. PubMed PMID: 23580651; PMCID: PMC3663524.
169. Kamelgarn M, Chen J, Kuang L, Arenas A, Zhai J, Zhu H, Gal J. Proteomic analysis of FUS interacting proteins provides insights into FUS function and its role in ALS. *Biochimica et biophysica acta*. 2016;1862(10):2004-14. Epub 2016/07/28. doi: 10.1016/j.bbadis.2016.07.015. PubMed PMID: 27460707; PMCID: PMC5055831.
170. Mills EW, Green R. Ribosomopathies: There's strength in numbers. *Science (New York, NY)*. 2017;358(6363). Epub 2017/11/04. doi: 10.1126/science.aan2755. PubMed PMID: 29097519.
171. Schmidt EK, Clavarino G, Ceppi M, Pierre P. SUnSET, a nonradioactive method to monitor protein synthesis. *Nat Meth*. 2009;6(4):275-7. doi: [http://www.nature.com/nmeth/journal/v6/n4/suppinfo/nmeth.1314\\_S1.html](http://www.nature.com/nmeth/journal/v6/n4/suppinfo/nmeth.1314_S1.html).
172. Shelkownikova TA, Dimasi P, Kukharsky MS, An H, Quintiero A, Schirmer C, Buee L, Galas MC, Buchman VL. Chronically stressed or stress-preconditioned neurons fail to maintain stress granule assembly. *Cell death & disease*. 2017;8(5):e2788. Epub 2017/05/12. doi: 10.1038/cddis.2017.199. PubMed PMID: 28492545; PMCID: PMC5520719.
173. Jackson RJ, Hellen CU, Pestova TV. The mechanism of eukaryotic translation initiation and principles of its regulation. *Nature reviews Molecular cell biology*. 2010;11(2):113.
174. Wang J, Ye Q, Cao Y, Guo Y, Huang X, Mi W, Liu S, Wang C, Yang HS, Zhou BP, Evers BM, She QB. Snail determines the therapeutic response to mTOR kinase inhibitors by transcriptional repression of 4E-BP1. *Nat Commun*. 2017;8(1):2207. Epub 2017/12/22. doi: 10.1038/s41467-017-02243-3. PubMed PMID: 29263324; PMCID: PMC5738350.

175. Hjerpe R, Aillet F, Lopitz-Otsoa F, Lang V, England P, Rodriguez MS. Efficient protection and isolation of ubiquitylated proteins using tandem ubiquitin-binding entities. *EMBO reports*. 2009;10(11):1250-8.
176. Schneider-Poetsch T, Ju J, Eyler DE, Dang Y, Bhat S, Merrick WC, Green R, Shen B, Liu JO. Inhibition of Eukaryotic Translation Elongation by Cycloheximide and Lactimidomycin. *Nature chemical biology*. 2010;6(3):209-17. doi: 10.1038/nchembio.304. PubMed PMID: PMC2831214.
177. Huang L, Lou CH, Chan W, Shum EY, Shao A, Stone E, Karam R, Song HW, Wilkinson MF. RNA homeostasis governed by cell type-specific and branched feedback loops acting on NMD. *Mol Cell*. 2011;43(6):950-61. Epub 2011/09/20. doi: 10.1016/j.molcel.2011.06.031. PubMed PMID: 21925383; PMCID: PMC4281029.
178. Yamashita A. Role of SMG-1-mediated Upfl phosphorylation in mammalian nonsense-mediated mRNA decay. *Genes to Cells*. 2013;18(3):161-75. doi: 10.1111/gtc.12033.
179. Durand S, Franks TM, Lykke-Andersen J. Hyperphosphorylation amplifies UPF1 activity to resolve stalls in nonsense-mediated mRNA decay. *Nat Commun*. 2016;7:12434. Epub 2016/08/12. doi: 10.1038/ncomms12434. PubMed PMID: 27511142; PMCID: PMC4987530.
180. Popp MW, Maquat LE. Attenuation of nonsense-mediated mRNA decay facilitates the response to chemotherapeutics. *Nat Commun*. 2015;6:6632. Epub 2015/03/27. doi: 10.1038/ncomms7632. PubMed PMID: 25808464; PMCID: PMC4375787.
181. Okada-Katsuhata Y, Yamashita A, Kutsuzawa K, Izumi N, Hirahara F, Ohno S. N- and C-terminal Upfl phosphorylations create binding platforms for SMG-6 and SMG-5:SMG-7 during NMD. *Nucleic Acids Research*. 2012;40(3):1251-66. doi: 10.1093/nar/gkr791. PubMed PMID: PMC3273798.
182. Kashima I, Yamashita A, Izumi N, Kataoka N, Morishita R, Hoshino S, Ohno M, Dreyfuss G, Ohno S. Binding of a novel SMG-1–Upfl–eRF1–eRF3 complex (SURF) to the exon junction complex triggers Upfl phosphorylation and nonsense-mediated mRNA decay. *Genes & development*. 2006;20(3):355-67. doi: 10.1101/gad.1389006. PubMed PMID: PMC1361706.
183. Imamachi N, Tani H, Mizutani R, Imamura K, Irie T, Suzuki Y, Akimitsu N. BRIC-seq: A genome-wide approach for determining RNA stability in mammalian cells. *Methods*. 2014;67(1):55-63.
184. Yepiskoposyan H, Aeschimann F, Nilsson D, Okoniewski M, Muhlemann O. Autoregulation of the nonsense-mediated mRNA decay pathway in human cells. *RNA (New York, NY)*. 2011;17(12):2108-18. Epub 2011/10/27. doi: 10.1261/rna.030247.111. PubMed PMID: 22028362; PMCID: PMC3222124.
185. Lee SR, Pratt GA, Martinez FJ, Yeo GW, Lykke-Andersen J. Target discrimination in nonsense-mediated mRNA decay requires Upfl ATPase activity. *Molecular cell*. 2015;59(3):413-25.
186. Mendell JT, Sharifi NA, Meyers JL, Martinez-Murillo F, Dietz HC. Nonsense surveillance regulates expression of diverse classes of mammalian transcripts and mutes genomic noise. *Nat Genet*. 2004;36(10):1073-8. Epub 2004/09/28. doi: 10.1038/ng1429. PubMed PMID: 15448691.

187. Viegas MH, Gehring NH, Breit S, Hentze MW, Kulozik AE. The abundance of RNPS1, a protein component of the exon junction complex, can determine the variability in efficiency of the Nonsense Mediated Decay pathway. *Nucleic Acids Research*. 2007;35(13):4542-51. doi: 10.1093/nar/gkm461. PubMed PMID: PMC1935013.
188. Gopal PP, Nirschl JJ, Klinman E, Holzbaur EL. Amyotrophic lateral sclerosis-linked mutations increase the viscosity of liquid-like TDP-43 RNP granules in neurons. *Proc Natl Acad Sci U S A*. 2017;114(12):E2466-e75. Epub 2017/03/08. doi: 10.1073/pnas.1614462114. PubMed PMID: 28265061; PMCID: PMC5373408.
189. Holt CE, Schuman EM. The central dogma decentralized: new perspectives on RNA function and local translation in neurons. *Neuron*. 2013;80(3):648-57.
190. Jung H, Yoon BC, Holt CE. Axonal mRNA localization and local protein synthesis in nervous system assembly, maintenance and repair. *Nature reviews Neuroscience*. 2012;13(5):308-24. Epub 2012/04/14. doi: 10.1038/nrn3210. PubMed PMID: 22498899; PMCID: PMC3682205.
191. Liu-Yesucevitz L, Bassell GJ, Gitler AD, Hart AC, Klann E, Richter JD, Warren ST, Wolozin B. Local RNA translation at the synapse and in disease. *The Journal of neuroscience : the official journal of the Society for Neuroscience*. 2011;31(45):16086-93. Epub 2011/11/11. doi: 10.1523/jneurosci.4105-11.2011. PubMed PMID: 22072660; PMCID: PMC3241995.
192. Beznoskova P, Wagner S, Jansen ME, von der Haar T, Valasek LS. Translation initiation factor eIF3 promotes programmed stop codon readthrough. *Nucleic Acids Res*. 2015;43(10):5099-111. Epub 2015/05/01. doi: 10.1093/nar/gkv421. PubMed PMID: 25925566; PMCID: PMC4446449.
193. Kolupaeva VG, Unbehaun A, Lomakin IB, Hellen CU, Pestova TV. Binding of eukaryotic initiation factor 3 to ribosomal 40S subunits and its role in ribosomal dissociation and anti-association. *RNA (New York, NY)*. 2005;11(4):470-86. Epub 2005/02/11. doi: 10.1261/rna.7215305. PubMed PMID: 15703437; PMCID: PMC1370736.
194. Protter DS, Parker R. Principles and properties of stress granules. *Trends in cell biology*. 2016;26(9):668-79.
195. Vance C, Scotter EL, Nishimura AL, Troakes C, Mitchell JC, Kathe C, Urwin H, Manser C, Miller CC, Hortobágyi T, Dragunow M, Rogelj B, Shaw CE. ALS mutant FUS disrupts nuclear localization and sequesters wild-type FUS within cytoplasmic stress granules. *Human molecular genetics*. 2013;22(13):2676-88. Epub 2013/03/07. doi: 10.1093/hmg/ddt117. PubMed PMID: 23474818.
196. Jackson KL, Dayton RD, Orchard EA, Ju S, Ringe D, Petsko GA, Maquat LE, Klein RL. Preservation of forelimb function by UPF1 gene therapy in a rat model of TDP-43-induced motor paralysis. *Gene therapy*. 2015;22(1):20-8. Epub 2014/10/31. doi: 10.1038/gt.2014.101. PubMed PMID: 25354681; PMCID: PMC4924570.
197. Neu-Yilik G, Raimondeau E, Eliseev B, Yeramala L, Amthor B, Deniaud A, Huard K, Kerschgens K, Hentze MW, Schaffitzel C, Kulozik AE. Dual function of UPF3B in early and late translation termination. *The EMBO journal*. 2017;36(20):2968-86. doi: 10.15252/embj.201797079. PubMed PMID: PMC5641913.
198. Tarpey PS, Raymond FL, Nguyen LS, Rodriguez J, Hackett A, Vandeleur L, Smith R, Shoubridge C, Edkins S, Stevens C, O'Meara S, Tofts C, Barthorpe S, Buck G, Cole J,

- Halliday K, Hills K, Jones D, Mironenko T, Perry J, Varian J, West S, Widaa S, Teague J, Dicks E, Butler A, Menzies A, Richardson D, Jenkinson A, Shepherd R, Raine K, Moon J, Luo Y, Parnau J, Bhat SS, Gardner A, Corbett M, Brooks D, Thomas P, Parkinson-Lawrence E, Porteous ME, Warner JP, Sanderson T, Pearson P, Simensen RJ, Skinner C, Hoganson G, Superneau D, Wooster R, Bobrow M, Turner G, Stevenson RE, Schwartz CE, Futreal PA, Srivastava AK, Stratton MR, Gecz J. Mutations in UPF3B, a member of the nonsense-mediated mRNA decay complex, cause syndromic and nonsyndromic mental retardation. *Nat Genet.* 2007;39(9):1127-33. Epub 2007/08/21. doi: 10.1038/ng2100. PubMed PMID: 17704778; PMCID: PMC2872770.
199. Jolly LA, Homan CC, Jacob R, Barry S, Gecz J. The UPF3B gene, implicated in intellectual disability, autism, ADHD and childhood onset schizophrenia regulates neural progenitor cell behaviour and neuronal outgrowth. *Hum Mol Genet.* 2013;22(23):4673-87. Epub 2013/07/04. doi: 10.1093/hmg/ddt315. PubMed PMID: 23821644.
200. Belly A, Moreau-Gachelin F, Sadoul R, Goldberg Y. Delocalization of the multifunctional RNA splicing factor TLS/FUS in hippocampal neurones: exclusion from the nucleus and accumulation in dendritic granules and spine heads. *Neuroscience letters.* 2005;379(3):152-7. Epub 2005/04/22. doi: 10.1016/j.neulet.2004.12.071. PubMed PMID: 15843054.
201. Sephton CF, Yu G. The function of RNA-binding proteins at the synapse: implications for neurodegeneration. *Cellular and molecular life sciences : CMLS.* 2015;72(19):3621-35. Epub 2015/06/07. doi: 10.1007/s00018-015-1943-x. PubMed PMID: 26047658; PMCID: PMC4565867.
202. Swanger SA, Bassell GJ. Dendritic protein synthesis in the normal and diseased brain. *Neuroscience.* 2013;232:106-27. doi: 10.1016/j.neuroscience.2012.12.003. PubMed PMID: PMC4502914.
203. Hug N, Longman D, Cáceres JF. Mechanism and regulation of the nonsense-mediated decay pathway. *Nucleic Acids Research.* 2016;44(4):1483-95. doi: 10.1093/nar/gkw010. PubMed PMID: PMC4770240.
204. Geloso MC, Corvino V, Marchese E, Serrano A, Michetti F, D'Ambrosi N. The Dual Role of Microglia in ALS: Mechanisms and Therapeutic Approaches. *Frontiers in Aging Neuroscience.* 2017;9:242. doi: 10.3389/fnagi.2017.00242. PubMed PMID: PMC5524666.
205. Yamanaka K, Komine O. The multi-dimensional roles of astrocytes in ALS. *Neuroscience research.* 2018;126:31-8. Epub 2017/10/22. doi: 10.1016/j.neures.2017.09.011. PubMed PMID: 29054467.
206. Sun S, Ling S-C, Qiu J, Albuquerque CP, Zhou Y, Tokunaga S, Li H, Qiu H, Bui A, Yeo GW, Huang EJ, Eggan K, Zhou H, Fu X-D, Lagier-Tourenne C, Cleveland DW. ALS-causative mutations in FUS/TLS confer gain- and loss-of-function by altered association with SMN and U1-snRNP. *Nature communications.* 2015;6:6171-. doi: 10.1038/ncomms7171. PubMed PMID: PMC4338613.
207. Yu Y, Chi B, Xia W, Gangopadhyay J, Yamazaki T, Winkelbauer-Hurt ME, Yin S, Eliasse Y, Adams E, Shaw CE, Reed R. U1 snRNP is mislocalized in ALS patient fibroblasts bearing NLS mutations in FUS and is required for motor neuron outgrowth in zebrafish. *Nucleic Acids Research.* 2015;43(6):3208-18. doi: 10.1093/nar/gkv157. PubMed PMID: PMC4381066.

208. Zhou Y, Liu S, Liu G, Ozturk A, Hicks GG. ALS-associated FUS mutations result in compromised FUS alternative splicing and autoregulation. *PLoS Genet.* 2013;9(10):e1003895. Epub 2013/11/10. doi: 10.1371/journal.pgen.1003895. PubMed PMID: 24204307; PMCID: PMC3814325.
209. Rogelj B, Easton LE, Bogu GK, Stanton LW, Rot G, Curk T, Zupan B, Sugimoto Y, Modic M, Haberman N, Tollervey J, Fujii R, Takumi T, Shaw CE, Ule J. Widespread binding of FUS along nascent RNA regulates alternative splicing in the brain. *Scientific reports.* 2012;2:603. doi: 10.1038/srep00603
- <https://www.nature.com/articles/srep00603#supplementary-information>.
210. Kino Y, Washizu C, Kurosawa M, Yamada M, Miyazaki H, Akagi T, Hashikawa T, Doi H, Takumi T, Hicks GG, Hattori N, Shimogori T, Nukina N. FUS/TLS deficiency causes behavioral and pathological abnormalities distinct from amyotrophic lateral sclerosis. *Acta neuropathologica communications.* 2015;3:24-. doi: 10.1186/s40478-015-0202-6. PubMed PMID: 25907258.
211. Kuroda M, Sok J, Webb L, Baechtold H, Urano F, Yin Y, Chung P, de Rooij DG, Akhmedov A, Ashley T. Male sterility and enhanced radiation sensitivity in TLS<sup>-/-</sup> mice. *The EMBO journal.* 2000;19(3):453-62.
212. Hicks GG, Singh N, Nashabi A, Mai S, Bozek G, Klewes L, Arapovic D, White EK, Koury MJ, Oltz EM. Fus deficiency in mice results in defective B-lymphocyte development and activation, high levels of chromosomal instability and perinatal death. *Nature genetics.* 2000;24(2):175.
213. Yamazaki T, Chen S, Yu Y, Yan B, Haertlein TC, Carrasco MA, Tapia JC, Zhai B, Das R, Lalancette-Hebert M, Sharma A, Chandran S, Sullivan G, Nishimura AL, Shaw CE, Gygi SP, Shneider NA, Maniatis T, Reed R. FUS-SMN protein interactions link the motor neuron diseases ALS and SMA. *Cell reports.* 2012;2(4):799-806. Epub 2012/09/27. doi: 10.1016/j.celrep.2012.08.025. PubMed PMID: 23022481.
214. Kamelgarn M, Chen J, Kuang L, Jin H, Kasarskis EJ, Zhu H. ALS mutations of FUS suppress protein translation and disrupt the regulation of nonsense-mediated decay. *Proc Natl Acad Sci U S A.* 2018. Epub 2018/11/21. doi: 10.1073/pnas.1810413115. PubMed PMID: 30455313.
215. Yang Y-CT, Di C, Hu B, Zhou M, Liu Y, Song N, Li Y, Umetsu J, Lu ZJ. CLIPdb: a CLIP-seq database for protein-RNA interactions. *BMC genomics.* 2015;16(1):51-. doi: 10.1186/s12864-015-1273-2. PubMed PMID: 25652745.
216. Yerbury JJ, Ooi L, Blair IP, Ciryam P, Dobson CM, Vendruscolo M. The metastability of the proteome of spinal motor neurons underlies their selective vulnerability in ALS. *Neuroscience letters.* 2019;704:89-94. Epub 2019/04/07. doi: 10.1016/j.neulet.2019.04.001. PubMed PMID: 30953736.
217. Singh AK, Choudhury SR, De S, Zhang J, Kissane S, Dwivedi V, Ramanathan P, Petric M, Orsini L, Hebenstreit D, Brogna S. The RNA helicase UPF1 associates with mRNAs co-transcriptionally and is required for the release of mRNAs from gene loci. *eLife.* 2019;8. Epub 2019/03/26. doi: 10.7554/eLife.41444. PubMed PMID: 30907728; PMCID: PMC6447362.

## VITA

### Education:

2009-2013 B.S.; Morehead State University, Morehead, Kentucky

Department of Biology

### Positions Held:

2015-2019: Ph.D. Candidate

2013-2019: Graduate Research Assistant

2010-2013: Undergraduate Research Fellow

### Awards:

- College of Medicine Fellowship for Excellence in Graduate Research (May 2018 – August 2017)
- Lyman T Johnson Fellowship Award (May 2018 – August 2013)
- Ruth L. Kirschstein National Research Service Award (April 2016 – April 2014)

### Abstracts and Meetings

#### 2018:

- *ALS Mutations of FUS Alter the Regulation of Nonsense Mediated Decay and Suppress Protein Translation*  
M. Kamelgarn, J. Chen, L. Kuang, H. Jin, E.J. Kasarskis, H. Zhu\*  
5th RNA Metabolism in Neurological Disease Conference
- *ALS Mutations of FUS Alter the Regulation of Nonsense Mediated Decay and Suppress Protein Translation*  
M. Kamelgarn, J. Chen, L. Kuang, H. Jin, E.J. Kasarskis, H. Zhu\*  
3rd Annual Midwest Motoneuron Consortium

#### 2017:

- *A Novel Method for Understanding the Mutant FUS Inclusion Interactome Demonstrates Sequestration of Proteins Critical for mRNA Metabolism*



M. Kamelgarn, J. Chen, H. Jin, H. Zhu\*  
International Symposium on ALS/MND

2015:

- *Proteomic Characterization of Cytoplasmic FUS Aggregates*  
M. Kamelgarn, J. Chen, H. Zhu\* International Symposium on ALS/MND  
Nominated for a poster award
- *Proteomic Characterization of Cytoplasmic FUS Aggregates*  
M. Kamelgarn, J. Chen, H. Zhu\*  
3rd RNA Metabolism in Neurological Disease Meeting
- *Proteomic Analysis of the Components of FUS Protein Aggregates with On-Membrane Tryptic Digestion;*  
Jing Chen; Marisa Kamelgarn; Haining Zhu;  
63rd ASMS Conference on Mass Spectrometry and Allied Topics

Marisa Elizabeth Kamelgarn